

การปรับปรุงความเข้ากันได้และความเหนียวของพอลิเมอร์ผสมระหว่าง
เทอร์โมพลาสติกสตาร์ชกับพอลิแลกติกแอซิด

นางสาวสุจารี เตชะพิบูลย์ทรัพย์



วิทยานิพนธ์นี้เป็นส่วนหนึ่งของการศึกษาตามหลักสูตรปริญญาวิศวกรรมศาสตรมหาบัณฑิต
สาขาวิชาวิศวกรรมพอลิเมอร์
มหาวิทยาลัยเทคโนโลยีสุรนารี
ปีการศึกษา 2556

**COMPATIBILITY AND TOUGHNESS IMPROVEMENT
OF THERMOPLASTIC STARCH/POLY(LACTIC ACID)
BLENDS**



Sujaree Tachaphiboonsap



**A Thesis Submitted in Partial Fulfillment of the Requirements for the
Degree of Master of Engineering in Polymer Engineering**

Suranaree University of Technology

Academic Year 2013

**COMPATIBILITY AND TOUGHNESS IMPROVEMENT OF
THERMOPLASTIC STARCH/POLY(LACTIC ACID)
BLENDS**

Suranaree University of Technology has approved this thesis submitted in partial fulfillment of the requirements for a Master's Degree.

Thesis Examining Committee

(Assoc. Prof. Dr. Yupaporn Ruksakulpiwat)

Chairperson

(Asst. Prof. Dr. Kasama Jarukumjorn)

Member (Thesis Advisor)

(Asst. Prof. Dr. Pranee Chumsamrong)

Member

(Prof. Dr. Sukit Limpijumnong)

Vice Rector for Academic Affairs
and Innovation

(Assoc. Prof. Flt. Lt. Dr. Kontorn Chamniprasart)

Dean of Institute of Engineering

สุจารี เตชะพิบูลย์ทรัพย์ : การปรับปรุงความเข้ากันได้และความเหนียวของพอลิเมอร์ผสมระหว่างเทอร์โมพลาสติกสตาร์ชกับพอลิแลคติกแอซิด (COMPATIBILITY AND TOUGHNESS IMPROVEMENT OF THERMOPLASTIC STARCH/POLY(LACTIC ACID) BLENDS) อาจารย์ที่ปรึกษา : ผู้ช่วยศาสตราจารย์ ดร.กษมา จารุกัจจร, 128 หน้า.

ในการศึกษานี้ พอลิเมอร์ผสมระหว่างเทอร์โมพลาสติกสตาร์ชกับพอลิแลคติกแอซิดที่อัตราส่วนต่างๆ คือ 10/90 20/80 30/70 40/60 และ 50/50 เปอร์เซ็นต์โดยน้ำหนัก ถูกเตรียมด้วยเครื่องบดผสมภายใน และชิ้นงานทดสอบถูกขึ้นรูปด้วยเครื่องกดอัด เทอร์โมพลาสติกสตาร์ชได้มาจากแป้งมันสำปะหลังและกลีเซอรอลที่อัตราส่วน 70/30 เปอร์เซ็นต์โดยน้ำหนัก ถูกเตรียมด้วยเครื่องบดผสมภายใน สมบัติทางกล ความร้อน และ สัณฐานวิทยาของพอลิเมอร์ผสมระหว่างเทอร์โมพลาสติกสตาร์ชกับพอลิแลคติกแอซิดถูกศึกษา ค่าความต้านแรงดึง ค่ามอดูลัสแรงดึง และ ค่าความต้านทานต่อแรงกระแทกของพอลิแลคติกแอซิดลดลง เมื่อใส่เทอร์โมพลาสติกสตาร์ช 10 เปอร์เซ็นต์โดยน้ำหนัก ในขณะที่ค่าความยืดสูงสุด ณ จุดขาดเพิ่มขึ้น สมบัติทางกลของพอลิเมอร์ผสมลดลงอย่างต่อเนื่องเมื่อเพิ่มปริมาณของเทอร์โมพลาสติกสตาร์ช พอลิเมอร์ผสมระหว่างเทอร์โมพลาสติกสตาร์ชกับพอลิแลคติกแอซิดที่อัตราส่วน 10/90 เปอร์เซ็นต์โดยน้ำหนัก แสดงค่าสมบัติทางกลที่สูงที่สุด อุณหภูมิเปลี่ยนสถานะคล้ายแก้ว อุณหภูมิการหลอมเหลว และอุณหภูมิการตกผลึกของพอลิแลคติกแอซิดลดลงเมื่อใส่เทอร์โมพลาสติกสตาร์ช 10 เปอร์เซ็นต์โดยน้ำหนัก ในขณะที่ปริมาณผลึกเพิ่มขึ้น เมื่อเพิ่มปริมาณของเทอร์โมพลาสติกสตาร์ช อุณหภูมิเปลี่ยนสถานะคล้ายแก้วและอุณหภูมิการหลอมเหลวของพอลิแลคติกแอซิดในพอลิเมอร์ผสมไม่เปลี่ยนแปลง แต่อุณหภูมิการตกผลึกลดลง เมื่อปริมาณของเทอร์โมพลาสติกสตาร์ชเพิ่มขึ้น ปริมาณผลึกของพอลิแลคติกแอซิดในพอลิเมอร์ผสมเพิ่มขึ้น ความเสถียรต่อความร้อนของพอลิแลคติกแอซิดลดลงเมื่อเพิ่มปริมาณของเทอร์โมพลาสติกสตาร์ช ภาพถ่ายจากกล้องจุลทรรศน์อิเล็กตรอนแบบส่องกราดแสดงให้เห็นว่าเทอร์โมพลาสติกสตาร์ชกับพอลิแลคติกแอซิดไม่เข้ากัน พอลิแลคติกแอซิดกราฟท์มาลิกแอนไฮไดรด์ถูกใช้เป็นการปรับปรุงความเข้ากันได้ และปริมาณของพอลิแลคติกแอซิดกราฟท์มาลิกแอนไฮไดรด์คือ 3 5 และ 7 ส่วนในร้อยส่วนของพอลิเมอร์ผสม สมบัติทางกลและความเสถียรต่อความร้อนของพอลิเมอร์ผสมระหว่างเทอร์โมพลาสติกสตาร์ชกับพอลิแลคติกแอซิดถูกปรับปรุงเมื่อปริมาณพอลิแลคติกแอซิดกราฟท์มาลิกแอนไฮไดรด์ เพิ่มขึ้นถึง 5 ส่วนในร้อยส่วนของพอลิเมอร์ผสม อย่างไรก็ตามที่ปริมาณพอลิแลคติกแอซิดกราฟท์มาลิกแอนไฮไดรด์ 7 ส่วนในร้อยส่วนของพอลิเมอร์ผสม สมบัติทางกลของพอลิเมอร์ผสมลดลง อุณหภูมิเปลี่ยนสถานะคล้ายแก้ว อุณหภูมิการหลอมเหลว และอุณหภูมิการตกผลึกของพอลิเมอร์ผสมลดลง เมื่อเพิ่มปริมาณของ

พอลิแลกติกแอซิดกราฟท์มาลิกแอนไฮไดรด์ ในขณะที่ปริมาณผลึกเพิ่มขึ้น ภาพถ่ายจากกล้องจุลทรรศน์อิเล็กตรอนแบบส่องกราดแสดงให้เห็นว่าพอลิแลกติกแอซิดกราฟท์มาลิกแอนไฮไดรด์ปรับปรุงความเข้ากันได้ระหว่างเทอร์โมพลาสติกสไตรซ์และพอลิแลกติกแอซิด

พอลิบิวทีลีนอะดิเปตโคเทอเรพทาเรต และยางธรรมชาติอีพ็อกซีไคร์ที่ 50 เปอร์เซ็นต์อีพ็อกซีเคชั่น ถูกใช้เป็นสารปรับปรุงความเหนียวสำหรับพอลิเมอร์ผสมที่มีการปรับปรุงความเข้ากันได้ และปริมาณของสารปรับปรุงความเหนียวคือ 10 20 และ 30 เปอร์เซ็นต์โดยน้ำหนัก ค่าความยืดสูงสุด ณ จุดขาดและค่าความต้านทานต่อแรงกระแทกเพิ่มขึ้นเมื่อเพิ่มปริมาณของพอลิบิวทีลีนอะดิเปตโคเทอเรพทาเรตแต่ค่าความต้านแรงดึงและค่ามอดูลัสแรงดึงลดลง เมื่อใส่พอลิบิวทีลีนอะดิเปตโคเทอเรพทาเรต 10 เปอร์เซ็นต์โดยน้ำหนัก อุณหภูมิเปลี่ยนสถานะคล้ายแก้วและอุณหภูมิการตกผลึกของพอลิแลกติกแอซิดในพอลิเมอร์ผสมลดลง ในขณะที่อุณหภูมิการหลอมเหลวไม่เปลี่ยนแปลง ปริมาณของพอลิบิวทีลีนอะดิเปตโคเทอเรพทาเรตไม่แสดงผลต่ออุณหภูมิเปลี่ยนสถานะคล้ายแก้ว อุณหภูมิการตกผลึก และอุณหภูมิหลอมเหลวของพอลิแลกติกแอซิดในพอลิเมอร์ผสม ปริมาณผลึกของพอลิแลกติกแอซิดในพอลิเมอร์ผสมเพิ่มขึ้นเมื่อใส่พอลิบิวทีลีนอะดิเปตโคเทอเรพทาเรต ความเสถียรต่อความร้อนของพอลิเมอร์ผสมเพิ่มขึ้น เมื่อเพิ่มปริมาณของพอลิบิวทีลีนอะดิเปตโคเทอเรพทาเรต ภาพถ่ายจากกล้องจุลทรรศน์อิเล็กตรอนแบบส่องกราดแสดงการแตกหักแบบเหนียวในพอลิเมอร์ผสมที่มีการปรับปรุงความเหนียวด้วยพอลิบิวทีลีนอะดิเปตโคเทอเรพทาเรต ค่าความต้านแรงดึงและค่ามอดูลัสแรงดึงของพอลิเมอร์ผสมลดลงเมื่อเพิ่มปริมาณของยางธรรมชาติอีพ็อกซีไคร์ที่ 50 เปอร์เซ็นต์อีพ็อกซีเคชั่น ค่าความยืดสูงสุด ณ จุดขาดและค่าความต้านทานต่อแรงกระแทกของพอลิเมอร์ผสมเพิ่มขึ้นอย่างต่อเนื่องเมื่อเพิ่มปริมาณยางธรรมชาติอีพ็อกซีไคร์ที่ 50 เปอร์เซ็นต์อีพ็อกซีเคชั่นถึง 20 เปอร์เซ็นต์โดยน้ำหนัก อย่างไรก็ตาม สมบัติทางกลของพอลิเมอร์ผสมลดลงเมื่อใส่ 30 เปอร์เซ็นต์โดยน้ำหนักของยางธรรมชาติอีพ็อกซีไคร์ที่ 50 เปอร์เซ็นต์อีพ็อกซีเคชั่น อุณหภูมิเปลี่ยนสถานะคล้ายแก้ว อุณหภูมิการหลอมเหลว และปริมาณผลึกของพอลิแลกติกแอซิดในพอลิเมอร์ผสมลดลง เมื่อเพิ่มปริมาณของยางธรรมชาติอีพ็อกซีไคร์ที่ 50 เปอร์เซ็นต์อีพ็อกซีเคชั่น แต่อุณหภูมิการตกผลึกเพิ่มขึ้น ความเสถียรต่อความร้อนของพอลิเมอร์ผสมลดลงเมื่อเพิ่มปริมาณของยางธรรมชาติอีพ็อกซีไคร์ที่ 50 เปอร์เซ็นต์อีพ็อกซีเคชั่น ภาพถ่ายจากกล้องจุลทรรศน์อิเล็กตรอนแบบส่องกราดแสดงการแตกหักแบบเหนียวในพอลิเมอร์ผสมที่มีการปรับปรุงความเหนียวด้วยยางธรรมชาติอีพ็อกซีไคร์ที่ 50 เปอร์เซ็นต์อีพ็อกซีเคชั่น

สาขาวิชา วิศวกรรมพอลิเมอร์

ปีการศึกษา 2556

ลายมือชื่อนักศึกษา _____

ลายมือชื่ออาจารย์ที่ปรึกษา _____

SUJAREE TACHAPHIBOONSAP : COMPATIBILITY AND
TOUGHNESS IMPROVEMENT OF THERMOPLASTIC STARCH/
POLY(LACTIC ACID) BLENDS. THESIS ADVISOR : ASST. PROF.
KASAMA JARUKUMJORN, Ph.D., 128 PP.

THERMOPLASTIC STARCH/POLY(LACTIC ACID)/POLY(LACTIC ACID)
GRAFTED WITH MALEIC ANHYDRIDE/POLY(BUTYLENE ADIPATE-CO-
TEREPHTHALATE)/EPOXIDIZED NATURAL RUBBER

In this study, thermoplastic starch (TPS)/poly(lactic acid) (PLA) blends at various ratios of 10/90, 20/80, 30/70, 40/60, and 50/50%wt were prepared using an internal mixer and their test specimens were molded using a compression molding machine. TPS obtained from cassava starch and glycerol at a ratio of 70/30%wt was mixed using an internal mixer. Mechanical, thermal, and morphological properties of TPS/PLA blends were studied. Tensile strength, tensile modulus, and impact strength of PLA were decreased with adding 10%wt TPS while elongation at break was increased. Mechanical properties of the blends were continuously decreased with increasing TPS content. TPS/PLA (10/90) blend showed the highest mechanical properties. Glass transition temperature (T_g), melting temperature (T_m), and cold crystallization temperature (T_{cc}) of PLA were decreased with incorporating 10%wt TPS whereas degree of crystallinity (χ_c) was increased. With increasing TPS content, T_g and T_m of PLA in the blends did not change but T_{cc} was decreased. As TPS content was increased χ_c of PLA in the blends was increased. Thermal stability of PLA was decreased with increasing TPS content. SEM micrographs showed that TPS and PLA were immiscible. PLA grafted with maleic anhydride (PLA-g-MA) was used as a

compatibilizer and its contents were 3, 5, and 7 phr. Mechanical properties and thermal stability of TPS/PLA blends were improved when PLA-g-MA content was increased to 5 phr. However, at PLA-g-MA content of 7 phr, mechanical properties of the blend were decreased. T_g , T_m , and T_{cc} of PLA in the blends were decreased with increasing PLA-g-MA content whereas χ_c was increased. SEM micrographs revealed that PLA-g-MA improved compatibility between TPS and PLA.

Poly(butylene adipate-co-terephthalate) (PBAT) and epoxidized natural rubber with 50% epoxidation (ENR50) were used as toughening agents for the compatibilized blends and their contents were 10, 20, and 30%wt. Elongation at break and impact strength of the blends were increased with increasing PBAT content but tensile strength and tensile modulus were decreased. With the addition of 10% wt PBAT, T_g and T_{cc} of PLA in the blend decreased whereas T_m did not change. PBAT content showed no effect on T_g , T_{cc} , and T_m of PLA in the blends. χ_c of PLA in the blends increased with adding PBAT. Thermal stability of the blends was enhanced with increasing PBAT content. SEM micrographs showed ductile fracture in the blends toughened with PBAT. Tensile strength and tensile modulus of the blends were decreased with increasing ENR50 content. Elongation at break and impact strength of the blends continuously increased with increasing ENR50 content up to 20%wt. However, mechanical properties of the blend were decreased with adding 30% wt ENR50. T_g , T_m , and χ_c of PLA in the blends were decreased with increasing ENR50 content but T_{cc} was increased. Thermal stability of the blends was decreased with increasing ENR50 content. SEM micrographs exhibited ductile fracture in the blends toughened with ENR50.

School of Polymer Engineering

Academic Year 2013

Student's Signature _____

Advisor's Signature _____

ACKNOWLEDGEMENTS

I gratefully acknowledge the financial supports from Suranaree University of Technology and Center of Excellence on Petrochemical and Materials Technology.

First, I would like to express my sincere grateful to my thesis advisor, Asst. Prof. Dr. Kasama Jarukumjorn, for her valuable supervision, inspiring guidance, support, and kindness throughout the period of the study. I am most grateful for her teaching and advice, not only the research methodologies but also many other methodologies in life. I would not have achieved this far and this thesis would not have been completed without all the support that I have always received from her. In addition, I wish to express my gratitude to Assoc. Prof. Dr. Yupaporn Ruksakulpiwat and Asst. Prof. Dr. Pranee Chumsamrong for their valuable suggestions and guidance given as committee members.

Furthermore, I am deeply indebted to lecturers, staff member, and all friend of School of Polymer Engineering for their helps, supports, and encouragement.

Finally, my graduation would not be achieved without best wish from my parent, Mr. Jirasak and Mrs. Samran Tachaphiboonsap, and my sister, Miss Pitcharee Tachaphiboonsap, who give me a valuable life with their endless love, support, and encouragement throughout my life.

Sujaree Tachaphiboonsap

TABLE OF CONTENTS

	Page
ABSTARCT (THAI)	I
ABSTARCT (ENGLISH).....	III
ACKNOWLEDGEMENTS	V
TABLE OF CONTENTS	VI
LIST OF TABLES	X
LIST OF FIGURES	XII
SYMBOLS AND ABBREVIATIONS	XVIII
CHAPTER	
I INTRODUCTION.....	1
1.1 Research objectives	3
1.2 Scope and limitation of the study.....	3
II LITERATURE REVIEW.....	5
2.1 Thermoplastic starch	5
2.2 TPS/poly(lactic acid) (PLA) blend	10
2.3 Compatibilization of TPS/PLA blend	14
2.3.1 Addition of compatibilizer.....	14
2.3.2 PLA modification	20
2.3.3 TPS modification	21
2.4 Toughness improvement of TPS/PLA blend	25

TABLE OF CONTENTS (Continued)

	Page
III EXPERIMENTAL	30
3.1 Materials.....	30
3.2 Experimental	30
3.2.1 Preparation of thermoplastic starch	30
3.2.2 Preparation and characterization of poly(lactic acid) grafted with maleic anhydride	31
3.2.2.1 Determination of maleic anhydride content.....	31
3.2.2.2 Fourier transform infrared spectroscopy	32
3.2.3 Preparation of TPS/PLA blends.....	32
3.2.4 Preparation of TPS/PLA/PBAT blends and TPS/PLA/ENR50 blends	33
3.2.5 Characterization of TPS, PLA, TPS/PLA blends, compatibilized TPS/PLA blends, compatibilized TPS/PLA/PBAT blends, and compatibilized TPS/PLA/ENR50 blends	33
3.2.5.1 Mechanical properties.....	33
3.2.5.2 Thermal properties.....	34
3.2.5.3 Morphological properties.....	35

TABLE OF CONTENTS (Continued)

	Page
IV RESULTS AND DISCUSSION	36
4.1 Characterization of poly(lactic acid) grafted with maleic anhydride (PLA-g-MA).....	36
4.1.1 Identification of PLA-g-MA and determination of graft content	36
4.2 Effect of blend composition on properties of TPS/PLA blends.....	40
4.2.1 Mechanical properties.....	40
4.2.2 Morphological properties.....	44
4.2.3 Thermal properties.....	45
4.3 Effect of compatibilizer content on properties of TPS/PLA blends.....	54
4.3.1 Mechanical properties.....	54
4.3.2 Morphological properties.....	59
4.3.3 Thermal properties.....	60
4.4 Effect of flexible polymer content on properties of compatibilized TPS/PLA blends	67
4.4.1 Effect of PBAT content on properties of compatibilized TPS/PLA blends	67
4.4.1.1 Mechanical properties.....	67

TABLE OF CONTENTS (Continued)

	Page
4.4.1.2 Morphological properties.....	72
4.4.1.3 Thermal properties.....	75
4.4.2 Effect of ENR50 content on properties of compatibilized TPS/PLA blends	81
4.4.2.1 Mechanical properties.....	81
4.4.2.2 Morphological properties.....	86
4.4.2.3 Thermal properties.....	88
V CONCLUSIONS	95
REFERENCES	98
APPENDIX A PUBLICATIONS	108
BIOGRAPHY	128

LIST OF TABLES

Table		Page
4.1	Mechanical properties of PLA, TPS, and TPS/PLA blends at various TPS contents.	43
4.2	Thermal characteristics of PLA and TPS/PLA blends at various TPS contents.	48
4.3	The thermal decomposition temperature of PLA, TPS, and TPS/PLA blends at various TPS contents.	53
4.4	Mechanical properties of TPS/PLA blend and TPS/PLA/PLA-g-MA blends at various PLA-g-MA contents.....	58
4.5	Thermal characteristics of TPS/PLA blend and TPS/PLA/PLA-g-MA blends at various PLA-g-MA contents.....	63
4.6	The thermal decomposition temperature of TPS/PLA blend and TPS/PLA/PLA-g-MA blends at various PLA-g-MA contents.....	66
4.7	Mechanical properties of compatibilized TPS/PLA blend and compatibilized TPS/PLA/PBAT blends at various PBAT contents.....	71
4.8	Thermal characteristics of compatibilized TPS/PLA blend and compatibilized TPS/PLA/PBAT blends at various PBAT contents.....	77
4.9	The thermal decomposition temperature of compatibilized TPS/PLA blend and compatibilized TPS/PLA/PBAT blends at various PBAT contents.....	80

LIST OF TABLES (Continued)

Table		Page
4.10	Mechanical properties of compatibilized TPS/PLA blend and compatibilized TPS/PLA/ENR50 blends at various of ENR50 contents.....	85
4.11	Thermal characteristics of compatibilized TPS/PLA blend and compatibilized TPS/PLA/ENR50 blends at various of ENR50 contents.....	91
4.12	The thermal decomposition temperature of compatibilized TPS/PLA blend and compatibilized TPS/PLA/ENR50 blends at various ENR50 contents.....	94

LIST OF FIGURES

Figure	Page
4.1 FTIR spectra of MA, PLA, and PLA-g-MA at 1.0% wt Luperox101 and 5.0% wt MA.....	37
4.2 FTIR second derivative spectra of MA, PLA, and PLA-g-MA at 1.0% wt Luperox101 and 5.0% wt MA.....	38
4.3 Proposed grafting reaction pathway for the reaction of MA on PLA.	39
4.4 Tensile strength of PLA, TPS, and TPS/PLA blends at various TPS contents.....	41
4.5 Tensile modulus of PLA, TPS, and TPS/PLA blends at various TPS contents.....	41
4.6 Elongation at break of PLA, TPS, and TPS/PLA blends at various TPS contents.....	42
4.7 Impact strength of PLA and TPS/PLA blends at various TPS contents.....	42
4.8 SEM micrographs of the freeze fractured surface at 1000x magnification of (a) PLA, (b) TPS/PLA 10/90 blend, (c) TPS/PLA 20/80 blend, (d) TPS/PLA 30/70 blend, (e) TPS/PLA 40/60 blend, and (f) TPS/PLA 50/50 blend.	44

LIST OF FIGURES (Continued)

Figure	Page
4.9 DSC thermograms of PLA, TPS, TPS/PLA blends at various TPS contents (the second heating, heating rate 5°C/min).	47
4.10 TGA curves of PLA, TPS, and cassava starch.	51
4.11 DTG curves of PLA, TPS, and cassava starch.	51
4.12 TGA curves of PLA, TPS, and TPS/PLA blends at various TPS contents.	52
4.13 DTG curves of PLA, TPS, and TPS/PLA blends at various TPS contents.	52
4.14 Tensile strength of TPS/PLA blend and TPS/PLA/PLA-g-MA blends at various PLA-g-MA contents.	56
4.15 Tensile modulus of TPS/PLA blend and TPS/PLA/PLA-g-MA blends at various PLA-g-MA contents.	56
4.16 Elongation at break of TPS/PLA blend and TPS/PLA/PLA-g-MA blends at various PLA-g-MA contents.	57
4.17 Impact strength of TPS/PLA blend and TPS/PLA/PLA-g-MA blends at various PLA-g-MA contents.	57
4.18 SEM micrographs of the freeze fractured surface at 1000x magnification of (a) TPS/PLA 10/90 blend, (b) TPS/PLA/PLA-g-MA 10/90/3 blend, (c) TPS/PLA/PLA-g-MA 10/90/5 blend, and (d) TPS/PLA/PLA-g-MA 10/90/7 blend.	60

LIST OF FIGURES (Continued)

Figure	Page
4.19 DSC thermograms of TPS/PLA blend and TPS/PLA/PLA-g-MA blends at various PLA-g-MA contents (the second heating, heating rate 5°C/min).	62
4.20 TGA curves of TPS/PLA blend and TPS/PLA/PLA-g-MA blends at various PLA-g-MA contents.	65
4.21 DTG curves of TPS/PLA blend and TPS/PLA/PLA-g-MA blends at various PLA-g-MA contents.	65
4.22 Tensile strength of compatibilized TPS/PLA blend and compatibilized TPS/PLA/PBAT blends at various PBAT contents.	68
4.23 Tensile modulus of compatibilized TPS/PLA blend and compatibilized TPS/PLA/PBAT blends at various PBAT contents.	69
4.24 Elongation at break of compatibilized TPS/PLA blend and compatibilized TPS/PLA/PBAT blends at various PBAT contents.	69
4.25 Impact strength of compatibilized TPS/PLA blend and compatibilized TPS/PLA/PBAT blends at various PBAT contents.	70

LIST OF FIGURES (Continued)

Figure	Page
4.26 SEM micrographs of the freeze fractured surface at 1000x (left) and 2000x (right) magnification of (a) TPS/PLA/PLA-g-MA 10/90/5phr blend, (b) TPS/PLA/PLA-g-MA/PBAT 9/81/5phr/10 blend, (c) TPS/PLA/PLA-g-MA/PBAT 8/72/5phr/20 blend, and (d) TPS/PLA/PLA-g-MA/PBAT 7/63/5phr/30 blend.	73
4.27 SEM micrographs of tensile fractured surface at 1500x magnification of (a) TPS/PLA/PLA-g-MA 10/90/5phr blend, (b) TPS/PLA/PLA-g-MA/PBAT 9/81/5phr/10 blend, (c) TPS/PLA/PLA-g-MA/PBAT 8/72/5phr/20 blend, and (d) TPS/PLA/PLA-g-MA/PBAT 7/63/5phr/30 blend.	74
4.28 DSC thermograms of compatibilized TPS/PLA blend and compatibilized TPS/PLA/PBAT blends at various PBAT contents (the second heating, heating rate 5°C/min).	76
4.29 TGA thermograms of compatibilized TPS/PLA blend and compatibilized TPS/PLA/PBAT blends at various PBAT contents.....	79
4.30 DTG thermograms of compatibilized TPS/PLA blend and compatibilized TPS/PLA/PBAT blends at various PBAT contents.	79

LIST OF FIGURES (Continued)

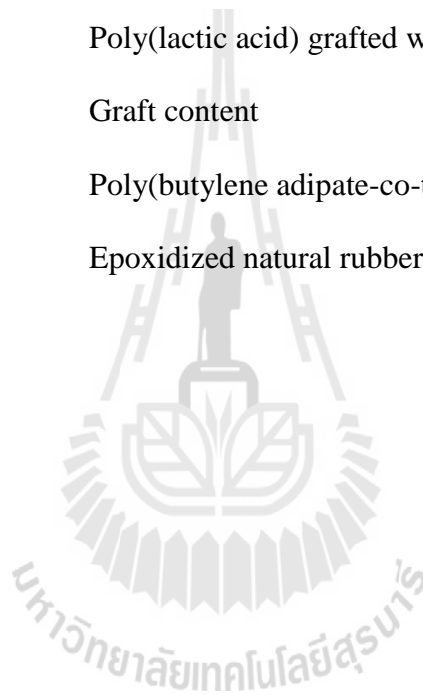
Figure	Page
4.31 Tensile strength of compatibilized TPS/PLA blend and compatibilized TPS/PLA/ENR50 blends at various ENR50 contents.....	83
4.32 Tensile modulus of compatibilized TPS/PLA blend and compatibilized TPS/PLA/ENR50 blends at various ENR50 contents.....	83
4.33 Elongation at break of compatibilized TPS/PLA blend and compatibilized TPS/PLA/ENR50 blends at various ENR50 contents.....	84
4.34 Impact strength of compatibilized TPS/PLA blend and compatibilized TPS/PLA/ENR50 blends at various ENR50 contents.....	84
4.35 SEM micrographs of the freeze fractured surface at 1000x magnification (a) TPS/PLA/PLA-g-MA 10/90/5phr blend, (b) TPS/PLA/PLA-g-MA/ENR50 9/81/5phr/10 blend, (c) TPS/PLA/PLA-g-MA/ENR50 8/72/5phr/20 blend, and (d) TPS/PLA/PLA-g-MA/ENR50 7/63/5phr/30 blend.	87

LIST OF FIGURES (Continued)

Figure	Page
4.36 SEM micrographs of the tensile fractured surface at 1000x magnification (a) TPS/PLA/PLA-g-MA 10/90/5phr blend, (b) TPS/PLA/PLA-g-MA/ENR50 9/81/5phr/10 blend, (c) TPS/PLA/PLA-g-MA/ENR50 8/72/5phr/20 blend, and (d) TPS/PLA/PLA-g-MA/ENR50 7/63/5phr/30 blend.	88
4.37 DSC thermograms of compatibilized TPS/PLA blend and compatibilized TPS/PLA/ENR50 blends (the second heating, heating rate 5°C/min).	90
4.38 TGA thermograms of compatibilized TPS/PLA blend and compatibilized TPS/PLA/ENR50 blends at various ENR50 contents.....	93
4.39 DTG thermograms of compatibilized TPS/PLA blend and compatibilized TPS/PLA/ENR50 blends at various ENR50 contents.....	93

SYMBOLS AND ABBREVIATIONS

TPS	=	Thermoplastic starch
PLA	=	Poly(lactic acid)
Luperox101	=	2,5-bis(tert-butylperoxy)-2,5 dimethylhexane
PLA-g-MA	=	Poly(lactic acid) grafted with maleic anhydride
%G	=	Graft content
PBAT	=	Poly(butylene adipate-co-terephthalate)
ENR50	=	Epoxidized natural rubber with 50% epoxidation



CHAPTER I

INTRODUCTION

Recently, biodegradable polymers have attracted considerable interest due to environmental concerns. Poly(lactic acid) (PLA), derived from renewable resources, is one of the most widely used biodegradable polymers. PLA has several advantages including biodegradability, high strength, high modulus, and gas permeability. However, its high brittleness and high cost limit its application.

In order to maintain its biodegradability and reduce cost of PLA, blending PLA with starch has been investigated. Starch, a hydrophilic renewable filler, is one of well-known biopolymers and often used in order to lower the cost of the finished product and enhance the biodegradable characteristics. However, melting temperature of starch is above the degradation temperature (Nashed, Rutgers, and Sopade, (2003); Yang, Yu, and Ma, (2006)). So, it does not soften and flows during blending with polymer. Therefore, starch is converted into thermoplastic starch (TPS) by the disruption of molecular interaction with the presence of plasticizer under heating and shearing process. This phenomena is known as gelatinization process. Polyols e.g. glycerol, glycol, sorbitol, xylitol are common plasticizers used in TPS preparation because these molecules are small and can easily separate from starch macromolecular chain. Glycerol has traditionally been considered as the most effective plasticizer due to high boiling point and low cost (Kaseem, Hamad, and Deri, (2012)). The addition of glycerol into starch results in a reduction in apparent viscosity and glass transition temperature

of starch (Rodriguez-Gonzalez, Ramsay, and Favis, (2004)). Higher glycerol content was beneficial for the improvement of processibility of TPS with both the reduction of the processing torque and the shortening of the time to attain the equilibrium. With increasing glycerol content, tensile strength of TPS decreased but elongation at break increased (Qiao, Tang, and Sun, (2011)).

However, TPS/PLA blend is an immiscible blend which leads to poor mechanical properties of the blend. The compatibility between PLA and TPS can be achieved by adding compatibilizers e.g. poly(lactic acid) grafted with amylose (PLA-g-A) (Schwach, Six, and Averous, (2008)), methylenediphenyl diisocyanate (MDI) (Yu, Petinakis, Dean, Liu, and Yuan, (2011)), poly(lactic acid) grafted with thermoplastic starch (PLA-g-TPS) (Wootthikanokkhan et al., (2012)), and poly(ethylene glycol) (PEG) (Ping, Kejian, Mingyin, Meijuan, (2013)). In addition, PLA modification e.g. poly(lactic acid) grafted with maleic anhydride (PLA-g-MA) (Huneault and Li, (2007)) and TPS modification e.g. thermoplastic acetylated starch (ATPS) (Zhang, Ran, Zhuang, Yao, and Dong, (2009)), maleated thermoplastic starch (MTPS) (Wootthikanokkhan et al., (2012)) are also used to enhance the compatibility between TPS and PLA.

Nevertheless, toughness of TPS/PLA blends need to be enhanced. In order to improve toughness of the blends, flexible polymers e.g. polycaprolactone (PCL), poly(butylene adipate-co-terephthalate) (PBAT), and poly(butylene succinate) (PBS) have been introduced into the blends. The addition of PCL improved ductility of TPS/PLA blends (Sarazin, Li, Orts, and Favis, (2008)). Ren, Fu, Ren, and Yuan, (2009) also reported that elongation at break of TPS/PLA blends greatly increased with increasing PBAT content. Shi et al., (2011) found that glycidyl methacrylate grafted

poly(ethylene octane) (GPOE) remarkably improved elongation at break and impact strength of TPS/PLA blends. In addition, research works focusing on the use of rubber as the third component to improve toughness of polymers have been reported. The incorporation of epoxidized natural rubber with 50% epoxidation (ENR50) increased tensile strength and elongation at break of PLA/rice starch composites (Yew, Mohd Yusof, MohdIshak, and Ishiaku, (2005)). Moreover, ENR50 enhanced biodegradability of the composites. Sharma et al. (2001) reported a small improvement of tensile strength of linear low density polyethylene (LLDPE)/sago starch composites with the addition of 6% wt of ENR50. Elongation at break of the composites changed insignificantly with adding ENR50 up to 6% wt.

1.1 Research objectives

The main objectives of this research are as below:

- (1) To study mechanical and thermal properties of TPS.
- (2) To study mechanical, thermal, and morphological properties of TPS/PLA blends.
- (3) To study effect of PLA-g-MA as a compatibilizer on mechanical, thermal, and morphological properties of TPS/PLA blends.
- (4) To study effect of PBAT and ENR50 on mechanical, thermal, and morphological properties of TPS/PLA blends.

1.2 Scope and limitation of the study

In this research, TPS was prepared using an internal mixer and then test specimens were molded by a compression molding machine. The ratio of glycerol/cassava starch was 30/70% wt. Mechanical and thermal properties of TPS were

investigated. Then, TPS/PLA blends at various ratios of 10/90, 20/80, 30/70, 40/60, and 50/50% wt were prepared using an internal mixer and test specimens were molded using a compression molding machine. Mechanical, thermal, and morphological properties of TPS/PLA blends were studied.

The TPS/PLA blend giving optimum mechanical properties was chosen to study the effect of compatibilizer content on mechanical, thermal, and morphological properties of the TPS/PLA blends. PLA-g-MA was used as a compatibilizer and its contents were 3, 5, and 7 phr. PLA-g-MA was prepared using an internal mixer. TPS/PLA/PLA-g-MA blends were prepared using an internal mixer and test specimens were processed using a compression molding machine. Mechanical, thermal, and morphological properties of the TPS/PLA blends were investigated.

The compatibilized TPS/PLA blend giving optimum mechanical properties was chosen to study the effect of poly(butylene adipate-co-terephthalate) (PBAT) and epoxidized natural rubber with 50% epoxidation (ENR50) content on mechanical, thermal, and morphological properties of the compatibilized TPS/PLA blend. PBAT and ENR50 contents were varied as 10, 20, and 30% wt. The blends were prepared using an internal mixer and test specimens were processed using a compression molding machine. Mechanical, thermal, and morphological properties of the TPS/PLA blends were studied.

CHAPTER II

LITERATURE REVIEW

2.1 Thermoplastic starch

Starch is a low cost polysaccharide derived from agricultural plants and it is susceptible to biological attack. However, melting temperature of starch is close to the degradation temperature thus it does not flow during processing. So, starch can be modified to be thermoplastic starch (TPS) by the disruption molecular interaction of starch with the presence of plasticizer under heating and shearing. This process is known as gelatinization process. Polyols such as glycerol, glycol, and sorbitol are common plasticizers used in TPS preparation. This is because these molecules are small and easily penetrate into starch chain.

Rodriguez-Gonzalez, Ramsay, and Favis (2004) studied rheological and thermal properties of TPS. Glycerol contents were 29, 33, 36, and 40%wt. Wheat starch was gelatinized and plasticized in a co rotating twin screw extruder. Shear viscosity of TPS decreased about 20% when glycerol was increased from 36 to 40%wt. This indicated that glycerol-rich soft region was shown on TPS. Loss and storage modulus of TPS were decreased as glycerol content was increased. In addition, a dramatic reduction of the moduli was observed when glycerol content from 29 to 33%wt. Glass transition temperature (T_g) was decreased as glycerol content was increased from 29 to 40%wt. Form time sweep measurement, TPS had excellent thermal stability at 150°C but became unstable at temperature above 180°C.

Huang, Yu, and Ma (2005) compared the effect of glycerol and ethanolamide as plasticizers on mechanical, thermal, and water absorption properties of TPS. Corn starch was mixed with the plasticizer using a high speed mixer at 300 rpm for 2 min. Then, the mixtures were fed into a single screw extruder with a screw speed of 20 rpm. The temperature profile was 110, 115, 120, and 125°C. Modulus, breaking energy, and water absorption of ethanolamide plasticized TPS (ETPS) were higher than glycerol plasticized TPS (GTPS). Ethanolamide could form hydrogen bond with starch during processing resulting in good mechanical properties of TPS. T_g of ETPS was lower than that of GTPS. However, water absorption of ETPS was lower than GTPS. This indicated that the hydrophilicity of ethanolamine was weaker than that of glycerol, thus it improved water resistance of TPS.

Ma, Yu, and Ma (2005) used urea and formamide as plasticizers to prepare thermoplastic flour (TPF). The ratio of urea and formamide was 1/2%wt. Plasticizer contents were 25, 30, 40, and 50% wt. Wheat flour and plasticizers were mixed using a high speed mixer with a rotating speed of 300 rpm for 2 min. After that, the mixtures were prepared in a single screw extruder with a rotating speed of 20 rpm. The temperature profile was 120, 130, 130, and 120°C. Tensile strength, modulus, and energy break of TPF were decreased but the elongation at break was improved with increasing plasticizer content. This was because hydrogen bond interaction between plasticizer and starch was formed and slippage movement of starch molecules was easy. Apparent viscosity of TPF was decreased when plasticizer content was increased due to a reduction of molecular interaction of starch by plasticizer. Water absorption results showed that TPF with low plasticizer content had a relatively good water resistance.

Da Roz, Carvalho, Gandini, and Curvelo (2006) investigated the effects of type and amount of plasticizer on mechanical, thermal, and water absorption properties of TPS. 1,4 butanediol (BUT), ethylene glycol (EG), propylene glycol (PG), diethyleneoxide glycol (DEG), and D-sorbitol (SOR) were used as plasticizers. Plasticizer contents were 15, 20, 30, and 40% wt. Corn starch and the selected plasticizer were mixed using an internal mixer at 150°C with a rotating speed of 60 rpm for 6 min. For EG and PG plasticized TPS, tensile modulus increased with increasing plasticizer content, except for EG contents above 30% wt due to an increase in crystallinity of TPS. However, tensile modulus of BUT, DEG, and SOR plasticized TPS decreased as plasticizer content was increased due to the plasticization. Tan δ curves of all samples showed two relaxations, which were observed between -75 and -40°C and between 70 and 150°C, respectively. A high temperature relaxation was attributed to T_g of TPS while a low temperature was related to a plasticizer-rich phase. Storage modulus of all TPS after the T_g displayed a plateau typical of semi-crystalline polymer. Equilibrium water uptake of all TPS increased with increasing plasticizer content.

Teixaira, Da Roz, Carvalho, and Curvelo (2007) studied the effect of glycerol/sugar/water and sugar/water mixtures on plasticization of TPS prepared from cassava starch. The ratio of glycerol/sugar/water was 30/2/18% wt while the ratio of sugar/water was approximately 25/25% wt. TPS was produced using an internal mixer with a temperature of 120°C for 6 min. The rotating speed was 60 rpm. Thermal and mechanical properties of TPS were investigated. The addition of 2% wt of sugar into starch-glycerol system showed the reduction in storage modulus of TPS due to lower crystallinity of TPS. The absence of glycerol from TPS sample made it more rigid resulting in high storage modulus. A small addition of sugar (2% wt) combined with

glycerol reduced glass transition temperature of TPS. The use of sugar and water as plasticizers without glycerol caused a considerable reduction in water uptake (by about 60%) of TPS due to lower efficiency of sugar as plasticizers.

Wang and Huang (2007) prepared TPS by using ethanolamine and glycerol as plasticizers. Plasticizer content was kept at 30% wt. Corn starch and plasticizer were blended using high speed mixer GH-100Y with a speed of 300 rpm for 2 min. After that, the mixtures were transferred into a single screw extruder with a screw speed of 20 rpm. The temperature profile was 110, 115, 120, and 125°C (from feed zone to die). Mechanical properties of ethanolamine plasticized TPS (ETPS) were higher than glycerol plasticized TPS (GTPS). This was because small molecules of ethanolamine penetrated into starch molecules and formed hydrogen bonds with starch which was stronger than the GTPS. DSC analysis revealed that T_g of ETPS was lower than GTPS. This was because ethanolamine formed hydrogen bonds with starch molecules which made the reaction between starch molecules weak and the degree of freedom of starch molecular chain relatively improved.

Zhang, Yu, Wu, and Ma (2008) used aliphatic amidediol and glycerol as plasticizers for TPS preparation. Plasticizer content was 30%wt and the ratios of glycerol/ aliphatic amidediol were 20/10 and 15/15%wt. Plasticizer and corn starch were blended using a high speed mixer GH-100Y and then stored overnight. The mixtures were fed into a single screw extruder. Barrel temperatures were 145, 150, 150, and 145°C (from feed zone to die). FTIR results confirmed that the mixture of aliphatic amidediol and glycerol formed stronger and stable hydrogen bond with starch molecules compared to native cornstarch. With increasing aliphatic amidediol content, T_g of TPS was increased. The strong hydrogen bond was formed between plasticizers

and starch resulting in a decrease in starch chain mobility and an increase in glass transition of TPS. Tensile stress and elongation at break of TPS were increased with increasing aliphatic amidediol content.

Sreekumar, Gopalakrishnan, Leblanc, and Saiter (2010) investigated the influence of glycerol content on viscoelastic behavior of thermoplastic flour (TPF). Glycerol content were 20, 23, 25, 30, and 35%wt. Wheat flour and glycerol were mixed using a thermo-regulated turbo mixer with a rotating speed of 750 rpm for 3 min. Then, the mixtures were mixed in a single screw extruder at 120°C with a rotating speed of 60 rpm. Two peaks were observed in damping curves. One at low temperature indicated glycerol rich phase and another at high temperature was starch rich phase. At high temperature region, the storage and loss moduli of TPS decreased as a function of glycerol content due to the variation in its T_g . The relaxation temperature was decreased with increasing glycerol content. This was because average molar mass of polymer-plasticizer mixture was decreased and free volume was increased.

Ahmad, Anuar, and Yusof (2011) studied the effect of glycerol content on mechanical, thermal, and morphological properties of TPS. Sago starch and glycerol was mixed using a stirrer. Then, the mixture was blended using a twin screw extruder. The mixing temperature was kept at 130°C with a screw speed of 100 rpm. Granulates were injection molded. The temperature profile was 110, 115, 120, 125, and 150°C. Glycerol contents were varied as 10, 20, 30, and 40%wt. TPS with less than 20% wt of glycerol had low tensile strength because plasticizing effect was not enough. The highest maximum tensile strength was obtained with adding 30% wt glycerol content. From SEM micrographs, TPS plasticized 20%wt of glycerol resulted in a less coarse granules when compared with the native sago starch. This suggested that starch granule

fused into homogeneous phase. This led to some empty space in TPS. Moreover, plasticized TPS with 30%wt of glycerol had a clear and smooth surface. As plasticizer content increased melt viscosity of TPS was decreased thus the plasticization of starch was difficult. This was due to a reduction of shear during processing.

Sreekumar, Leblance, and Saiter (2013) investigated the effect of glycerol on thermal, mechanical, and morphological properties of TPS. Glycerol contents were 20, 23, 25, 30, and 35%wt. Wheat flour was mixed with glycerol using a thermo-regulated turbo mixer at a rotating speed of 750 rpm over 3 min. The mixture was extruded using a single screw extruder at 120°C. The mixing speed was set at 60 rpm. The samples were molded into thick sheets using hydraulic press at 120°C and a pressure of 10 kg/cm³. Elongation at break of TPS was increased with increasing glycerol content whereas tensile strength, modulus and hardness decreased. This suggested that glycerol modified the state of starch from solid to that of a rubber phase. From SEM micrograph, surface of TPS with less amount of glycerol was rough. With increasing TPS content, the surface of TPS become smoother. When glycerol content was increased, MFI values were increased. This indicated that plasticization effect improved the mobility of starch molecules by a reduction in its viscosity. When the glycerol content was increased from 20 to 25%wt impact strength was increased. Glycerol showed no significant effect on thermal stability of TPS.

2.2 TPS/poly(lactic acid) (PLA) blend

PLA is considered as a substitute of non-biodegradable polymers for commodity applications due to its good physical properties and commercial availability. However, the main limitation of PLA is high cost. Blending TPS with PLA is a solution to reduce the cost and maintain biodegradability of PLA.

Martin and Averous (2001) studied mechanical and thermal properties of TPS/PLA blends. TPS contents were 10, 25, 40, and 75%wt. TPS/PLA blends were mixed using a single screw extruder. The temperature range was from 120 to 180°C. Tensile strength, elongation at break, and impact strength of PLA were decreased with increasing TPS content. T_g of PLA was decreased when TPS content was increased. This indicated a small degree of compatibility between TPS and PLA. Moreover, melting temperature (T_m) of PLA in TPS/PLA blend was lower than pure PLA. This result may be explained by two reasons. Firstly, the reduction in T_m was observed when a semi-crystalline component was miscible with an amorphous polymer. Secondly, T_m was decreased due to plasticizing effect of glycerol.

Wang, Yu, and Ma (2008) studied mechanical, thermal, and rheological properties of TPS/PLA blends. Glycerol and formamide were used as plasticizers. The ratios of formamide/glycerol were varied as 0/40, 10/30, 20/20, and 30/10%wt. Corn starch/plasticizer ratio was 100/40%wt. The plasticizers were firstly mixed and then blended with starch using a high speed mixer with a rotating speed of 3000 rpm for 2 min. After that, the mixtures were blended with PLA using a high speed mixer. TPS/PLA blends were prepared using a single screw extruder with a screw speed of 10 rpm. The temperature profile was 130, 140, 150, and 130°C. Mechanical, thermal, and rheological properties of TPS/PLA blends were tested. Tensile strength and elongation at break of the blend were decreased with adding TPS due to poor interfacial adhesion between TPS and PLA. With increasing formamide content, tensile strength and elongation at break of TPS/PLA blends were increased because of an increase in fluidity of TPS. When glycerol was replaced by formamide, the temperature corresponding to 5% weight loss ($T_{5\%}$) of TPS decreased due to low boiling point of formamide. After

blending with PLA, the decomposition temperature (T_d) of glycerol based TPS in the blend decreased when compared with pure glycerol based TPS. However, T_d of formamide based TPS in the blend was slightly higher than that pure formamide based TPS. This improvement was ascribed to good compatibility between PLA and TPS. Apparent viscosity of TPS/PLA blends decreased with increasing formamide content. This indicated that formamide which had small size and high polarity penetrated into starch chain and deteriorated starch chain entanglement.

Wang, Yu, Chang, and Ma (2008) studied mechanical, thermal, and rheological properties of TPS/PLA blend and thermoplastic dry starch (DTPS)/PLA blend. TPS was prepared from corn starch, formamide, glycerol, and water. Water content was fixed at 10%wt while the ratios of formamide/glycerol were 0/30, 10/20, 15/15, 20/10, and 30/0%wt. Thermoplastic dry starch (DTPS) was prepared from corn starch, formamide, and glycerol without water. The ratios of formamide/glycerol were 0/40, 10/30, 20/20, 30/10, and 40/0%wt. Corn starch and plasticizer ratio was 100/40%wt. The content of TPS or DTPS was 50%wt. The plasticizers were firstly mixed and then blended with corn starch by using a high speed mixer with a rotating speed of 3000 rpm for 2 min. Then, mixtures were premixed with PLA in a high speed mixer. After that the mixtures were fed into a single screw extruder with a screw speed of 10 rpm. The temperature profile was 130, 140, 150, and 130°C. When glycerol was replaced by formamide, tensile strength of DTPS/PLA blend was similar to that pure PLA while elongation at break was increased. $T_{5\%}$ and apparent viscosities of DTPS/PLA and TPS/PLA blends were decreased with increasing formamide content due to low boiling point of formamide.

Cai, Liu, Wang, Yao, Li, and Xiong (2011) investigated crystallization kinetics of TPS/PLA blends using differential scanning calorimeter (DSC). The analysis based on the Avrami theory indicated that spherulite growth rate, crystallization rate, and activation energy (ΔE_a) of TPS/PLA blends were influenced by the addition of TPS. Crystallization kinetic constant (K) was increased with incorporating TPS into PLA which indicated that TPS acted as a nucleating agent and accelerated crystallization rate of PLA in the blends. ΔE_a of TPS/PLA blends calculated from Arrhenius formula was lower than pure PLA. This was suggested that the addition of TPS into PLA induced the heterogeneous nucleating and improved the crystallization ability of PLA matrix during crystallization processes.

Teixeira, Curvelo, Correa, Marconcini, Glenn, and Mattoso (2012) studied tensile and thermal properties of TPS/PLA blends. Cassava starch and cassava bagasse were used to prepare TPS. Glycerol and water were used as plasticizers. The ratio of starch/glycerol/water was 50/30/20% wt. TPS/PLA blends were prepared using a co-rotating twin screw extruder. The temperature profile was set between 140 and 160°C. When compared with PLA, tensile strength and tensile modulus of TPS/PLA blend were reduced 70% and 51% respectively. However, elongation at break of the blend was increased from 2.6% to 14.5% because TPS had high elongation at break (33.1%). T_g was not affected by incorporating TPS in the blends. Crystallization temperature (T_c) of PLA was decreased with adding TPS due to nucleating effect of TPS on PLA crystallization.

Li, Xiong, Fei, Cai, Xiong, Tan, and Yu (2013) investigated crystallization of TPS/PLA blends by using a differential scanning calorimeter (DSC). TPS/PLA blends were prepared by a stirring kneader at temperature from 175 to 180°C. TPS contents

were 20, 40, 60, 80, and 100%wt. Crystallization enthalpy (ΔH_c) of TPS/PLA blends was higher than pure PLA which indicated that TPS acted as a nucleating agent for PLA. When TPS content was increased ΔH_c of TPS/PLA blends was decreased. This result indicated that TPS hindered the mobility of PLA chains and influenced crystallinity of PLA during the crystallization process. TPS/PLA blends showed different crystallization because of their different contents. TPS could act as a nucleating agent resulting in an improvement of the crystallinity of PLA and constrained the mobility of PLA chain.

2.3 Compatibilization of TPS/PLA blend

The major problem of TPS/PLA blend is poor interfacial adhesion between hydrophilic starch and hydrophobic PLA leading to the blend with poor mechanical properties. The compatibility between TPS and PLA can be enhanced by addition of compatibilizer, PLA modification, and TPS modification.

2.3.1 Addition of compatibilizer

The incompatibility between TPS and PLA resulting from differences in polarity and hydrophilicity of the phases leads to poor mechanical properties of the TPS/PLA blends. The addition of compatibilizer can be used to improve the compatibility of the blends.

Li and Huneault (2008) studied crystallization of TPS/PLA blends. TPS contents were 10, 15, 20, 42%wt. PLA grafted with maleic anhydride (PLA-g-MA) as a compatibilizer was 20%wt. TPS/PLA blends were prepared using a co-rotating twin screw extruder. Starch and plasticizer were supplied in the primary feed hopper. PLA and PLA-g-MA were dry-blended prior to extruder. Then, PLA and PLA-g-MA were fed at mid-extruder. A relatively low extruder temperature of 180°C was used. The

mixture were extruded at a rate of 10hg/h through a 2-strand die. The presence of TPS phase increased the crystallization rate of PLA potentially by playing the role of nucleating agent. Cold crystallization temperature (T_{cc}) of PLA was shifted to higher temperature as the TPS content increased. When PLA-g-MA was added, the crystallization rate of PLA increased due to increased blend interfacial area. SEM micrographs showed fine morphology. TPS phase size was decreased with adding PLA-g-MA. This dispersed phase size reduction was a typical effect of compatibilization and was due to the interfacial tension reduction provided by the presence PLA-g-MA created in situ at the blends interface. The reduction TPS phase size led to an increase of the interfacial area. This may increase the crystallization rate.

Phetwarotai, Potiyaraj, and Aht-Ong (2010) studied the effect of methylenediphenyl diisocyanate (MDI) content and starch type on tensile, thermal, and morphological properties of TPS/PLA blends. Corn and tapioca starch were used. Water and glycerol contents were 10 and 25% wt, respectively. TPS was prepared using a high-speed mixer and then mixed in a two roll mill at a rolling speed of 10 rpm at temperature of 130°C for 10 min until TPS was in homogeneous form. MDI was used as a compatibilizer and its contents were varied as 0.62, 1.25, 2.50, 5, and 10%wt. TPS and PLA (40/60% wt) were mixed using an internal batch mixer at 180°C for 4 min. The rotating speed was 90 rpm. The addition of MDI led to an increase in tensile properties of the blend films. This was due to the improvement of interfacial adhesion between TPS and PLA. The blend film with 1.25%wt of MDI showed the highest tensile properties. At MDI content of 2.50, 5, and 10%wt, defects were generated in the blend films which resulted in a decrease in mechanical properties. This was because MDI could react with TPS resulting in agglomeration of TPS phase which eventually caused

defects and cracks in the blend films. Tensile properties of TPS prepared from corn starch were higher than TPS prepared from tapioca starch. SEM micrographs showed TPS prepared from corn starch showed smaller gaps and holes between TPS and PLA when compared with TPS prepared from tapioca starch. The different types of starch had no effect on T_g and T_m of the blend films. With increasing MDI content, T_g of PLA decreased gradually whereas T_g of TPS phase increased. In other words, these T_g shifts indicated that the interfacial adhesion of two phases was improved with the presence of MDI. SEM micrographs of the blend showed a few gaps and holes between TPS and PLA when MDI was added. This indicated that TPS was well wet by PLA phase.

Yu, Petinakis, Dean, Lin, and Yuan (2011) studied the effect of methylenediphenyl diisocyanate (MDI) as a compatibilizer on mechanical and thermal properties of TPS/PLA blends. Corn starch was plasticized with water at a ratio of 75/25%wt using a twin screw extruder with a screw speed of 120 rpm. The 10 temperature zones from feeder to die were set to 70, 90, 120, 150, 170, 160, 140, 120, 115, and 110°C. TPS was compounded with PLA in a twin screw extruder with a maximum temperature of 180°C. MDI was added into the blends at different stages to control its distribution. For the first stage, MDI was added into starch phase. For the second stage, MDI was added into PLA phase. MDI contents were 0.5 and 1%wt. The addition of MDI improved modulus, tensile strength, and impact strength of the blends. With increasing MDI content, mechanical properties of the blends continuously increased. This was due to a formation of a compatibilizing block copolymer between isocyanate group in MDI and hydroxyl group associated with starch and PLA. When MDI was distributed in the PLA phase, modulus, yield strength, and impact strength of the blend were increased. This was because the isocyanate group in the MDI grafted

polyester reacted with hydroxyl groups in the starch to produce a compatibilizing starch/polyester block copolymer. Mechanical properties of the blend which MDI was distributed in the starch phase were lower than the blend which MDI distributed in PLA phase. This was because MDI distributed in the starch phase resulted in hydrolysis of the ester groups in PLA via the water bound in the TPS. T_g of PLA in the blend was unchanged with the addition of TPS due to phase separation. T_{cc} of PLA in the blends which MDI was distributed in the PLA phase was decreased due to a nucleating effect of starch. T_d of the blend which MDI was distributed in starch phase did not change with the addition of MDI whereas T_d of the blend which MDI was distributed in PLA phase was increased about 5°C due to improved interfacial adhesion between TPS and PLA.

Ferrarezi, Taipina, Silva, and Goncalves (2013) used poly(ethylene glycol) (PEG) as a compatibilizer in TPS/PLA blends. Mechanical, thermal, and morphological properties of the blends were investigated. Cassava starch and glycerol were mixed by using a twin-screw micro-compounder. The chamber temperature was 150°C and a mixing speed was fixed at 50 rpm. TPS/PLA blends were prepared using a twin-screw micro-compounder at a temperature of 170°C and a mixing speed of 100 rpm. PEG content was 25% wt. SEM micrographs of TPS/PLA blend showed large TPS phase size and low adhesion between TPS and PLA. Impact strength of TPS/PLA blend increased with adding PEG while elastic modulus did not change. This suggested that PEG acted as an efficient compatibilizer for TPS/PLA blend by promoting chemical interaction between TPS and PLA as well as acting as physical bridges. Crystallization of PLA was enhanced with incorporating PEG due to plasticizing effect and enhanced interfacial adhesion between TPS and PLA.

Karagoz and Ozkoc (2013) used phenylene diisocyanate (PDI) as a compatibilizer in citric acid (CA) modified TPS/PLA blends. Mechanical, thermal, and morphological properties of the blends were studied. Corn starch, glycerol, and CA were mixed with a co-rotating twin-screw micro-compounder. The temperature was 150°C and the screw speed was 100 rpm. CA contents were 1 and 5% wt. CA modified TPS and PLA were blended using a co-rotating twin-screw micro-compounder at 180°C. The screw speed was 100 rpm. PDI was incorporated into the blends at contents of 0.5, 1, and 2% wt. FTIR results presented that CA interacted with starch and PDI interacted with both starch and PLA through the hydroxyl groups. SEM micrographs revealed that combination of CA and PDI enhanced the distribution of TPS in PLA matrix. Impact strength of CA modified TPS/PLA blends was improved by the addition of PDI. This related to a decrease in TPS phase size. It was known that as the particle size of dispersed phase was reduced, the impact strength of the blends was increased. With increasing CA content, impact strength of the blends increased. The addition of PDI improved tensile strength of CA modified TPS/PLA blend which was attributed to enhanced interfacial adhesion between two phase resulting in the retarded premature crack formation phenomena. With increasing PDI content, tensile strength of the blends slightly increased. Elastic modulus of CA modified TPS/PLA blend was enhanced with incorporating PDI due to possible co-polymerization reaction between TPS and PLA. However, elastic modulus did not change with further increasing PDI content. The change in elastic modulus of the blends was not directly associated with the interfacial interaction since modulus was measured at very low strain where the interfacial adhesion did not play any role, but the modulus depended on the molecular weight of the system. The change in the modulus indicated that molecular weight of the system

increased due to co-polymerization between TPS and PLA. Elongation at break of the blends increased when CA and PDI were added. T_g of PLA in the blends decreased as PDI content was increased resulting a possible urethane linkage to form TPS-g-PLA copolymers and formed at interface between TPS and PLA. T_c of PLA in the blend decreased by increasing PDI content due to the improvement of interfacial interaction with the presence of PDI. T_m of PLA in the blends decreased with the addition of both PDI and CA. With the incorporation of CA into TPS/PLA blend, thermal stability was improved due to enhanced intermolecular interaction between TPS and PLA.

Ping, Kejian, Mingyin, and Meijuan (2013) studied the effect of poly(ethylene glycol) (PEG) as a compatibilizer on mechanical and thermal properties of TPS/PLA blends. TPS/PLA blends at various contents of PGE were dry-blended in a 5 L high intensity kinetic mixer at 3200 rpm. Then, all blends were prepared by using a twin-screw extruder with a screw speed of 330 rpm. The temperatures from feed zone to die zone were 160, 165, 165, 170, and 170°C. The ratio of TPS/PLA blend was fixed at 20/80%wt. PEG contents were 1, 3, and 5% wt. T_g and T_m of TPS/PLA blends were decreased with adding PEG. T_c of TPS/PLA blends were decreased with increasing PEG content due to enhanced chain mobility as the PEG content increased. The distance of double melting peaks of PLA was narrow with increasing PEG up to 3%wt due to enhanced interfacial interaction of the blends. However, the distance of double melting peak became large when PEG content was more than 3%wt due to aggregate of redundant PEG. MFI of TPS/PLA blend was increased with adding PEG due to enhanced plasticization and processability of the TPS/PLA blends. Tensile strength, flexural strength, and impact strength of TPS/PLA blends increased with increasing PEG up to 3%wt due to improved interfacial adhesion between TPS and PLA.

However, mechanical properties were decreased when PEG content was more than 3% wt. At large amount of PEG, the redundant part of PEG penetrated into the inside of TPS particles and broke the internal hydrogen bond resulting in a decrease of the force between TPS molecules.

2.3.2 PLA modification

Currently, a more promising interfacial modification route may come from the modification of polymer matrix itself. This could be obtained by grafting a reactive agent into polymer matrix.

Huneault and Li (2007) studied morphology and mechanical properties of TPS/PLA blends. TPS was prepared from wheat starch, glycerol, and water. Glycerol contents were varied from 30 to 39% wt. TPS contents were varied from 27 to 60% wt. The blends were prepared using a co-rotating twin screw extruder. The first half of the twin-screw extrusion line was used to prepare TPS. Temperature was kept at 130°C. Then, water was removed from TPS by vacuum venting located before mid-extruder. PLA was added at mid-extruder using a single-screw extruder as a side feeder to the twin-screw line at 180°C. Interfacial modification was obtained by free-radical grafting of maleic anhydride (MA) into PLA and then reacted the modified PLA with TPS. The first half of the extruder was kept at 100°C to prevent free-radical initiation prior to MA melting and complete mixing of the component. The next section was kept at 180°C to operate maleation reaction. The modified PLA was pelletized and used in replacement of pure PLA in the TPS/PLA blend. MA content was fixed at 2 % wt. 2,5-dimethyl-2,5-di-(tert-butyperoxy)-hexane (L101) contents were 0.1, 0.25, and 0.5% wt. Tensile modulus of TPS/PLA-g-MA blends decreased with increasing TPS content. However, tensile modulus was unaffected by the interfacial modification. This was because

modulus was measured at low strain before any interfacial de-bonding occurred. The interfacial modification slightly increased tensile properties of the blend. Elongation at break of TPS/PLA-g-MA blend was higher than TPS/PLA blend. TPS/PLA-g-MA blend showed a remarkable improvement of ductility due to enhanced interfacial adhesion between TPS and PLA. High elongation at break was obtained when TPS consisted 36% of glycerol. The compatibilized blends showed a long plastic deformation plateau leading to elongation at break of blends in excess of 150%. TPS/PLA-g-MA blends had fine morphology indicating that interfacial adhesion between TPS and PLA was increased.

2.3.3 TPS modification

The utilization of TPS to tailor biobased and biodegradable PLA blends for applications requires a balance between cost and properties. Alternatively, many starch can be blends with PLA without the used any compatibilizers. To enhance compatibility between the starch and PLA, it is important that chemical structure of starch was modified by partially replacing hydroxyl group of starch with some less hydrophilic functional groups such as ether and ester groups.

Shin, Jo, Kang, Lee, and Kim (2007) studied rheological and morphological properties of chemically modified plasticized starch (CMPS)/PLA blends. Corn starch was reactively modified using maleic anhydride (MA) and plasticized using glycerol. MA was ground to a fine powder and then mixed with starch using a tumber blender for 15 min. The mixture was blended using a twin screw co-rotating extruder. Glycerol was mixed with 2,5-bis((tert-butylperoxide)-2,5-dimethyl hexane (Luperox) and pumped to the extruder using peristaltic pump. The extruder was operated at 150 rpm. Starch/glycerol ratio was 8/2% wt, MA content was 2 phr, and

Luperox was 0.2 phr on basis of the total weight of starch and glycerol. PLA and CMPS were blended using a twin screw co-rotating extruder. The barrel temperature range was 65 to 195°C with a die temperature of 185°C and a screw speed of 150 rpm. CMPS contents were 10, 20, 30, 40, 50, 60, 70, and 80%wt. From SEM micrographs, sphere-shaped CMPS dispersed phase was observed in PLA at low CMPS content. Deformed CMPS phase which extended to complete co-continuous with long rods CMPS phase bridged was occurred with increasing CMPS content. CMPS/PLA blends exhibited Newtonian fluid with power-law index around 0.95. Pseudoplastic fluid was observed with increasing CMPS content and power-law index was about 0.65 to 0.11 indicating the tendency of easy molecular alignment tendency to the flow direction under shear stress.

Zhang, Ran, Zhuang, Yao, and Dong (2009) prepared the blends of PLA and thermoplastic acetylated starch (ATPS). Acetylation is an efficient chemical modification to raise hydrophobicity, thermal stability, and mechanical properties of starch material. Acetylated starch and glycerol were per-mixed with a high speed mixer until a homogeneous material was obtained. The mixture was processed using Haake Rheomix600 batch mixer with a rotor speed of 50 rpm for 8 min. ATPS/PLA blends were mixed using Haake Rheomix600 batch mixer for 8 min. The rotor speed was 50 rpm. ATPS contents were 10, 20, and 40%wt. Mechanical, thermal, and rheological properties were analyzed. For all ATPS/PLA blends, an obvious yield process and stable neck growth cold drawing were observed from stress-strain curves. A transition from brittle fracture of pure PLA to ductile fracture for ATPS/PLA blend was found. With increasing ATPS content, elongation at break and impact strength of ATPS/PLA blends were increased due to compatibility between ATPS and PLA. T_g of PLA in the

ATPS/PLA blends slightly decreased as the content of ATPS was increased. This result indicated that there was some degree of miscibility between ATPS and PLA. T_{cc} of PLA was decreased approximately 15°C indicating an enhancement of crystallization ability of PLA. The incorporation of ATPS gradually shifted down T_m of PLA in the ATPS/PLA blend. Peak of derivative weight of ATPS in the ATPS/PLA blends moved to higher temperature with adding PLA. This suggested that PLA increased the thermal stability of ATPS. Melt elasticity and viscosity of the blends decreased with increasing ATPS content which was favorable to the processing properties of PLA.

Wootthikanokkhan, Wongta, Sombatsompop, Kositchaiyong, Wong-On, Isarankura na Ayutthaya, and Kaabbuathong (2012) studied the effect of chemical modification and blending time on mechanical, thermal, rheological, and morphological properties of TPS/PLA blends. TPS was modified to be maleated thermoplastic starch (MTPS). MTPS was obtained by blending cassava starch, glycerol, and maleic anhydride. MTPS contents were 20, 30, and 40%wt. MTPS/PLA blends were prepared using an internal mixer with a rotor speed of 40 rpm. The temperature was 190°C. The mixing time was 12 min. Tensile strength and modulus of MTPS/PLA blends were increased with increasing blending time whereas elongation at break and tensile toughness were decreased. Viscosity of the blends was decreased when blending time increased due to chain scission of polymer during process. T_g of MTPS/PLA blends was higher when compared to pure PLA. This could be attributed to the presence of some bulky PLA-g-MTPS molecules produced from trans-esterification between MTPS and PLA during blending. SEM micrographs revealed that MTPS/PLA blends were immiscible. Various sizes of starch particles were dispersed in a continuous PLA matrix. This morphology corresponded to a decrease in of tensile properties of the

blends. Phase separation between TPS and PLA insignificantly changed when blending time was increased. This suggested that the changes in tensile properties of the blends with blending time were predominated by the effect of chain scission. Moreover, elongation at break and tensile toughness of MTPS/PLA blends were higher than TPS/PLA blend whereas tensile strength and modulus were lower.

Shin, Jang, and Kim (2011) investigated mechanical, thermal, biodegradability, and morphological properties of chemical modified thermoplastic starch (CMPS)/PLA blends. FTIR result was used to confirm interaction between CMPS and PLA. CPMS was obtained from corn starch, MA, and glycerol using a twin-screw micro-compounder. The extruder was processed at the temperature range from 65 to 155°C with a screw speed of 150 rpm. CPMS/PLA blends were prepared by using a twin-screw micro-compounder with temperature range from 65 to 185°C. The screw speed was fixed at 150 rpm. The contents of CPMS were varied from 10 to 80%wt. FTIR results revealed that the interfacial adhesion between CMPS and PLA was improved by PLA-g-starch which formed at interface through a transesterification reaction between CMPS and PLA. SEM micrograph showed CMPS dispersed phase size did not vary too much when CMPS content was up to 30%wt whereas the number of CMPS phases was increased with increasing CMPS content. In addition, when CMPS content was up to 40%wt, CMPS dispersed sizes were increased and CMPS became aggregated. This indicated the beginning of the phase inversion phenomenon. Tensile strength and elongation at break of the blends reduced with increasing CPMS content while modulus insignificantly changed. Biodegradability of the blends increased with increasing CPMS content. A single melting peak of the blends was observed when CPMS content was less than 30%wt. On the other hand, a double

melting peak was shown as CMPS content was higher than 40% wt. This was attributed to slow crystallization kinetics of PLA and partial melting followed by recrystallization of molecules during DSC scan. Moreover, crystallinity of PLA was increased with the incorporation of CPMS due to nucleating effect of CMPS. However, at CPMS content more than 50% wt, the crystallinity of the blends decreased. This was because CMPS phase was not expected to exert an effective nucleating effect on PLA.

2.4 Toughness improvement of TPS/PLA blend

Toughness of TPS/PLA blends is still not enough for some applications. TPS/PLA blends is brittle. Blending TPS/PLA blend with flexible polymers provides a new material with excellent integrated performance.

Sarazin, Li, Orts, and Favis (2008) investigated physical and morphological properties of TPS/PLA/polycaprolactone (PCL) ternary blends. TPS was prepared from wheat starch/glycerol/water at ratios of 48.5/28.15/23.35% wt for TPS36 and 48.5/15.65/35.85% wt for TPS24. The extrusion system was composed of a single screw connected to a co-rotating extruder. The starch/water/glycerol suspension was fed in the first zone of the twin screw extruder set at 150 rpm, while PLA was fed in single screw extruder. After gelatinization of starch followed by extraction of the volatiles, TPS was mix with molten PLA on the twin screw extruder. The temperature of in the zones crossed by PLA was set at 150°C. The ratio of TPS/PLA/PCL ternary blend was 50/40/10% wt. The morphology analysis of the ternary blend showed a substantial number of fine dispersed particles in the system. PCL formed disperse phase in PLA. The addition 10% wt of PCL into TPS/PLA blend resulted in a significant increase in strain at break and notched Izod impact energy but a decrease in elastic modulus and maximum strength due to ductile behavior of TPS and PCL.

Ren, Fu, Ren, and Yuan (2009) prepared ternary blends of TPS, PLA, and poly(butylenesadipate-co-terephthalate) (PBAT). Maleic anhydride (MA) was used to improve the compatibility of the blends and its content was fixed at 1%wt. TPS was prepared from corn starch and glycerol using a high speed mixer at 2880 rpm. The ratio of starch/glycerol was 80/20%wt. The mixing temperature was kept at 120°C for 20 min. TPS/PLA binary blends and TPS/PLA/PBAT ternary blends were prepared by a twin screw extruder with a temperature profile of 155 to 175°C and a rotating speed of 80 rpm. TPS content was fixed at 50%wt. PBAT contents were 10, 20, 30, and 40%wt. With increasing PBAT content, elongation at break of the blends was remarkably increased but tensile strength, flexural strength, and flexural modulus were decreased. The compatibilized blends exhibited higher tensile and flexural properties when compared with the uncompatibilized blend due to improved interfacial adhesion between the blend components.

Li and Huneault (2011) used epoxy-acrylic-styrene copolymer as a chain extender to increase toughness of TPS/PLA blends. PLA-g-MA was used as a compatibilizer in the blends. TPS/PLA blends were prepared using a co-rotating twin screw extruder. Sorbitol, glycerol, and water were used as plasticizers for TPS preparation. The first haft of the extruder was used to prepare TPS at a temperature of 140°C. Wheat starch and sorbitol were fed in a dry powder form. Then, glycerol and water were added to starch through the plasticizer injection port. The water/glycerol ratio was kept at 0.1/1%wt. After that water was removed by devolatilization in subsequent extruder portion to obtain a TPS. The plasticizer content in TPS was fixed at 36%wt. TPS and PLA were mixed in the second part of extruder at a temperature of 180°C and a rotating speed of 100 rpm. TPS content was kept at 27%wt. In case of

compatibilized blends, 20% wt of PLA was substituted by PLA-g-MA. Chain extender contents were various as 0.5, 1, 2, and 5% wt. PLA-g-MA and/or chain extender were dry-blended with PLA before extrusion. Tensile and rheological properties were investigated. The addition of chain extender and PLA-g-MA into TPS/PLA blend dramatically increased elongation at break which related to ability of the material to deform through a necking mechanism after yield point. The incorporation of the chain extender decreased melting enthalpy progressively. When 2% wt of chain extender was added into TPS/PLA blend, the viscosity was increased. This indicated that the length of polymer chain was increased and the mobility of chain was difficult. The combination of interfacial modification and chain extender strategies led to greatly improved ductility. This was probably because of the improvement of PLA molecular weight and chain entanglement at the interface, which improved the stress transfer between PLA and TPS phase.

Shi, Chen, Gao, Jiao, Xu, and Guo (2011) studied mechanical, thermal, and morphological properties of TPS/PLA/glycidyl methacrylate grafted poly(ethylene octane) (GPOE) ternary blends. GPOE acted as a flexible polymer which played an important role in improving interfacial adhesion and toughness. TPS was prepared from corn starch and 20% wt of glycerol using an internal mixer with a temperature of 120°C and a rotating speed of 60 rpm for 10 min. TPS contents were 0, 10, 20, 30, 40, and 50 %wt. GPOE contents were 0, 5, 10, 15, and 20%wt. The blends were mixed using an internal mixer with a temperature of 180°C and a rotating speed of 60 rpm for 10 min. With the addition of GPOE, elongation at break and impact strength of the ternary blends were greatly increased but tensile strength was decreased due to the effect of the rubbery nature of GPOE. With increasing TPS content, tensile strength of the blends

was decreased. Elongation at break of the blend increased with adding 10%wt of TPS. However, at TPS content higher than 10% wt, elongation at break of the blend decreased due to phase separation of TPS and PLA. Adding GPOE decreased T_g of all blends. This indicated that epoxy groups of GPOE could react with carboxyl or hydroxyl group of PLA and TPS which enhanced the compatibility between the blend components. GPOE reduced TPS phase size and improved the compatibility of the blends. Comparing to TPS/PLA binary blends, TPS/PLA/GPOE ternary blends had higher water uptake and need a long time to equilibrate.

Yokesahachart and Yoksan (2011) used amphiphilic molecules such as tween 60, linoleic acid, and zein, as additives for TPS in TPS/PLA blends. The addition of amphiphilic molecules resulted in: (i) improved plasticization and processability, (ii) enhanced extensibility, (iii) increased crystallinity, and (iv) decreased stiffness of the material. Cassava starch and mung bean starch were mixed in a ribbon mixer with at weight ratio of 70/30%wt. Glycerol and water at ratio of 3/1%wt were used as a plasticizer. The starch mixture and plasticizers were fed into a twin screw extruder. The barrel temperature was set in range from 70 to 120°C. Amphiphiles at content of 1.55%wt were blended with TPS at the same condition for preparing TPS. TPS and PLA were blended in a twin screw extruder with temperature range from 130 to 160°C. TPS content were varied as 30, 50, and 70%wt. The addition of amphiphiles resulted in improved plasticization, processability, and extensibility of TPS but decreased stiffness. In addition, the incorporation of amphiphiles improved extensibility, flowability, and processability of TPS/PLA blends. The type of amphiphiles also affected tensile and rheological properties of TPS/PLA blends. Tween 60 and linoleic acid provided more extensible blends than zein whereas zein led to strong and rigid

blend. Moreover, tween 60 and linoleic acid enhanced more flowability of the blends when compared with zein.



CHAPTER III

EXPERIMENTAL

3.1 Materials

Poly(lactic acid) (PLA, 4043D) was supplied from Natural Works LLC. Poly(butylene adipate-co-terephthalate) (PBAT, Ecoflex FBX 7011) was obtained from BASF Co., Ltd. Maleic anhydride monomer (MA monomer, AR grade) and 2,5-bis(tert-butylproxy)-2,5 dimethylhexane (Luperox101, AR grade) were supplied from Sigma-Aldrich. Cassava starch was purchased from Bangkok Interfood Co., Ltd. Glycerol was supplied from Carlo Erba Reagenti Co., Ltd. Epoxidized natural rubber with 50% epoxidation (ENR50) was purchased from Muang Mai Guthrie Co., Ltd.

3.2 Experimental

3.2.1 Preparation of thermoplastic starch

Thermoplastic starch (TPS) was prepared using an internal mixer (Hakke Rheomix, 3000P). TPS was obtained from cassava starch and glycerol at a ratio of 70/30% wt. Cassava starch was dried at 70°C for 4 h. The mixing temperature was kept at 120°C and the rotor speed was 60 rpm. The mixing time was 10 min. The test specimens were prepared by a compression molding machine (Labtech, LP20-B) at the temperature of 120°C and the pressure of 100 MPa.

3.2.2 Preparation and characterization of poly(lactic acid) grafted with maleic anhydride

Poly(lactic acid) grafted with maleic anhydride (PLA-g-MA) was prepared using an internal mixer (Haake Rheomix, 3000P) at 170°C for 10 min. The rotor speed was 50 rpm. PLA was dried at 70°C for 4 h before mixing. Maleic anhydride and 2,5-bis(tert-butylproxy)-2,5 dimethylhexane were 5.0 and 1.0% wt, respectively (Teamsinsungvon, 2011).

3.2.2.1 Determination of maleic anhydride content

Maleic anhydride on PLA was determined by a titration of acid groups derived from anhydride functions using phenolphthalein as an indicator. Sample was dissolved in chloroform and precipitated with methanol to remove residual MA and initiator. After that, the grafted PLA was accurately weighed and completely dissolved in chloroform:methanol (80/20%v). Then, it was titrated with 0.025 mol/l potassium hydroxide solution (KOH). The acid number and the graft content (%G) were calculated using Equation (3.1) and Equation (3.2), respectively. Pure PLA without MA was also titrated under the same condition to obtain blank values (Wu, 2003)

$$\text{Acid number (mg KOH/g)} = \frac{V_{\text{KOH}}(\text{ml}) \times N_{\text{KOH}}(\text{M})}{\text{sample (g)}} \times 56.1 \quad (3.1)$$

$$\%G = \frac{(\text{Acid number} - M_0)}{2 \times 56.1} \times 98.06 \quad (3.2)$$

Where M is morality (mol/l), V is the volume (ml), and M_0 is the blank titration value of pure PLA. 98.06 is molecular weight of MA.

3.2.2.2 Fourier transform infrared spectroscopy

Infrared spectrum of PLA-g-MA was characterized by a Fourier transform infrared spectrometer (FTIR, Bruker/Tenser27) using attenuated total reflectance (ATR) equipped with platinum diamond crystal (TYPE A225/QL). The spectrum was recorded in a wavenumber range from 4000 to 600 cm^{-1} with a resolution of 4 cm^{-1} and a number of scan of 32.

3.2.3 Preparation of TPS/PLA blends

TPS/PLA blends were prepared using an internal mixer (Hakke Rheomix, 3000P). TPS contents were 10, 20, 30, 40, and 50%wt. TPS and PLA were dried at 70°C for 4 h before blending. The mixing temperature was 170°C and the rotor speed was 60 rpm. The mixing time was 10 min. The test specimens were processed by a compression molding machine (Labtech, LP20-B) at the temperature of 170°C and the pressure of 100 MPa. Furthermore, TPS/PLA blend giving the optimum mechanical properties was selected to study the effect of compatibilizer content on mechanical, thermal, and morphological properties of TPS/PLA blends.

In cases of compatibilized TPS/PLA blends, PLA-g-MA was used as a compatibilizer and its contents were 3, 5, and 7 phr. TPS and PLA were dried at 70°C for 4 h before blending. The compatibilized TPS/PLA blends were mixed using an internal mixer (Hakke Rheomix, 3000P). The temperature was 170°C and the rotor speed was 60 rpm. The mixing time was 10 min. The test specimens were processed by a compression molding machine (Labtech, LP20-B) at the temperature of 170°C and the pressure of 100 MPa. In addition, the compatibilized TPS/PLA blend giving the optimum mechanical properties was chosen to study the effect of PBAT and ENR50 content on the properties of the compatibilized TPS/PLA blends.

3.2.4 Preparation of TPS/PLA/PBAT blends and TPS/PLA/ENR50 blends

PBAT or ENR50 was added into the compatibilized TPS/PLA blend at 10, 20, and 30%wt. TPS, PLA, and PBAT were dried at 70°C for 4 h before blending. Then, TPS/PLA/PBAT blends and TPS/PLA/ENR50 blends were prepared using an internal mixer (Hakke Rheomix, 3000P) at the temperature of 170°C and the rotor speed of 60 rpm. The mixing time was kept at 10 min. The test specimens were prepared using a compression molding machine (Labtech, LP20-B) at 170°C and the pressure of 100 MPa.

3.2.5 Characterization of TPS, PLA, TPS/PLA blends, compatibilized TPS/PLA blends, compatibilized TPS/PLA/PBAT blends, and compatibilized TPS/PLA/ENR50 blends

3.2.5.1 Mechanical properties

Tensile properties of TPS, PLA, TPS/PLA blends, compatibilized TPS/PLA blends, compatibilized TPS/PLA/PBAT blends, and compatibilized TPS/PLA/ENR50 blends were tested according to ASTM D638 using a universal testing machine (Instron, 5565) with a load cell of 5 kN and a crosshead speed of 5 mm/min.

Impact test of TPS, PLA, TPS/PLA blends, compatibilized TPS/PLA blends, compatibilized TPS/PLA/PBAT blends, and compatibilized TPS/PLA/ENR50 blends was performed according to ASTM D256 using an impact testing machine (Atlas, BPI). A pendulum of 2.7 J was chosen.

3.2.5.2 Thermal properties

Thermal properties of TPS, PLA, TPS/PLA blends, compatibilized TPS/PLA blends, compatibilized TPS/PLA/PBAT blends, and compatibilized TPS/PLA/ENR50 blends were tested using a differential scanning calorimeter (NETZSCH, DSC 204F1). All samples were heated from 25 to 200°C with the heating rate of 5°C/min and kept isothermal for 5 min under nitrogen atmosphere to delete previous thermal history. After that, the specimens were cooled to -50°C with the cooling rate of 5°C/min and heated again to 200°C with the heating rate of 5°C/min (2nd heating scan). The degree of crystallinity of PLA (χ_c) was calculated using the following equation:

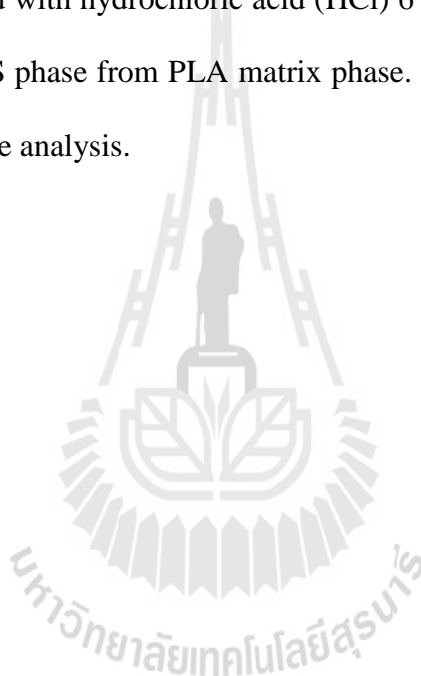
$$\chi_c = \frac{\Delta H_m}{W_f \times \Delta H_m^0} \times 100\% \quad (3.3)$$

Where ΔH_m is the enthalpy of fusion during the heating. ΔH_m^0 is the enthalpy for 100% crystalline PLA homopolymer (93.7 J/g) (Garlotta, (2001)), and W_f is the weight fraction of PLA component in blends.

Thermogravimetric analysis of TPS, PLA, TPS/PLA blends, compatibilized TPS/PLA blends, compatibilized TPS/PLA/PBAT blends, and compatibilized TPS/PLA/ENR50 blends was analyzed using a thermogravimetric analyzer (Perkin Elmer, SDT 2960). Thermal decomposition was examined under nitrogen atmosphere. The weight of specimens between 5 to 10 mg was used. The specimen was heated from room temperature to 600°C with the heating rate of 10°C/min.

3.2.5.3 Morphological properties

Morphological properties of freeze-fractured surfaces and tensile fractured surface of PLA, TPS/PLA blends, compatibilized TPS/PLA blends, compatibilized TPS/PLA/PBAT blends, and compatibilized TPS/PLA/ENR50 blends were performed by a scanning electron microscope (JEOL, JSM-6010LV). Acceleration voltage of 10 kV was used to collect SEM images of the samples. The specimens were etched with hydrochloric acid (HCl) 6 M at room temperature for 3 h in order to extract TPS phase from PLA matrix phase. After that, the specimens were coated with gold before analysis.



CHAPTER IV

RESULTS AND DISCUSSION

4.1 Characterization of poly(lactic acid) grafted with maleic anhydride (PLA-g-MA)

4.1.1 Identification of PLA-g-MA and determination of graft content

PLA-g-MA was obtained by melt grafting using an internal mixer. Fourier transform infrared spectrophotometer (FTIR) was used to identify the grafting reaction of PLA-g-MA. FTIR spectra of MA, PLA, and PLA-g-MA are shown in Figure 4.1. Succinic anhydride exhibited an intensive absorption band near 1780 cm^{-1} and a weak band near 1850 cm^{-1} due to symmetric and asymmetric stretch of C=O (John, Tang, Yang, and Bhattacharya, (1997); Mani, Bhattacharya, and Tang, (1999)). The absorption at 1780 cm^{-1} was weak and might be overlapped with the carbonyl peak of PLA which was much stronger as shown in Figure 4.1. So, the second derivative of FTIR spectra were used for improving resolution of strongly overlapping peaks.

The second derivative FTIR spectra of MA, PLA, and PLA-g-MA are shown in Figure 4.2. PLA-g-MA spectrum showed the absorption at 1780 cm^{-1} corresponding to the symmetric stretch of C=O of the cyclic anhydride groups absorption (Tserki, Matzinos, and Panayiotou, (2006)). Moreover, the absorption at 1850 cm^{-1} was occurred as a small peak in PLA-g-MA spectrum which indicated the asymmetric stretch of C=O of cyclic anhydride groups. This result confirmed that MA was grafted onto PLA.

Graft content of MA onto PLA was determined by a titration of acid groups derived from anhydride functions using phenolphthalein as an indicator. The graft content of PLA-g-MA achieved from 1.0% wt Luperox101 and 5.0% wt MA was 0.86%. This PLA-g-MA was used as a compatibilizer in this study.

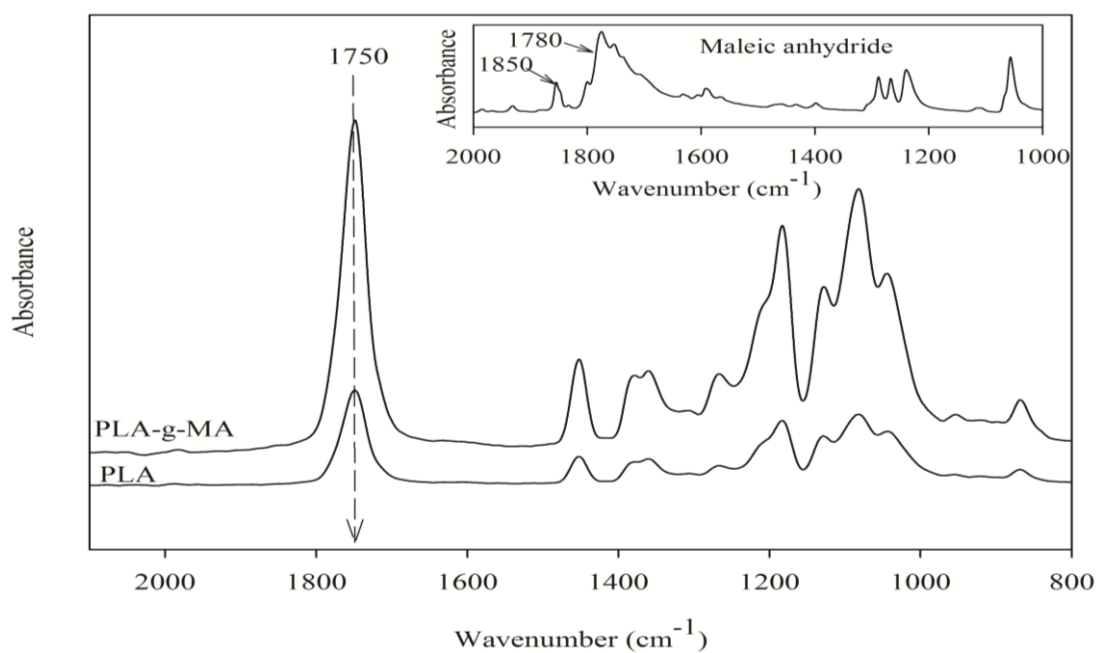


Figure 4.1 FTIR spectra of MA, PLA, and PLA-g-MA at 1.0% wt Luperox101 and 5.0% wt MA.

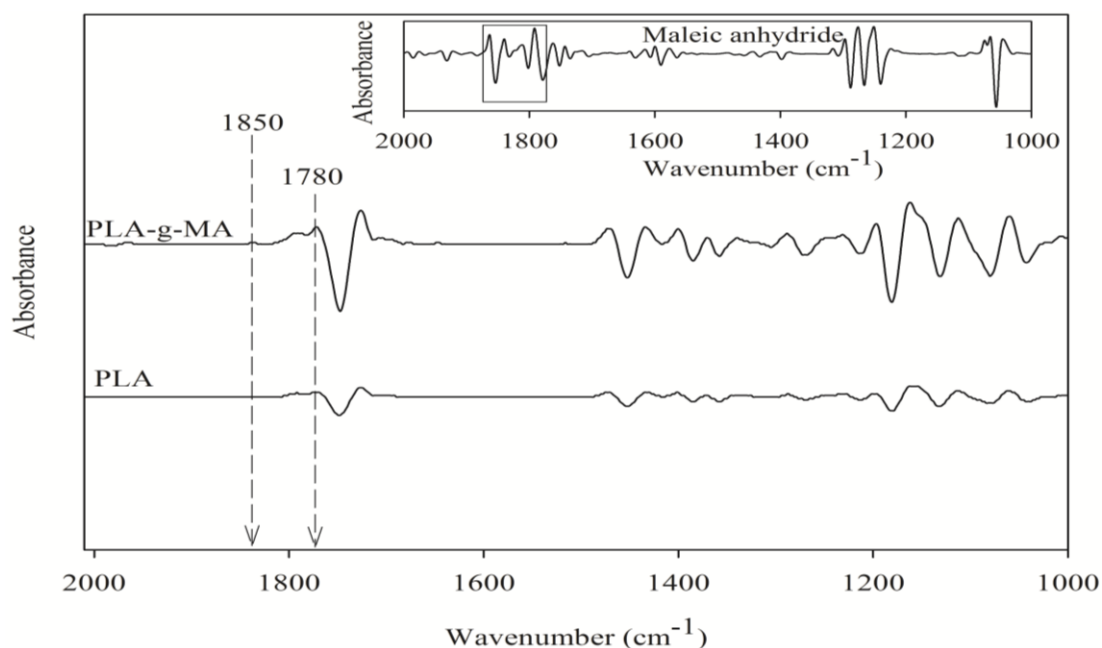


Figure 4.2 FTIR second derivative spectra of MA, PLA, and PLA-g-MA at 1.0% wt Luperox101 and 5.0% wt MA.

On the basis of the evidence from FTIR, the probable mechanism for the grafting reaction was suggested in Figure 4.3. The reaction started with the homolytical scission of organic peroxide. This was followed by the hydrogen abstraction of the α -carbon atom of the ester carbonyl group and resulted in the formation of a polyester macroradical. After that, a single molecule of MA might graft onto the macroradical (Mani, Bhattacharya, and Tang, (1999)).

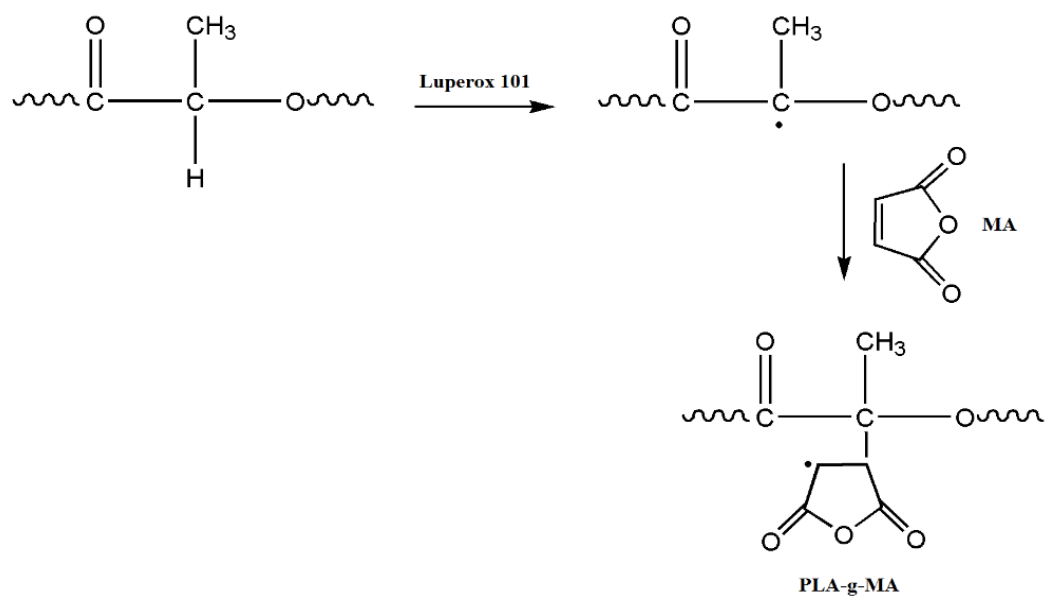
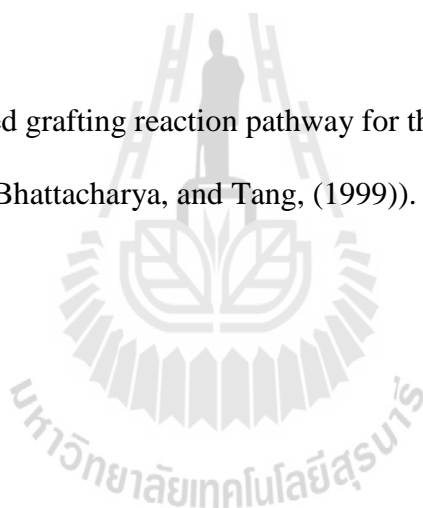


Figure 4.3 Proposed grafting reaction pathway for the reaction of MA on PLA (Mani, Bhattacharya, and Tang, (1999)).



4.2 Effect of blend composition on properties of TPS/PLA blends

4.2.1 Mechanical properties

Mechanical properties of PLA, TPS, and TPS/PLA blends at various TPS contents are listed in Table 4.1. Tensile strength, tensile modulus, and elongation at break of PLA, TPS, and TPS/PLA blends are shown in Figure 4.4, Figure 4.5, and Figure 4.6, respectively. PLA demonstrated high tensile modulus, high tensile strength, but low elongation at break. Tensile strength and tensile modulus of PLA decreased with adding 10%wt TPS because TPS had lower tensile strength and tensile modulus than pure PLA whereas elongation at break of PLA increased. This suggested that the presence of TPS led to ductile behavior (Leadprathom, Suttiruengwong, Threepopnatkul, and Seadan, (2010); Ferrarezi, Taipina, Silva, and Goncalves, (2013)). With increasing TPS content, tensile properties of the blends were decreased due to poor interfacial adhesion between TPS and PLA (Schwach, Six, and Averous, (2008); Wootthikanokkhan et al., (2012); Wang, Yu, Chang, and Ma, (2008); Leadprathom, Suttiruengwong, Threepopnatkul, and Seadan, (2010)).

Impact strength of PLA and TPS/PLA blends is shown in Figure 4.7. TPS did not break under testing condition. Impact strength of PLA was reduced with adding 10%wt TPS due to incompatibility between TPS and PLA (Martin and Averous, (2001)). Moreover, impact strength of the TPS/PLA blends was continuously decreased with further increasing TPS content due to coalescence of TPS phase in the blend as shown in Figure 4.8(b-f). The TPS dispersed phase could act as stress concentrator in the blends resulting in decreased impact strength. Sarazin, Orts, and Favis, (2008) also found that impact strength of TPS/PLA blends was decreased with increasing TPS content.

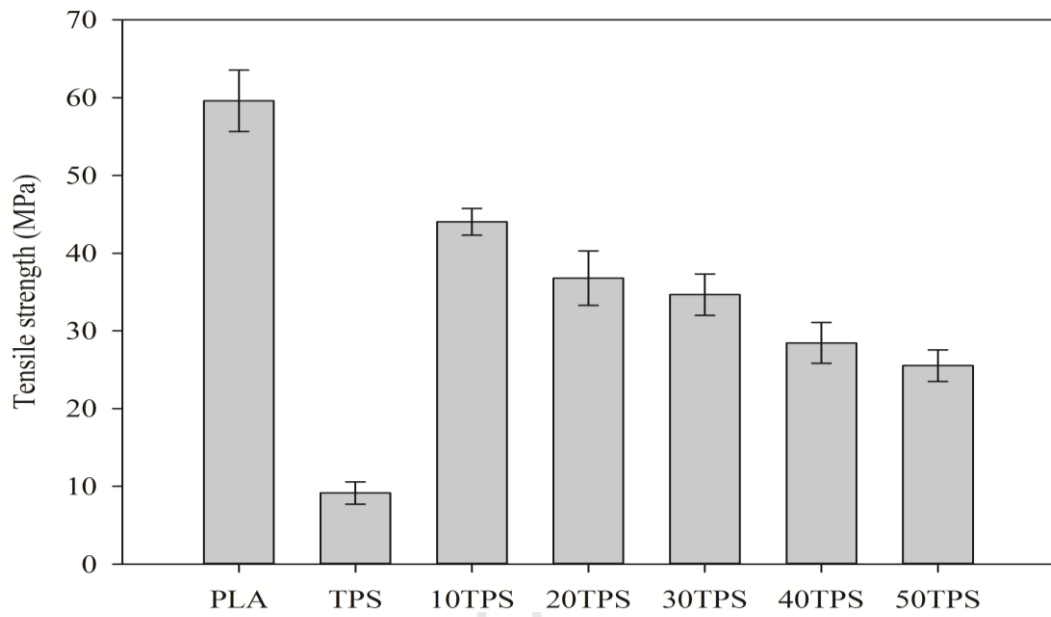


Figure 4.4 Tensile strength of PLA, TPS, and TPS/PLA blends at various TPS contents.

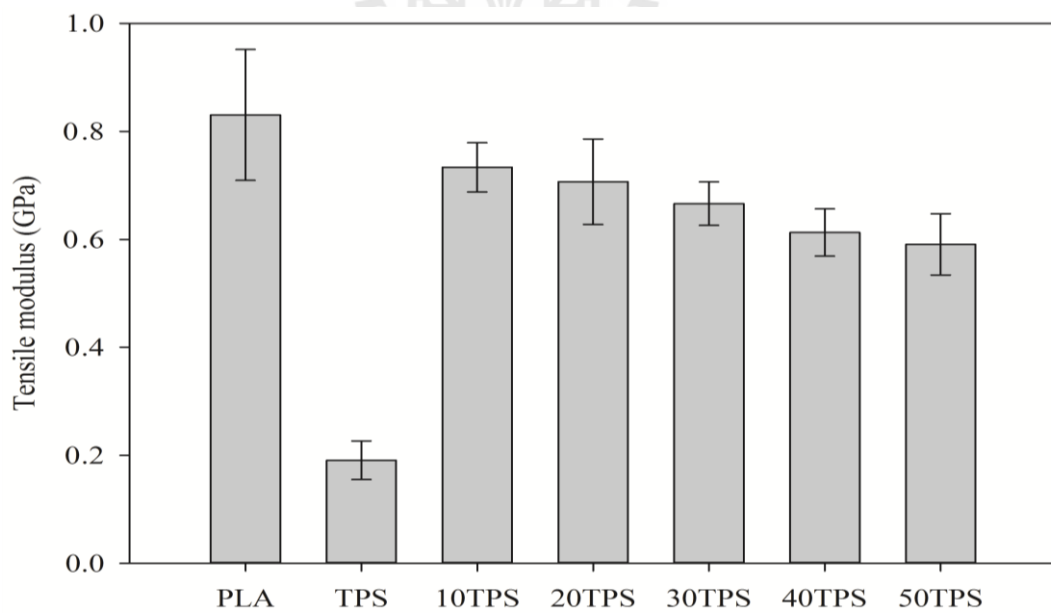


Figure 4.5 Tensile modulus of PLA, TPS, and TPS/PLA blends at various TPS contents.

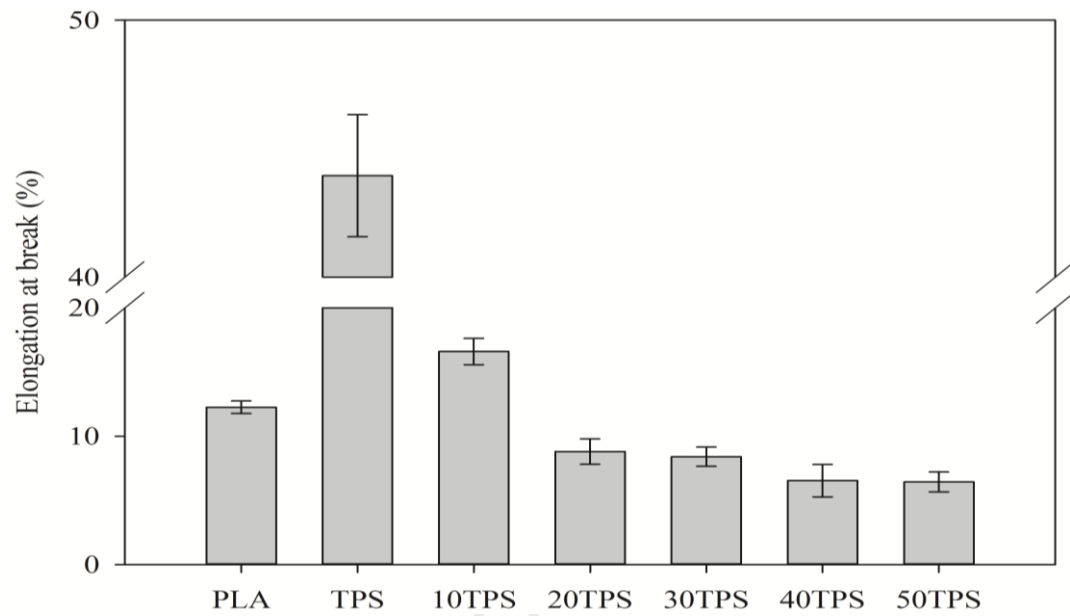


Figure 4.6 Elongation at break of PLA, TPS, and TPS/PLA blends at various TPS contents.

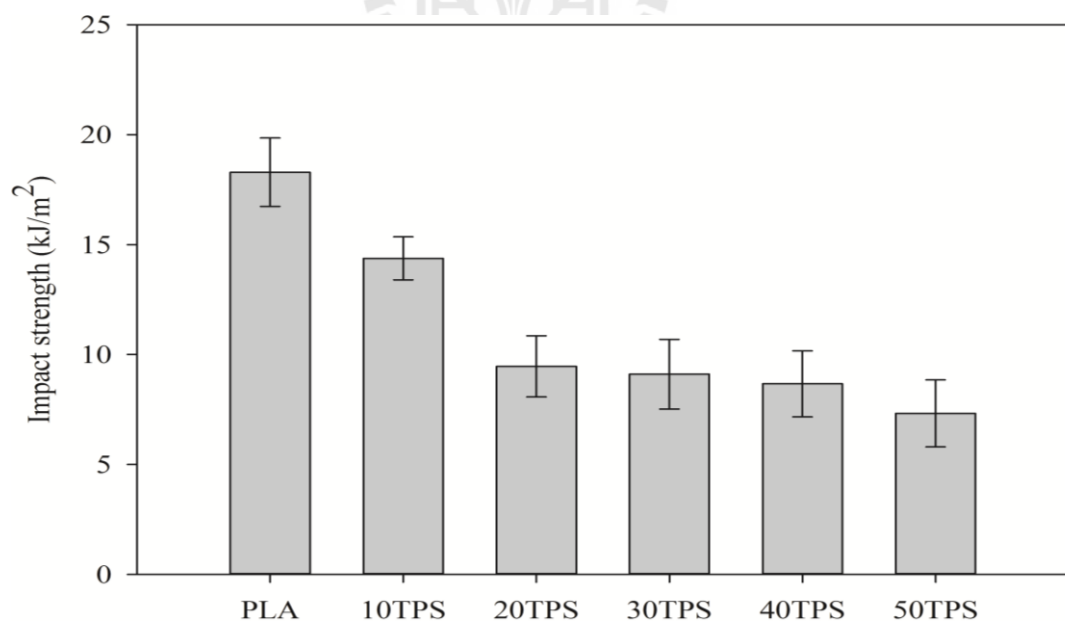


Figure 4.7 Impact strength of PLA and TPS/PLA blends at various TPS contents.

Table 4.1 Mechanical properties of PLA, TPS, and TPS/PLA blends at various TPS contents.

Composition (%wt)	Tensile strength (MPa)	Tensile modulus (GPa)	Elongation at break (%)	Impact strength (kJ/m²)
PLA	59.59±3.95	0.83±0.12	12.25±0.48	18.29±1.56
TPS	9.15±1.43	0.19±0.04	43.95±2.37	NB
TPS/PLA (10/90)	44.03±1.72	0.73±0.05	16.59±1.02	14.37±0.98
TPS/PLA (20/80)	36.79±3.51	0.71±0.08	8.80±0.99	9.45±1.39
TPS/PLA (30/70)	34.66±2.67	0.67±0.04	8.40±0.75	9.10±1.58
TPS/PLA (40/60)	28.45±2.61	0.61±0.04	6.54±1.26	8.67±1.50
TPS/PLA (50/50)	25.53±2.03	0.59±0.06	6.44±0.77	7.32±1.52

Note: NB = Not broken

4.2.2 Morphological properties

SEM micrographs of the freeze fractured surface of PLA and TPS/PLA blends at various TPS contents are shown in Figure 4.8. TPS/PLA blends were etched by 6 M HCl solution by wiping out TPS in PLA matrix. The smooth fractured surface was demonstrated on surface of PLA as shown in Figure 4.8(a). From Figure 4.8(b) – (f), separated coarse phase of TPS was shown in PLA matrix phase. This indicated that PLA and TPS were immiscible. The incompatibility between TPS and PLA led to poor mechanical properties of the blend. When TPS content was increased, TPS phase size was increased due to coalescence of TPS phase. Wootthikanokkhan et al., (2012) reported that with increasing TPS content, phase separation between TPS and PLA was more noticeable. This morphology well corresponded with the mechanical properties of the blends.

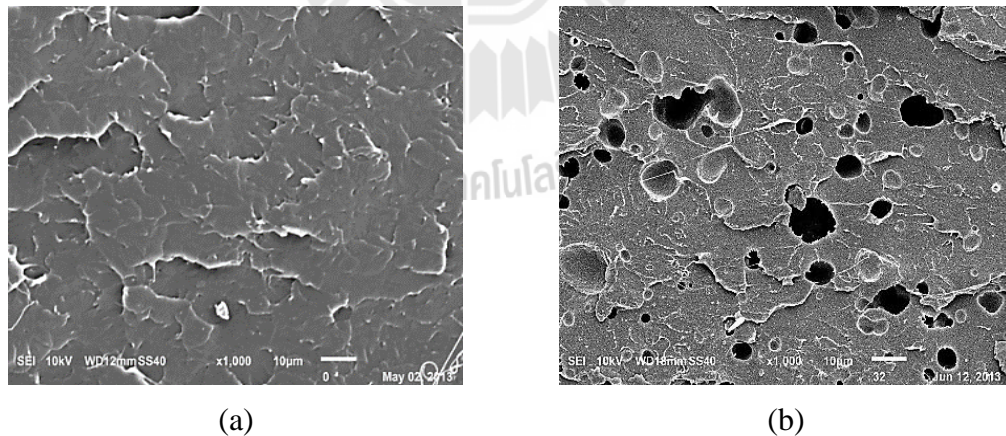


Figure 4.8 SEM micrographs of the freeze fractured surface at 1000x magnification of (a) PLA, (b) TPS/PLA 10/90 blend, (c) TPS/PLA 20/80 blend, (d) TPS/PLA 30/70 blend, (e) TPS/PLA 40/60 blend, and (f) TPS/PLA 50/50 blend.

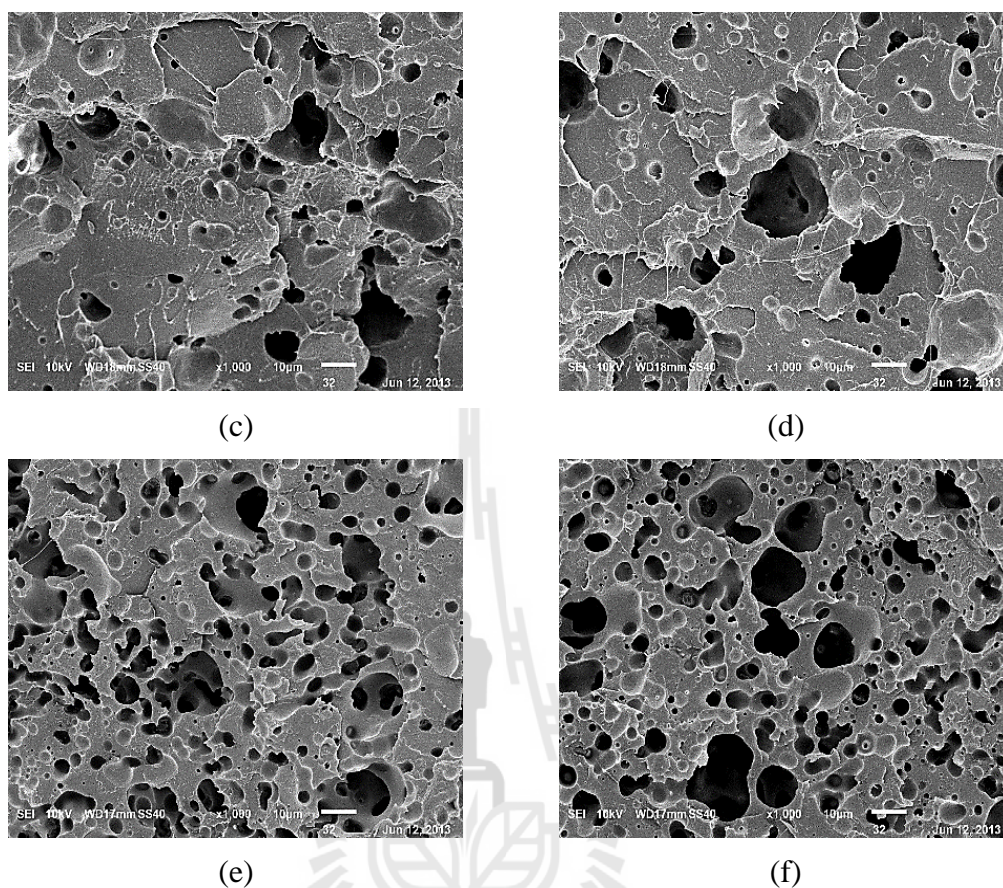


Figure 4.8 SEM micrographs of the freeze fractured surface at 1000x magnification of (a) PLA, (b) TPS/PLA 10/90 blend, (c) TPS/PLA 20/80 blend, (d) TPS/PLA 30/70 blend, (e) TPS/PLA 40/60 blend, and (f) TPS/PLA 50/50 blend (continued).

4.2.3 Thermal properties

DSC thermograms of PLA, TPS, and TPS/PLA blends are shown in Figure 4.9. The second heating curves of melt samples were chosen in order to remove previous thermal history. Thermal properties of PLA and TPS/PLA blends at various TPS contents are presented in Table 4.2. There was no discernible change of

the thermogram of TPS since thermal signal of TPS was weaker than conventional polymers (Yu, Petinakis, Dean, Liu, and Yuan, (2011)). Moreover, TPS behaved rather as an amorphous material almost without any crystal and melting peak (Yu and Christie, (2001)). Glass transition temperature (T_g), cold crystallization temperature (T_{cc}), and double melting temperature (T_{m1} , T_{m2}) of pure PLA were observed at 54.3, 99.5, 144.9, and 154.6°C, respectively. The double melting temperature of pure PLA indicated that small and imperfect crystals changed successively into more stable crystals through the melt-recrystallization mechanism (Yasuniwa, Tsubakihara, Sugimoto, and Nakafuku, (2004)).

With incorporating 10%wt TPS into PLA, T_g and T_m of PLA in TPS/PLA blends decreased due to some degree of miscibility between the blend components (Martin and Averous, (2001); Shi et al., 2010). Moreover, T_{cc} of PLA in TPS/PLA blends was lower than pure PLA due to nucleating effect of TPS (Li et al., (2011)). Heat of crystallinity (ΔH_c) and heat of fusion (ΔH_m), and degree of crystallinity (χ_c) of TPS/PLA blends were higher than pure PLA. This suggested that TPS acted as a nucleating agent in PLA (Park, Im, Kim, and Kim (2000); Li et al., (2013); Ke and Sun, (2003); Xiong et al., (2013)). Shin, Jang, and Kim, (2011) found that in PLA/chemical modified plasticized starch (CMPS) blends with high crystallinity, the dispersed CMPS phases acted as nucleating agent enhancing crystallization of PLA.

T_g of PLA in the blends insignificantly changed with increasing TPS content. Yu, Petinakis, Dean, Liu, and Yuan, (2011) also found that T_g of PLA in the TPS/PLA blends did not change with increasing TPS content. TPS content had no effect on T_m of PLA in the blends. However, T_{cc} was slightly decreased when TPS content was increased. ΔH_c and ΔH_m of PLA in the blends were reduced when TPS

content was increased. χ_c of PLA in the blends was slightly increased with increasing TPS content due to nucleating effect of TPS (Park and Im, (2000); Li and Huneault, (2011); Oza, Thompson, Hrymak, and Liu, (2012)). With increasing TPS content, the size of TPS phases were much larger due to coalescence of TPS phases. The larger TPS phases were known to be less effective nucleating agents compared to smaller particles (Shin, Jang, and Kim, (2011)). Park, Im, Kim, and Kim (2000) also reported that a decrease in the nucleating effect of TPS was because the TPS phases size was large.

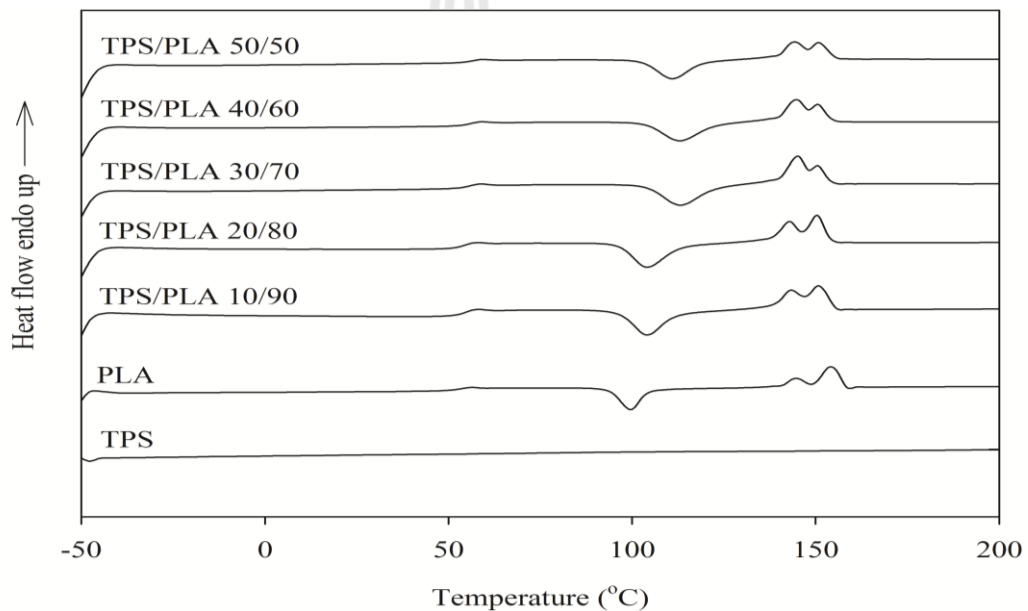


Figure 4.9 DSC thermograms of PLA, TPS, TPS/PLA blends at various TPS contents (the second heating, heating rate 5°C/min).

Table 4.2 Thermal characteristics of PLA and TPS/PLA blends at various TPS contents.

Composition (%wt)	T_g (°C)	T_{cc} (°C)	T_{m1} (°C)	T_{m2} (°C)	ΔH_c (J/g)	ΔH_m (J/g)	χ_c (%)
PLA	54.3	99.5	144.9	154.6	35.33	32.91	35.12
TPS/PLA (10/90)	50.7	93.1	139.5	150.4	37.38	40.16	47.62
TPS/PLA (20/80)	50.2	92.3	138.7	148.9	34.52	38.61	51.50
TPS/PLA (30/70)	50.5	91.0	137.7	147.7	31.18	35.17	53.62
TPS/PLA (40/60)	51.0	91.3	137.5	147.5	27.71	30.36	54.00
TPS/PLA (50/50)	50.3	90.8	137.2	146.9	22.48	25.70	54.85

TGA and DTG curves of PLA, TPS, and cassava starch are shown in Figure 4.10 and 4.11, respectively. It can be seen that there were two steps of thermal decomposition of cassava starch. The first step below 150°C was mainly caused by water evaporation. The second step was initiated at 250°C and ended at 350°C indicating the degradation of starch component. The initial shoulder of weight loss of cassava starch was due to its linear structure of amylose. The final weight loss of cassava starch indicated cross-linked structures of amylopectin (Mano, Koniarova, and Reis, (2003)). Thermal decomposition temperature at 5% weight loss (T_5), thermal decomposition temperature at 50% weight loss (T_{50}), and thermal decomposition temperature (T_d) of cassava starch were 123.77, 309.69, and 313.69°C, respectively. TGA curve of TPS exhibited three steps of thermal decomposition. The first step was obtained below 250°C which related to the volatilization of moisture and glycerol. The second step was observed from 250 to 300°C due to the decomposition of linear structure of amylose (Mano Koniarova, and Reis, (2003); Yunos and Rahman, (2011)). The third step from 300 to 350°C indicated cross-linked structures of amylopectin in TPS. TGA curve of pure PLA showed one step of thermal decomposition of PLA polymer chain at 363.92°C.

TGA and DTG curves of PLA, TPS, and TPS/PLA blends are shown in Figure 4.12 and Figure 4.13, respectively. TPS/PLA blend exhibited two steps of thermal decomposition. The first step below 250°C indicated volatilization of moisture and glycerol. Then, the second step around 250 to 380°C indicated the overlap thermal decomposition of TPS and PLA (Gao, Hu, Su, Zhang, and Tang, (2011)). T_5 , T_{50} , and T_d of cassava starch, TPS, PLA, and TPS/PLA blends were listed in Table 4.3. T_5 , T_{50} , and T_d of TPS were observed at 133.91, 311.37, and 317.79°C, respectively.

TPS displayed higher T_5 , T_{50} , and T_d than cassava starch. This indicated TPS had better thermal stability than cassava starch. T_5 , T_{50} , and T_d of PLA were 321.14, 361.94, and 363.92°C, respectively. It can be seen that PLA had better thermal stability than TPS.

T_5 , T_{50} , and T_d of TPS/PLA blend were lower than pure PLA. Similar results were also found by Wang, Yu, and Ma, (2008) and Schwach, Six, and Averous, (2008). It was well known that thermal decomposition of PLA was operated by random chain or specific chain scissions because its repeated aliphatic ester structure was relatively easy to hydrolyze and break down (McNeill and Leiper, (1985)). So, the reduction of T_5 , T_{50} , and T_d of TPS/PLA blend was probably because the products of pyrolytic decomposition of TPS including carbon monoxide, water, volatile organic compounds, and carbonaceous residue involved thermal the degradation of PLA chain (Vasques et al., (2007); Ferrarezi, Taipina, Silva, and Goncalves, (2013)). Petinakis et al., (2010) also reported that small polar molecules such as CO, CO₂, H₂O, CH₄, C₂H₄, and CH₂O were produced when starch decomposed. These molecules could break down PLA chain giving rise to a decrease in T_d of PLA. Increasing TPS content resulted in a reduction of T_5 , T_{50} , and T_d of TPS/PLA blends because the amount of pyrolytic decomposition products of TPS was increased and these products accelerated the decomposition of PLA (Petinakis et al., (2010)).

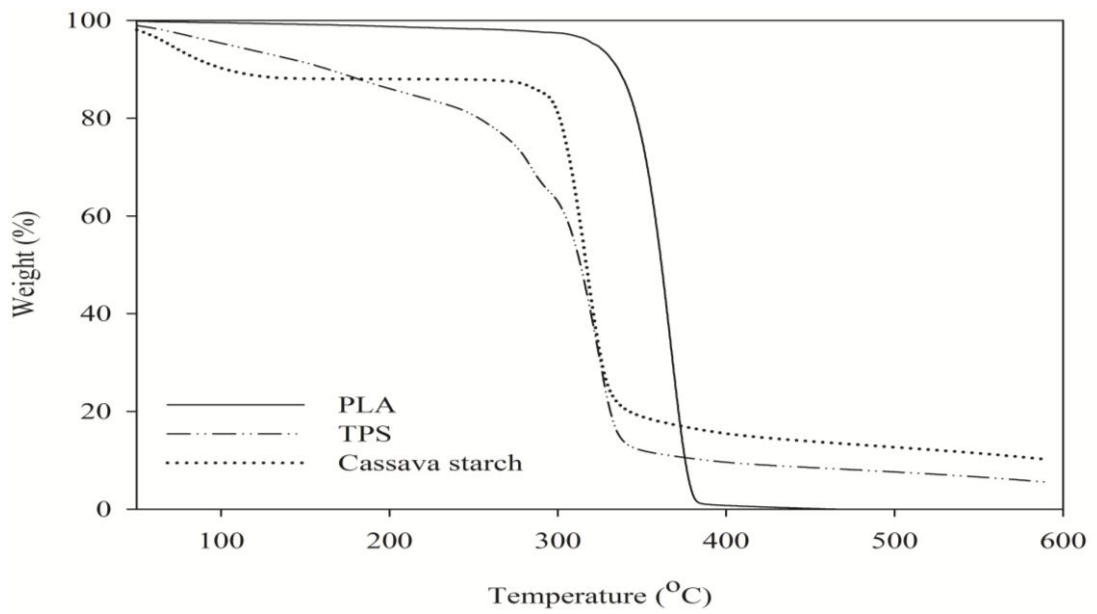


Figure 4.10 TGA curves of PLA, TPS, and cassava starch.

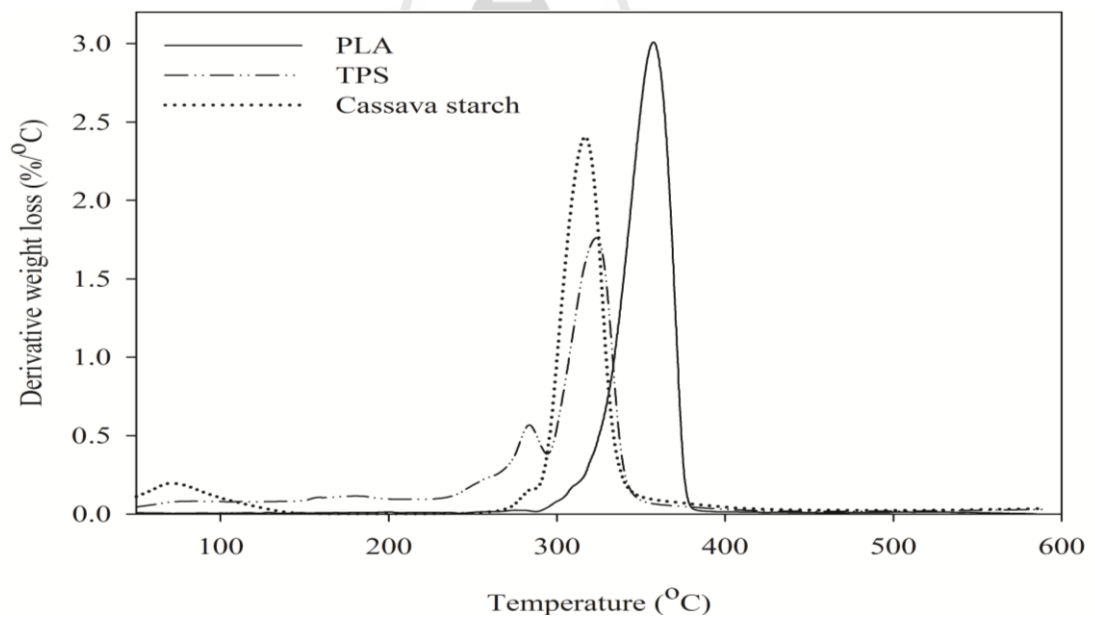


Figure 4.11 DTG curves of PLA, TPS, and cassava starch.

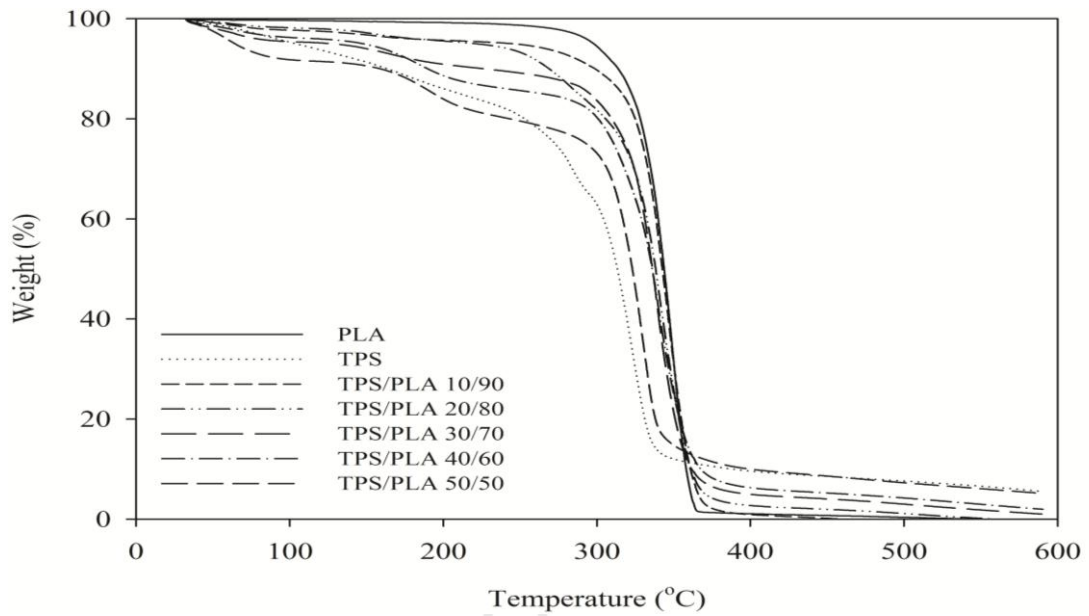


Figure 4.12 TGA curves of PLA, TPS, and TPS/PLA blends at various TPS contents.

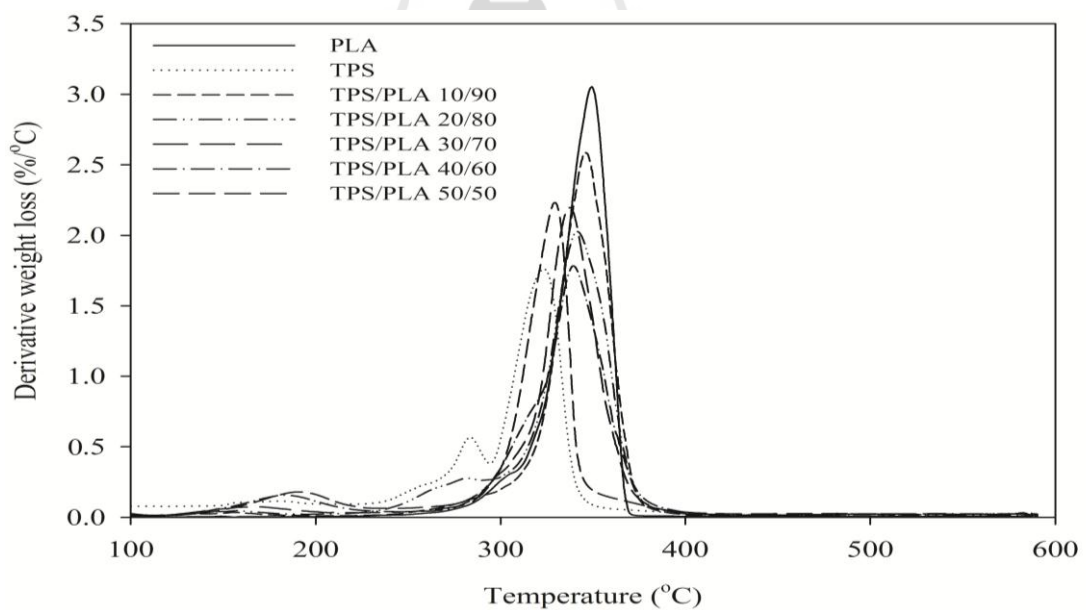


Figure 4.13 DTG curves of PLA, TPS, and TPS/PLA blends at various TPS contents.

Table 4.3 The thermal decomposition temperature of PLA, TPS, and TPS/PLA blends at various TPS contents.

Composition (%wt)	T₅ (°C)	T₅₀ (°C)	T_d (°C)
Cassava starch	123.77	309.69	313.69
TPS	133.91	311.37	317.79
PLA	321.14	361.94	363.92
TPS/PLA (10/90)	246.06	340.54	341.46
TPS/PLA (20/80)	221.95	338.29	340.19
TPS/PLA (30/70)	128.16	336.18	337.71
TPS/PLA (40/60)	125.72	332.88	334.06
TPS/PLA (50/50)	120.16	321.25	322.44

Among TPS/PLA blends, TPS/PLA (10/90) blend showed the highest tensile and impact properties. So, this blend was selected to study the effect of compatibilizer content on the properties of TPS/PLA blends.

4.3 Effect of compatibilizer content on properties of TPS/PLA blends

To study the effect of PLA-g-MA content on mechanical, thermal, and morphological properties of TPS/PLA blends, TPS/PLA (10/90) blend was chosen since the blend exhibited the highest mechanical properties.

4.3.1 Mechanical properties

Mechanical properties of uncompatibilized TPS/PLA blend and compatibilized TPS/PLA blends at various PLA-g-MA contents are shown in Table 4.4.

Tensile strength, tensile modulus, and elongation at break of the compatibilized TPS/PLA blends were higher when compared to the uncompatibilized TPS/PLA blend due to enhanced compatibility between TPS and PLA as shown in Figure 4.14, 4.15, and 4.16, respectively. The anhydride groups of PLA-g-MA reacted with hydroxyl groups of starch to form a graft copolymer which acted as an emulsifier for the blend (Huneault and Li, (2007)). This led to increased tensile properties. Wang and Huang, (2007), Schwach, Six, and Averous, (2008), and Wootthikanokkhan et al., (2012) reported that tensile properties of TPS/PLA blends improved with the presence of compatibilizers. Tensile properties of the blends were continuously increased when PLA-g-MA content was increased up to 5 phr. With incorporating 7 phr of PLA-g-MA, tensile properties of the blend slightly decreased. This may be because with increasing PLA-g-MA content, more anhydride molecules were capable of activating chain scissions of PLA molecules during melt blending via hydrolysis mechanism (Tsuji, (2002); Wootthikanokkhan et al., (2012)). This was attributed to a decrease in the tensile properties of the blends. Phetwarotai, Potiyaraj, and Aht-Ong (2010) also found tensile

properties of PLA/TPS blends decreased with increasing methylenediphenyl diisocyanate (MDI) content over 1.25%wt. This was because MDI could react between TPS and TPS molecules, some agglomeration of TPS molecules appeared, which eventually caused defects and cracks in the blend films.

Impact strength of the TPS/PLA/PLA-g-MA blends was shown in Figure 4.17. Impact strength of the blends was continuously increased when PLA-g-MA content was increased up to 5 phr. This suggested that the improvement of interfacial adhesion between TPS and PLA might enhance the ductility of the materials (Huneault and Li, (2007)). However, impact strength of the blend was decreased with the addition of 7 phr PLA-g-MA due to saturation of PLA-g-MA on interface between TPS and PLA (Sailaja, Reddy, and Chanda, (2001)). Ping, Kejian, Mingyin, and Meijuan, (2013) also observed that impact strength of TPS/PLA blends increased with adding 3%wt poly(ethylene glycol) (PEG) and then trended to decrease with further increasing PEG content. This was because more content of PEG easily induced the aggregation and decreased the dispersibility of PEG.

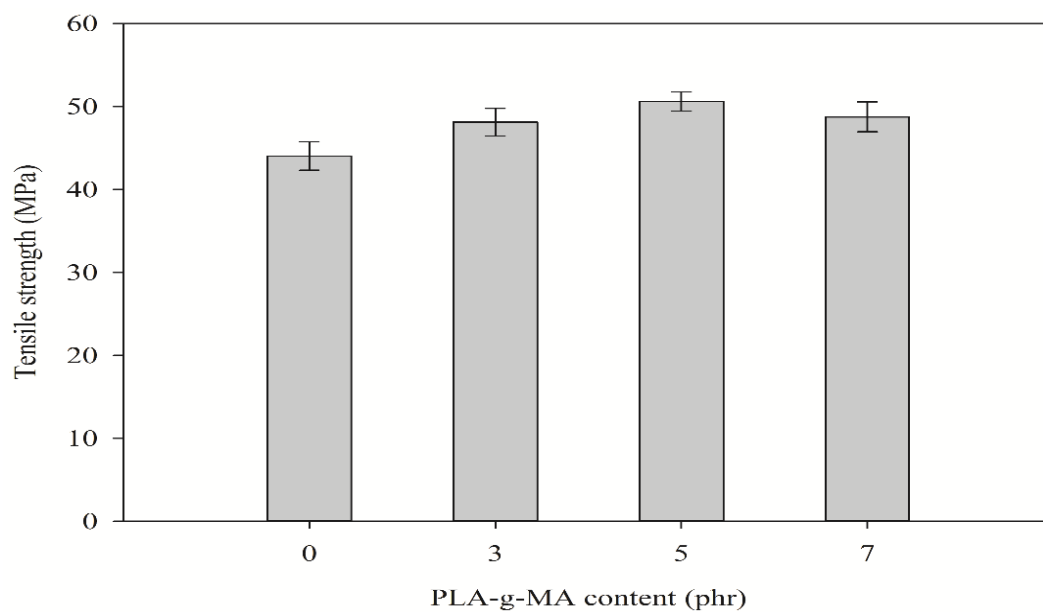


Figure 4.14 Tensile strength of TPS/PLA blend and TPS/PLA/PLA-g-MA blends at various PLA-g-MA contents.

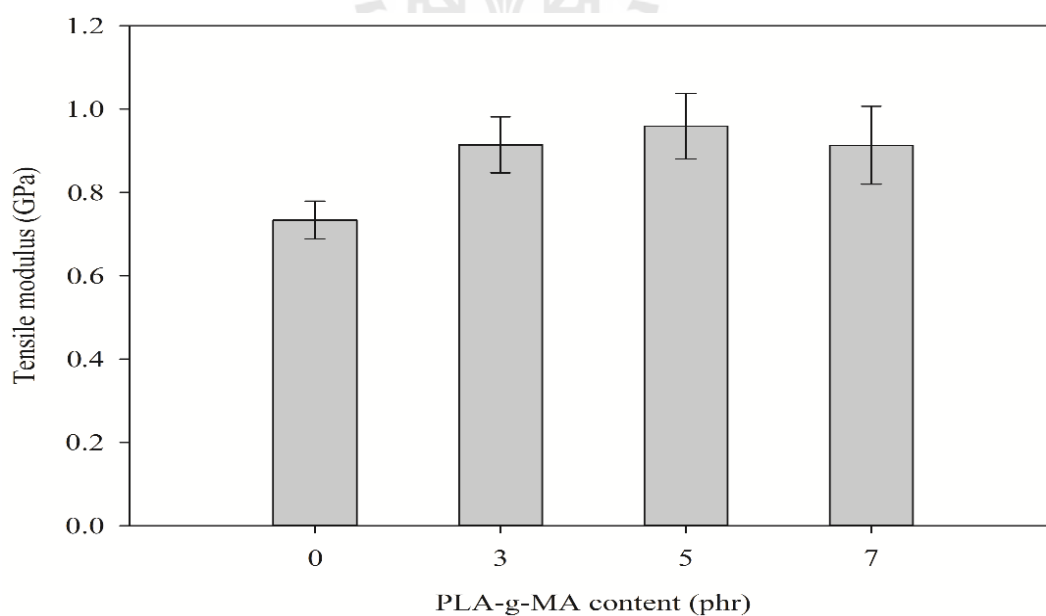


Figure 4.15 Tensile modulus of TPS/PLA blend and TPS/PLA/PLA-g-MA blends at various PLA-g-MA contents.

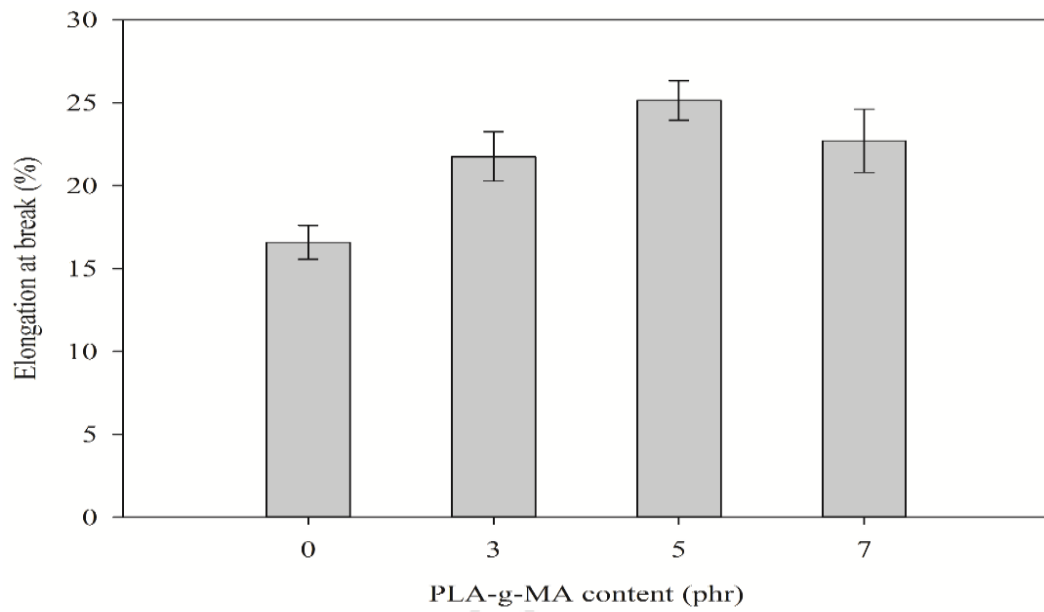


Figure 4.16 Elongation at break of TPS/PLA blend and TPS/PLA/PLA-g-MA blends at various PLA-g-MA contents.

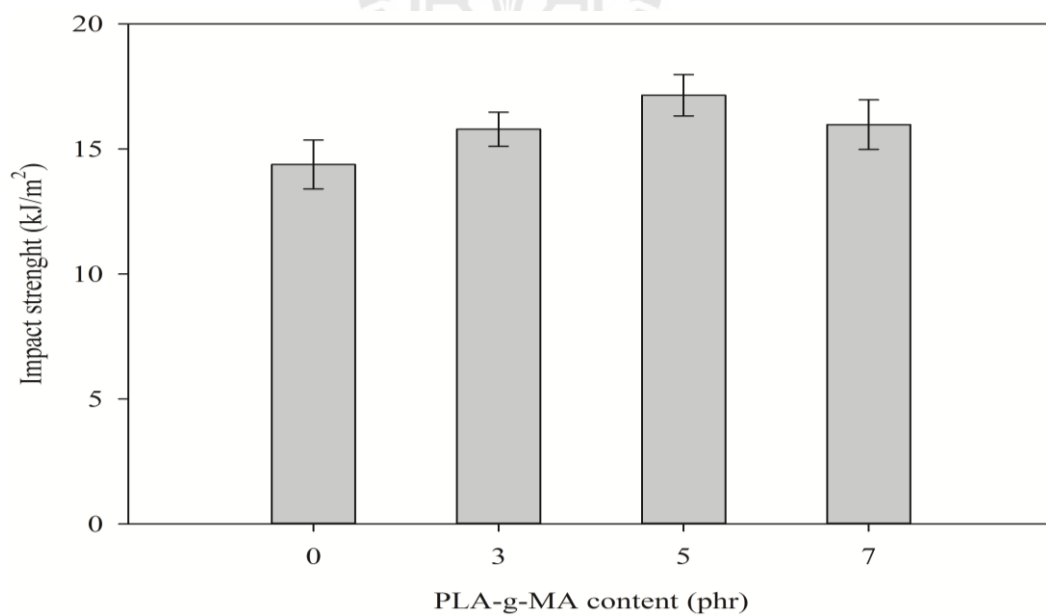


Figure 4.17 Impact strength of TPS/PLA blend and TPS/PLA/PLA-g-MA blends at various PLA-g-MA contents.

Table 4.4 Mechanical properties of TPS/PLA blend and TPS/PLA/PLA-g-MA blends at various PLA-g-MA contents.

Composition (%wt)	Tensile strength (MPa)	Tensile modulus (GPa)	Elongation at break (%)	Impact strength (kJ/m²)
TPS/PLA (10/90)	44.03±1.72	0.73±0.05	16.59±1.02	14.37±0.98
TPS/PLA/PLA-g-MA (10/90/3)	48.12±1.66	0.91±0.06	21.75±1.49	15.79±0.68
TPS/PLA/PLA-g-MA (10/90/5)	50.60±1.13	0.95±0.07	25.14±1.19	17.15±0.83
TPS/PLA/PLA-g-MA (10/90/7)	48.75±1.80	0.91±0.09	22.70±1.90	15.97±0.99



4.3.2 Morphological properties

SEM micrographs of the freeze fractured surface of TPS/PLA blend and TPS/PLA/PLA-g-MA blends are shown in Figure 4.18. TPS phase was removed by 6 M HCl solution. In a case of the uncompatibilized TPS/PLA blend, the large holes of TPS were observed in PLA matrix as shown in Figure 4.18(a). From Figure 4.18(b-d), the size of TPS phase in the compatibilized TPS/PLA blends was finer than the uncompatibilized blend. This indicated the improvement of the compatibility between TPS and PLA leading to increased mechanical properties of the blends. Wootthikanokkhan et al. (2012) suggested that compatibilizer reduced coalescence and surface tension of TPS phase in TPS/PLA blends resulting in enhanced mechanical properties of the blends. TPS phase size was continuously decreased with increasing PLA-g-MA up to 5 phr. However, further increasing PLA-g-MA content to 7 phr, no remarkable change in TPS size was found.

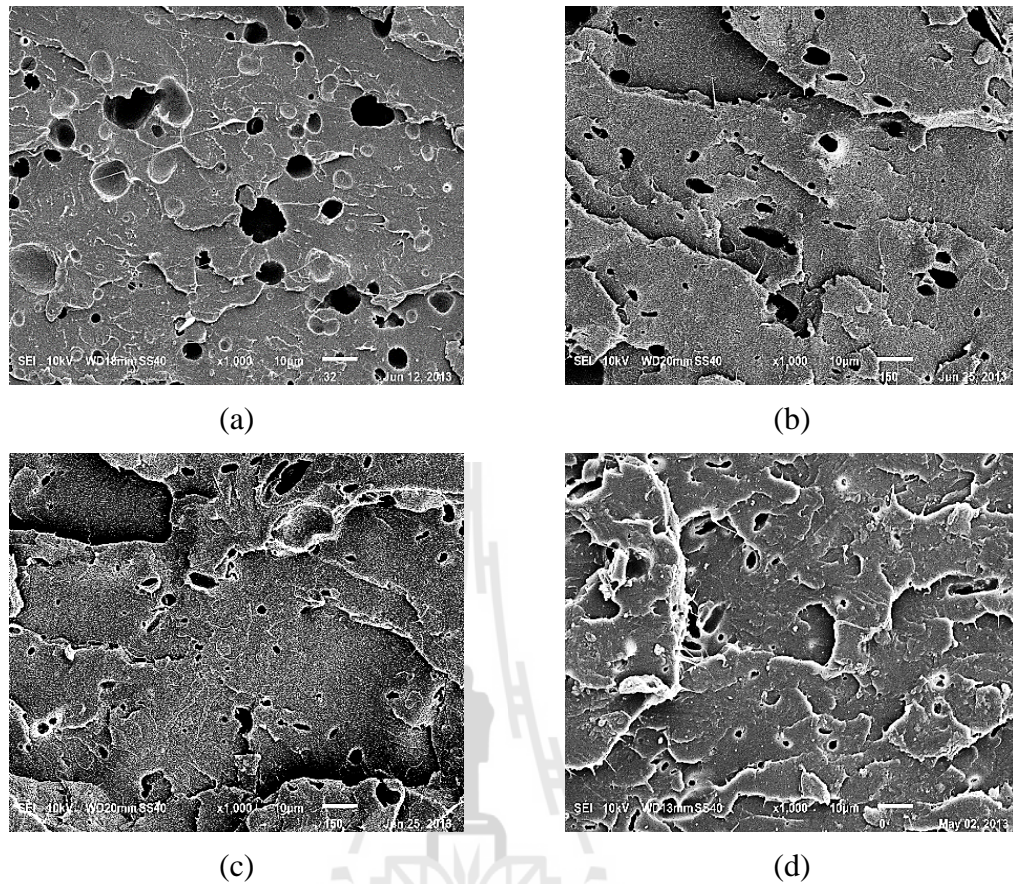


Figure 4.18 SEM micrographs of the freeze fractured surface at 1000x magnification of (a) TPS/PLA 10/90 blend, (b) TPS/PLA/PLA-g-MA 10/90/3 blend, (c) TPS/PLA/PLA-g-MA 10/90/5 blend, and (d) TPS/PLA/PLA-g-MA 10/90/7 blend.

4.3.3 Thermal properties

DSC thermograms of uncompatibilized TPS/PLA blend and compatibilized TPS/PLA blends are shown in Fig. 4.19 and their DSC data are listed in Table 4.5. The uncompatibilized TPS/PLA blend showed T_g , T_{cc} , T_{m1} , and T_{m2} at 50.7, 93.1, 139.5, and 150.4°C, respectively. T_g of PLA in the compatibilized TPS/PLA blend at PLA-g-MA content of 3 phr was lower than the uncompatibilized TPS/PLA blend

due to improved interfacial adhesion between TPS and PLA (Karagoz and Ozkoc, (2013); Ferrarezi, Taipina, Silva, and Goncalves, (2013)). T_m of PLA in the compatibilized TPS/PLA blend slightly decreased approximately 1°C with adding 3 phr PLA-g-MA due to enhanced compatibility between TPS and PLA (Karagoz and Ozkoc, (2013)). Similar result was also found by Ping, Keijian, Mingyin, and Meijuan, (2013). T_{cc} of PLA in the compatibilized TPS/PLA blend was decreased with incorporating 3 phr PLA-g-MA which indicated the enhancement of chain mobility of PLA (Ferrarezi, Taipina, Silva, and Goncalves, (2013)). ΔH_c , ΔH_m , and χ_c were increased with adding PLA-g-MA due to effect of nucleating agent of TPS. Small size of TPS phase could act as a good nucleating agent of the blends (Shin, Jang, and Kim, (2011)).

T_g and T_m of PLA the compatibilized TPS/PLA blends continuously decreased when PLA-g-MA content was increased to 5 phr due to improved compatibility between TPS and PLA (Karagoz and Ozkoc, (2013)). Moreover, T_{cc} of PLA in the compatibilized TPS/PLA blend was decreased when PLA-g-MA content was increased due to improved chain mobility of PLA. ΔH_m , ΔH_c , and χ_c of the compatibilized TPS/PLA blend were increased when PLA-g-MA content was increased. This suggested that fine TPS disperse phase might act as an effective nucleating agent (Shin, Jang, and Kim, (2011)). Li and Huneault, (2008) explained that the reduction of dispersed phase size led to an increase in interfacial area thus enhanced the crystallization of PLA.

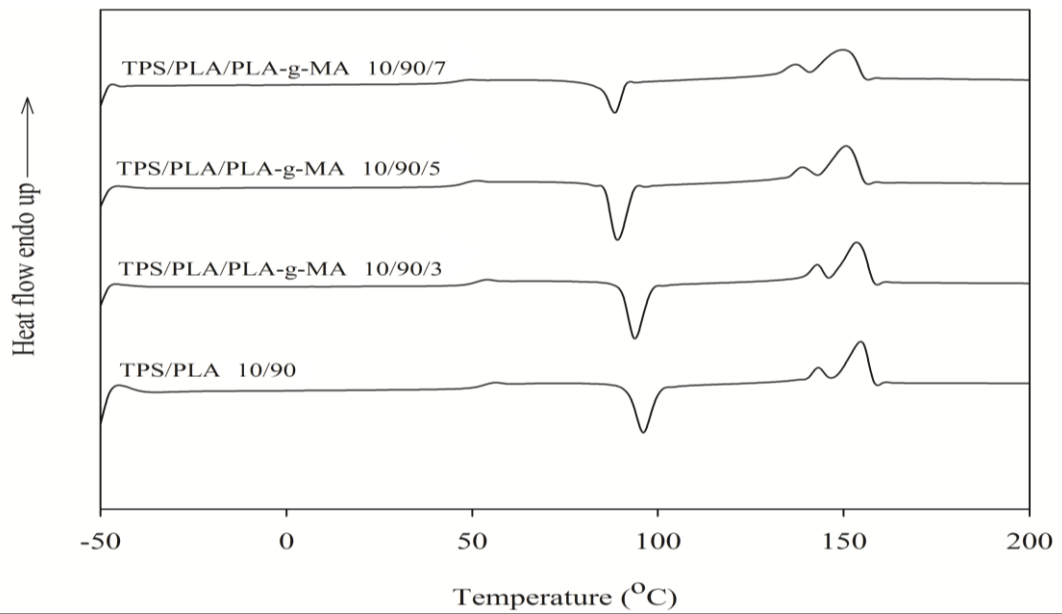


Figure 4.19 DSC thermograms of TPS/PLA blend and TPS/PLA/PLA-g-MA blends at various PLA-g-MA contents (the second heating, heating rate 5°C/min).

Table 4.5 Thermal characteristics of TPS/PLA blend and TPS/PLA/PLA-g-MA blends at various PLA-g-MA contents.

Composition (%wt)	T_g (°C)	T_{cc} (°C)	T_{m1} (°C)	T_{m2} (°C)	ΔH_c (J/g)	ΔH_m (J/g)	χ_c (%)
TPS/PLA (10/90)	50.7	93.1	139.5	150.4	37.38	40.16	47.62
TPS/PLA/PLA-g-MA (10/90/3)	49.6	91.4	138.0	149.0	40.63	44.26	55.09
TPS/PLA/PLA-g-MA (10/90/5)	46.3	86.9	135.7	147.1	41.49	46.55	57.71
TPS/PLA/PLA-g-MA (10/90/7)	45.0	85.1	136.9	147.7	42.11	47.89	59.25



TGA and DTG curves of uncompatibilized TPS/PLA blend and compatibilized TPS/PLA blends are presented in Figure 4.20 and Figure 4.21, respectively. The uncompatibilized TPS/PLA blend and the compatibilized TPS/PLA blends showed two steps of weight loss. First step was related to decomposition of moisture and glycerol. The second step was the decomposition of TPS and PLA which was overlapped. Similar result was also found by Gao, Hu, Su, Zhang, and Tang, (2011) and Victor, Brostow, Chonkaew, and Lopez, (2009). Thermal decomposition temperature at 5% weight loss (T_5), thermal decomposition temperature at 50% weight loss (T_{50}), and thermal decomposition temperature (T_d) of the uncompatibilized TPS/PLA blend and the compatibilized TPS/PLA blends are listed in Table 4.6. T_5 , T_{50} , T_d of the uncompatibilized TPS/PLA blend were at 246.06, 340.54, and 341.46°C, respectively. When 3 phr of PLA-g-MA was incorporated into the uncompatibilized TPS/PLA blend, T_5 , T_{50} , T_d of the compatibilized TPS/PLA blend were 284.70, 361.13, and 364.11°C, respectively. This indicated that thermal stability of the blend was enhanced with adding PLA-g-MA due to improved interfacial adhesion between TPS and PLA (Wang, Yu, and Ma, (2008); Shi et al., (2011)). T_d of the compatibilized TPS/PLA blend did not change significantly with increasing PLA-g-MA content. Victor, Brostow, Chonkaew, and Lopez, (2009) also reported that PLA-g-MA showed little effect on thermal stability of PLA/starch blends.

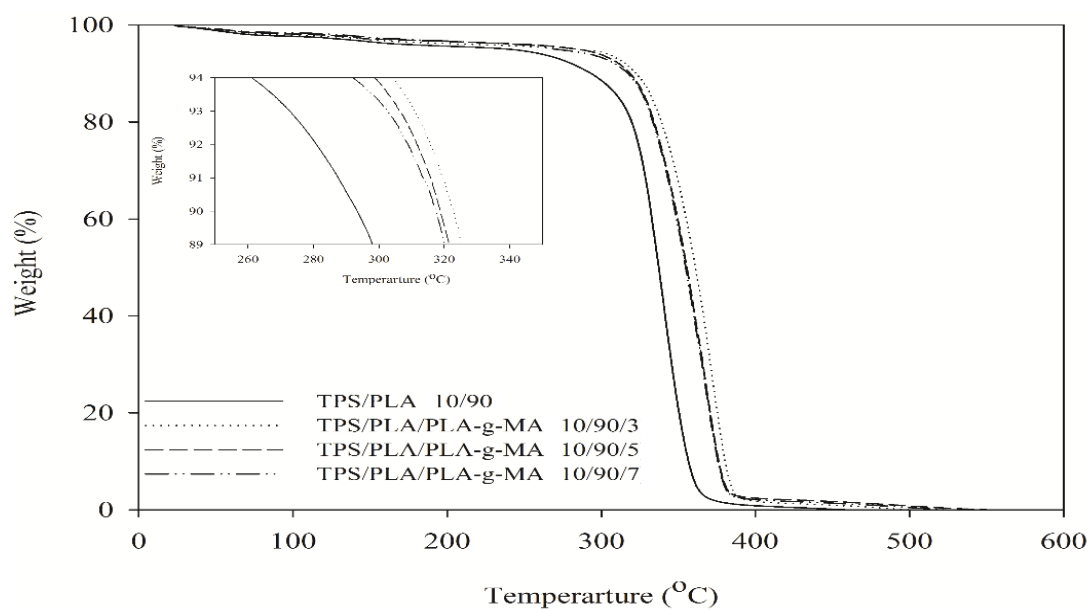


Figure 4.20 TGA curves of TPS/PLA blend and TPS/PLA/PLA-g-MA blends at various PLA-g-MA contents.

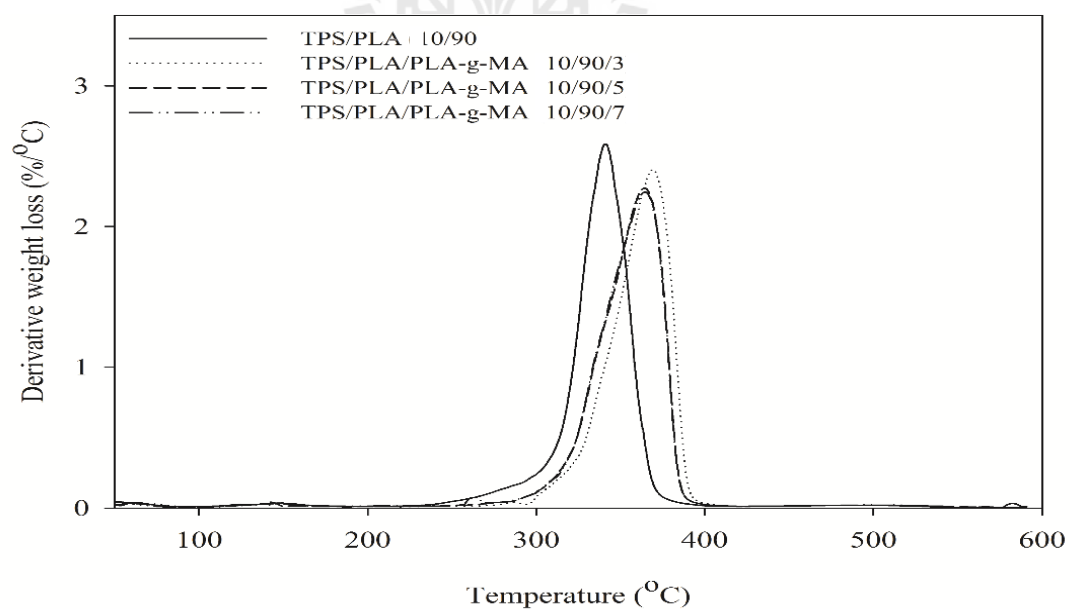


Figure 4.21 DTG curves of TPS/PLA blend and TPS/PLA/PLA-g-MA blends at various PLA-g-MA contents.

Table 4.6 The thermal decomposition temperature of TPS/PLA blend and TPS/PLA/PLA-g-MA blends at various PLA-g-MA contents.

Composition (%wt)	T ₅ (°C)	T ₅₀ (°C)	T _d (°C)
TPS/PLA (10/90)	246.06	340.54	341.46
TPS/PLA/PLA-g-MA (10/90/3)	284.70	361.13	364.11
TPS/PLA/PLA-g-MA (10/90/5)	284.83	360.11	364.15
TPS/PLA/PLA-g-MA (10/90/7)	284.88	360.14	364.20

The compatibilized TPS/PLA blend containing 5 phr PLA-g-MA showed the highest tensile and impact properties. Therefore, the TPS/PLA/PLA-g-MA (10/90/5) blend was selected to study effect of PBAT and ENR50 content on the properties of compatibilized TPS/PLA/PBAT blends and compatibilized TPS/PLA/ENR50 blends.

4.4 Effect of flexible polymer content on properties of compatibilized TPS/PLA blends

To study the effect of flexible polymer content on mechanical, thermal, and morphological properties of the compatibilized TPS/PLA blends, TPS/PLA/PLA-g-MA (10/90/5phr) blend was chosen according to its optimum mechanical properties. Poly(butylene adipate-co-terephthalate) (PBAT) and epoxidized natural rubber with 50% epoxidation (ENR50) were used as flexible polymers.

4.4.1 Effect of PBAT content on properties of compatibilized TPS/PLA blends

4.4.1.1 Mechanical properties

Mechanical properties of compatibilized TPS/PLA blend and compatibilized TPS/PLA/PBAT blends at various PBAT contents are shown in Table 4.7. Tensile strength and tensile modulus of the compatibilized TPS/PLA blends were continuously decreased with increasing PBAT content whereas elongation at break was increased as shown in Figure 4.22, Figure 4.23, and Figure 4.24, respectively. This was due to the rubber nature of PBAT (Ren, Fu, Ren, and Yuan, (2009)). Phetwarotai and Aht-Ong, (2011) also found that adding PBAT increased elongation at break of TPS/PLA blend but decreased tensile strength. This was because PBAT had lower tensile strength than PLA resulting in the ductility improvement of TPS/PLA blend.

Impact strength of the compatibilized TPS/PLA blends also increased with increasing PBAT content as shown in Figure 4.25. PBAT particles may act as sites of local stress concentration and these sites were capable of initiation

of craze and shear band (Lin, Guo, Chan, Ma, and Wang, (2012); Zhao, Liu, Wu, and Ren, (2010)). This resulted in improved toughness of the blends.

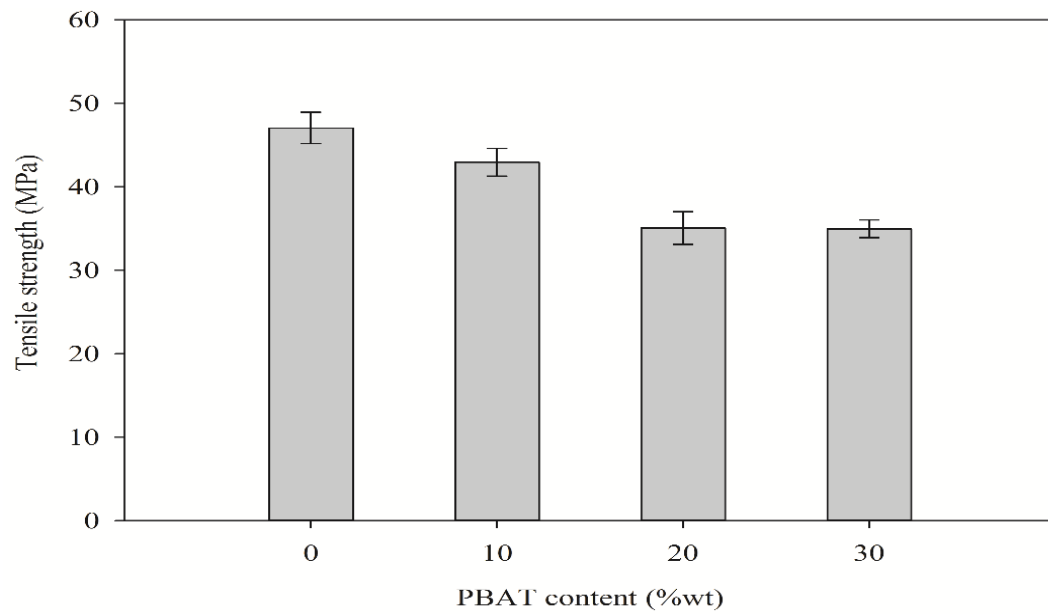


Figure 4.22 Tensile strength of compatibilized TPS/PLA blend and compatibilized TPS/PLA/PBAT blends at various PBAT contents.

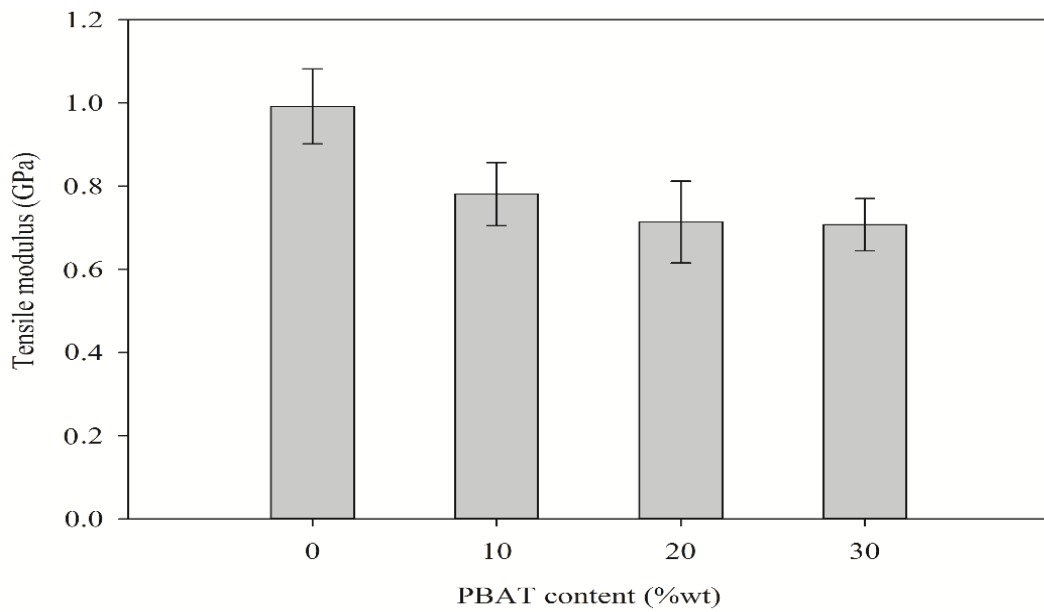


Figure 4.23 Tensile modulus of compatibilized TPS/PLA blend and compatibilized TPS/PLA/PBAT blends at various PBAT contents.

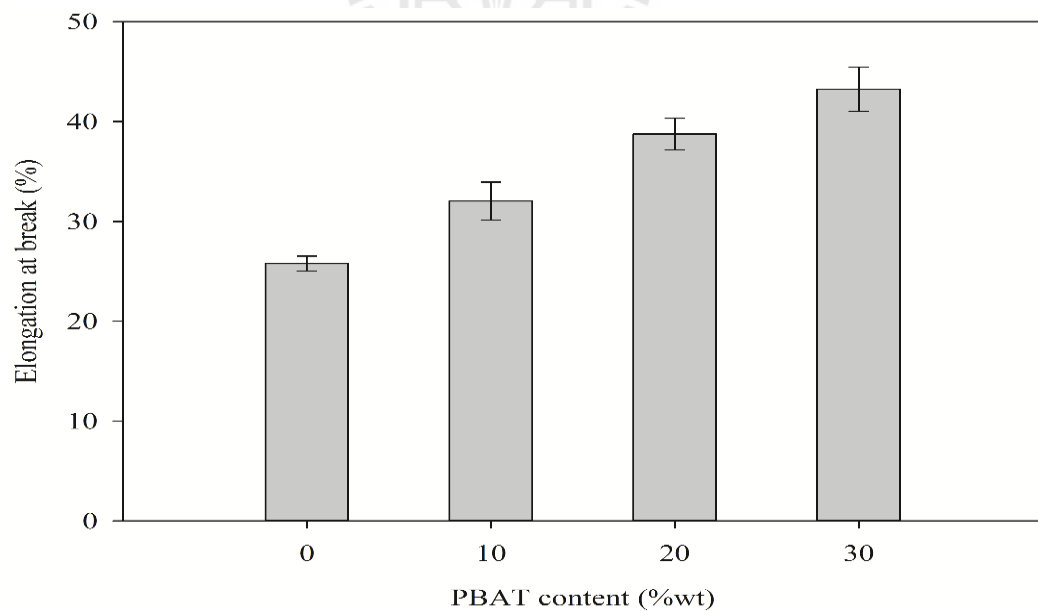


Figure 4.24 Elongation at break of compatibilized TPS/PLA blend and compatibilized TPS/PLA/PBAT blends at various PBAT contents.

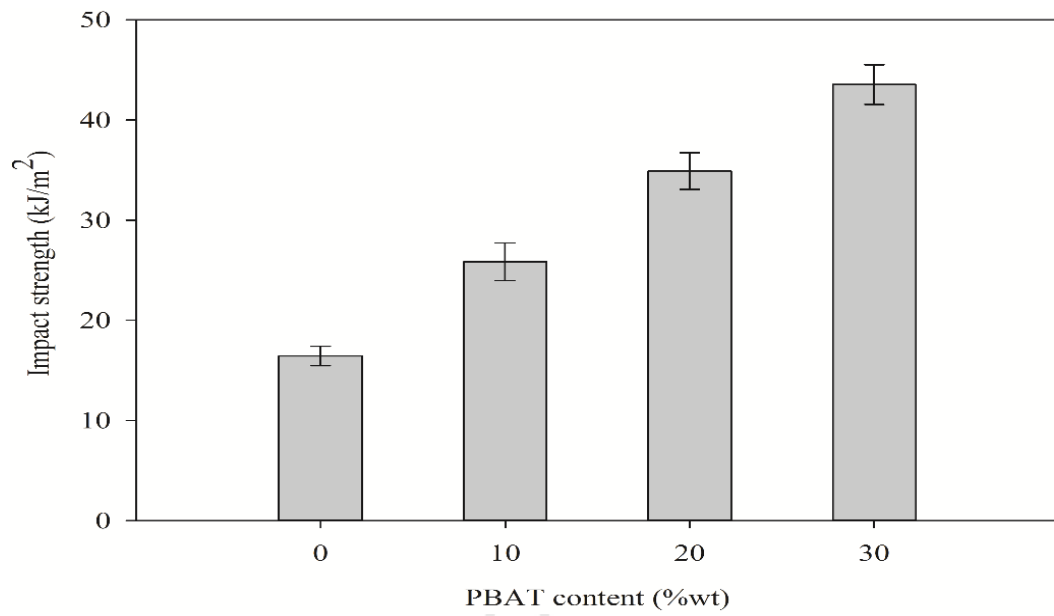


Figure 4.25 Impact strength of compatibilized TPS/PLA blend and compatibilized TPS/PLA/PBAT blends at various PBAT contents.

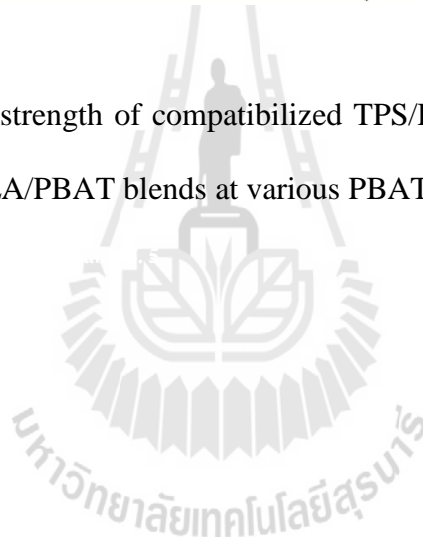
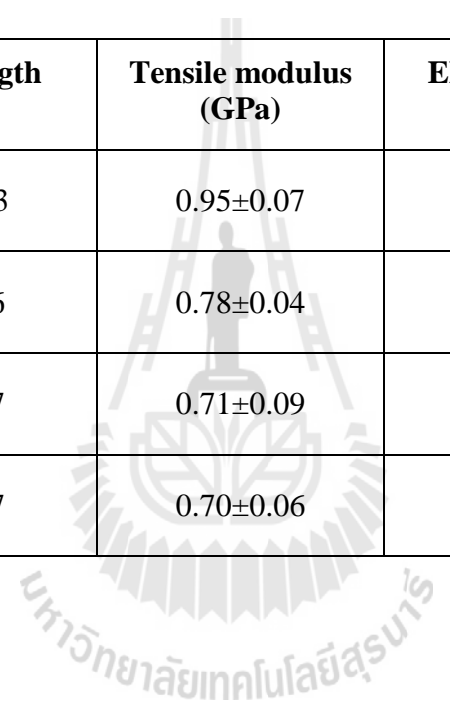


Table 4.7 Mechanical properties of compatibilized TPS/PLA blend and compatibilized TPS/PLA/PBAT blends at various PBAT contents.

Composition (%wt)	Tensile strength (MPa)	Tensile modulus (GPa)	Elongation at break (%)	Impact strength (kJ/m²)
TPS/PLA/PLA-g-MA (10/90/5phr)	50.60±1.1.3	0.95±0.07	25.14±1.19	17.15±0.83
TPS/PLA/PLA-g-MA/PBAT (9/81/5phr/10)	42.94±1.66	0.78±0.04	31.17±2.59	25.85±1.87
TPS/PLA/PLA-g-MA/PBAT (8/72/5phr/20)	35.06±1.97	0.71±0.09	39.49±2.31	34.91±1.82
TPS/PLA/PLA-g-MA/PBAT (7/63/5phr/30)	34.95±1.07	0.70±0.06	43.24±2.19	43.54±1.98



4.4.1.2 Morphological properties

SEM micrographs of the freeze fractured surface of compatibilized TPS/PLA blend and compatibilized TPS/PLA/PBAT blends at various PBAT contents are shown in Figure 4.26. TPS phases well dispersed in PLA matrix with adding PLA-g-MA as shown in Figure 4.26(a). From Figure 4.26(b), the small droplets of PBAT were observed in the compatibilized TPS/PLA/PBAT blend. This indicated that PLA and PBAT were immiscible. PBAT phase size was increased with increasing PBAT content as shown in Figure 4.26(b-d) due to coalescence of PBAT phase (Kim and Michler, (1998); Kumar, Mohanty, Nayak, and Rahail Parvaiz, (2010)). SEM micrographs of the tensile fractured surface of compatibilized TPS/PLA blend and compatibilized TPS/PLA/PBAT blends at various PBAT contents are shown in Figure 4.27. From Figure 4.27(b-d), some elongated matrix during tensile test was occurred. This indicated a ductile deformation.

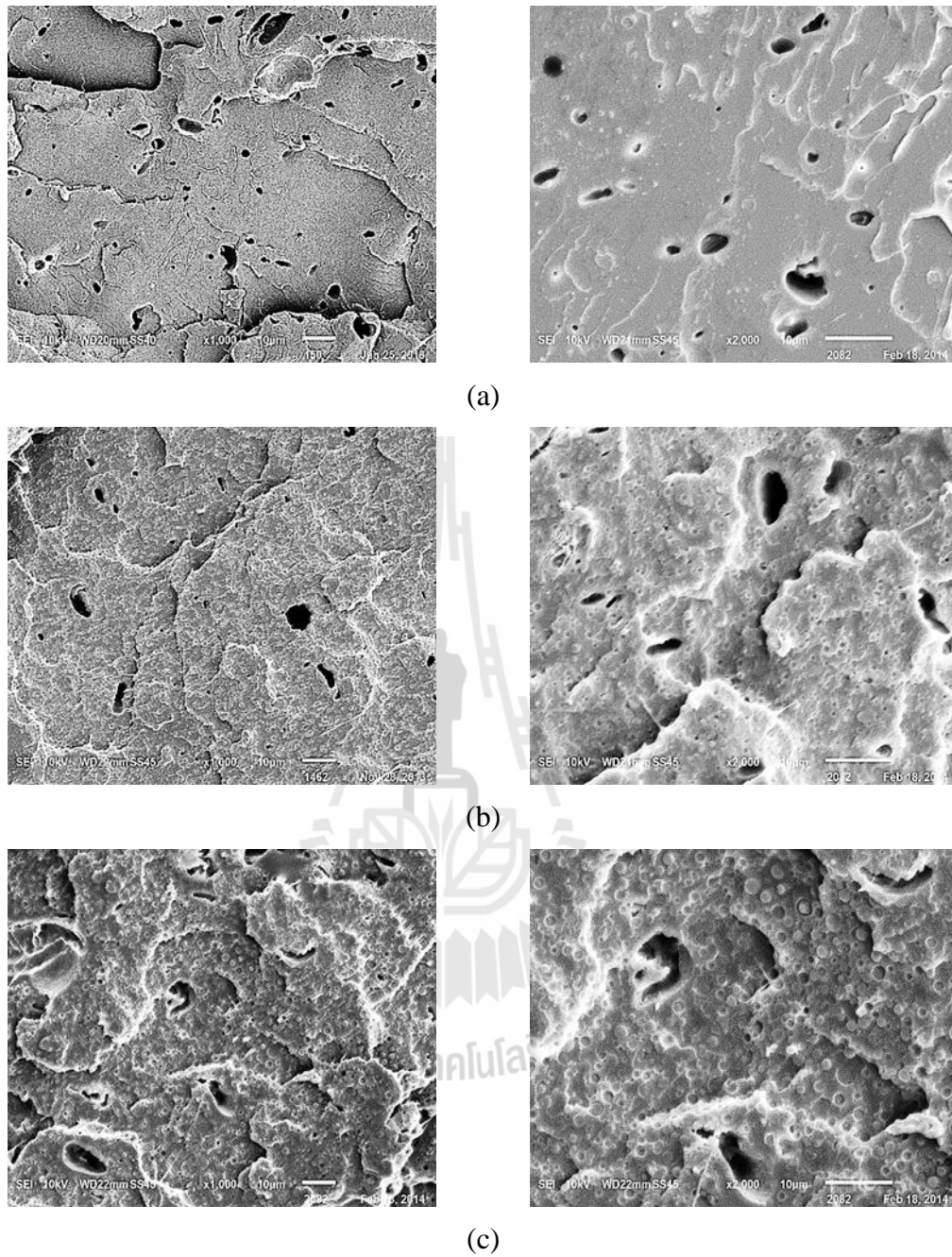


Figure 4.26 SEM micrographs of the freeze fractured surface at 1000x (left) and 2000x (right) magnification of (a) TPS/PLA/PLA-g-MA 10/90/5phr blend, (b) TPS/PLA/PLA-g-MA/PBAT 9/81/5phr/10 blend, (c) TPS/PLA/PLA-g-MA/PBAT 8/72/5phr/20 blend, and (d) TPS/PLA/PLA-g-MA/PBAT 7/63/5phr/30 blend.

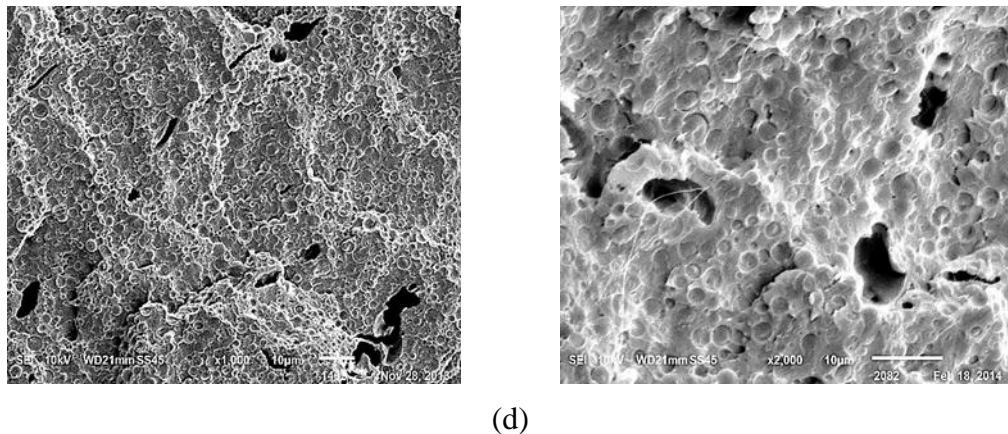


Figure 4.26 SEM micrographs of the freeze fractured surface at 1000x (left) and 2000x (right) magnification of (a) TPS/PLA/PLA-g-MA 10/90/5phr blend, (b) TPS/PLA/PLA-g-MA/PBAT 9/81/5phr/10 blend, (c) TPS/PLA/PLA-g-MA/PBAT 8/72/5phr/20 blend, and (d) TPS/PLA/PLA-g-MA/PBAT 7/63/5phr/30 blend (continued).

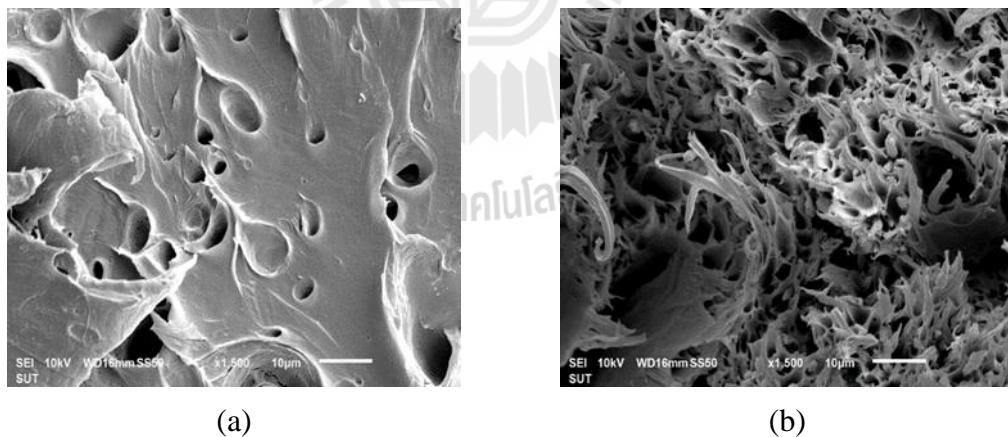


Figure 4.27 SEM micrographs of tensile fractured surfaced at 1500x magnification of (a) TPS/PLA/PLA-g-MA 10/90/5phr blend, (b) TPS/PLA/PLA-g-MA/PBAT 9/81/5phr/10 blend, (c) TPS/PLA/PLA-g-MA/PBAT 8/72/5phr/20 blend, and (d) TPS/PLA/PLA-g-MA/PBAT 7/63/5phr/30 blend.

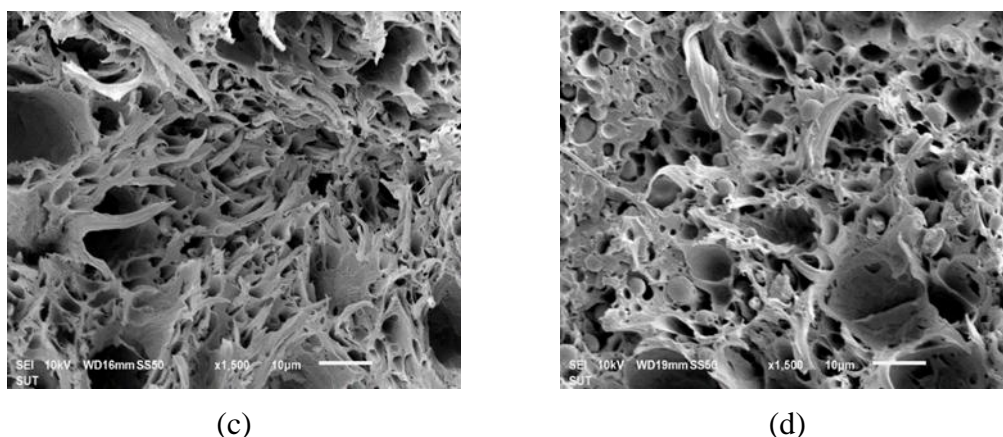


Figure 4.27 SEM micrographs of tensile fractured surface at 1500x magnification of (a) TPS/PLA/PLA-g-MA 10/90/5phr blend, (b) TPS/PLA/PLA-g-MA/PBAT 9/81/5phr/10 blend, (c) TPS/PLA/PLA-g-MA/PBAT 8/72/5phr/20 blend, and (d) TPS/PLA/PLA-g-MA/PBAT 7/63/5phr/30 blend (continued).

4.4.1.3 Thermal properties

DSC thermograms of compatibilized TPS/PLA blend and compatibilized TPS/PLA/PBAT blends are shown in Fig. 4.28 and their DSC data are listed in Table 4.8. T_g of PLA in the compatibilized TPS/PLA blend was decreased with adding 10%wt PBAT which indicated that PLA and PBAT were partially immiscible (Jiang, Wolcott, and Zhang, (2006)). The incorporation of 10%wt PBAT decreased T_{cc} of PLA in the compatibilized TPS/PLA blends which suggested that PBAT improved crystalline ability of PLA (Zhao, Liu, Wu, and Ren, (2010)). T_m of PLA in the compatibilized TPS/PLA blend insignificantly changed when 10%wt PBAT was incorporated. ΔH_c and ΔH_m of PLA in the compatibilized TPS/PLA/PBAT blend were lower when compared with the compatibilized TPS/PLA blend. However, χ_c of

PLA in the compatibilized TPS/PLA blend was increased with adding 10%wt PBAT content. This could be implied that PBAT acted as a nucleating agent in the blend (Dong, Zou, Yan, Ma, and Chen, (2013)). With increasing PBAT content, T_g , T_c , and T_m of PLA in the compatibilized TPS/PLA blends did not change. The reduction of ΔH_c and ΔH_m of the compatibilized TPS/PLA blends was observed when PBAT content was increased. PBAT content exhibited insignificant effect on χ_c of PLA in the compatibilized TPS/PLA/PBAT blends.

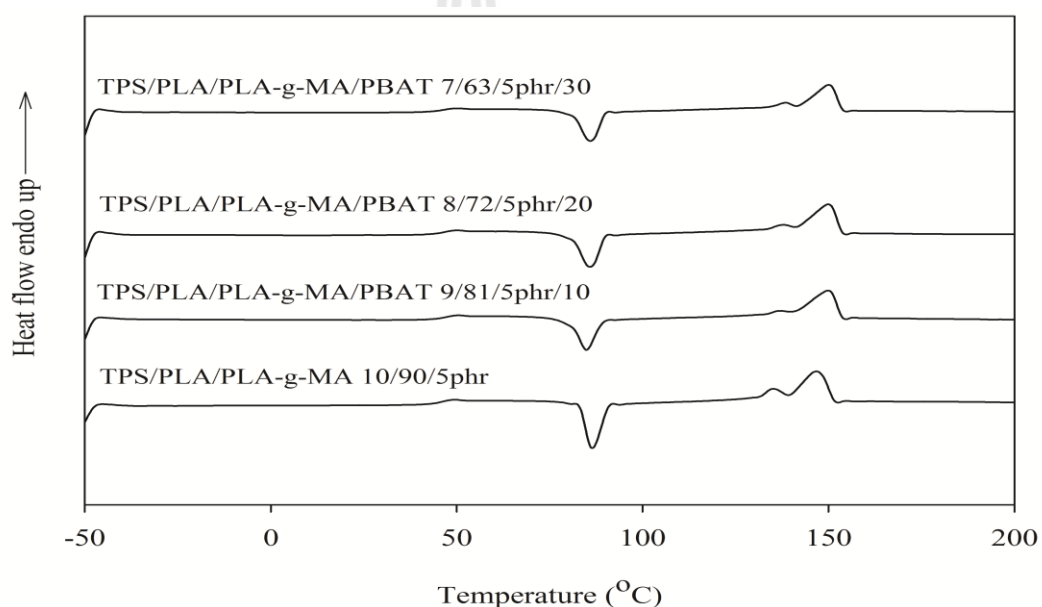


Figure 4.28 DSC thermograms of compatibilized TPS/PLA blend and compatibilized TPS/PLA/PBAT blends at various PBAT contents (the second heating, heating rate 5°C/min).

Table 4.8 Thermal characteristics of compatibilized TPS/PLA blend and compatibilized TPS/PLA/PBAT blends at various PBAT contents.

Composition (%wt)	T_g (°C)	T_{cc} (°C)	T_{m1} (°C)	T_{m2} (°C)	ΔH_c (J/g)	ΔH_m (J/g)	χ_c (%)
TPS/PLA/PLA-g-MA (10/90/5phr)	46.3	86.9	135.7	147.1	41.49	46.55	57.77
TPS/PLA/PLA-g-MA/PBAT (9/81/5phr/10)	45.1	84.1	135.6	147.0	39.51	43.51	59.97
TPS/PLA/PLA-g-MA/PBAT (8/72/5phr/20)	44.8	84.4	135.9	147.1	36.18	39.28	60.88
TPS/PLA/PLA-g-MA/PBAT (7/63/5phr/30)	44.2	84.9	135.0	147.2	30.80	34.22	60.57



TGA and DTG curves of compatibilized TPS/PLA blend and compatibilized TPS/PLA/PBAT blends at various PBAT contents are shown in Figure 4.29 and Figure 4.30, respectively. PLA and PBAT showed a single step of weight loss and thermal decomposition temperature of PLA and PBAT were 363.92 and 410.87°C, respectively. The compatibilized TPS/PLA/PBAT blend showed two steps of weight loss. The first step was attributed to the decomposition of TPS/PLA blend. The second step was assigned to PBAT decomposition. Thermal decomposition temperature at 5% weight loss (T_5), thermal decomposition temperature at 50% weight loss (T_{50}), and their thermal decomposition temperature of TPS/PLA blends (T_{d1}) and PBAT (T_{d2}) in the compatibilized TPS/PLA blend and the compatibilized TPS/PLA/PBAT blends are summarized in Table 4.9. T_5 , T_{50} , and T_{d1} of the compatibilized TPS/PLA blend were 284.83, 356.28, and 364.15°C, respectively. T_5 , T_{50} , and T_{d1} of the compatibilized TPS/PLA/PBAT blend were higher than the compatibilized TPS/PLA blend. This indicated that the incorporation of PBAT led to enhanced thermal stability of the blends (Phetwarotai and Aht-Ong, (2011); Kumar, Mohanty, Nayak, Rahail Parvaiz, (2010)). T_{d2} of the compatibilized TPS/PLA/PBAT blend was decreased when compared with PBAT. This was because PBAT had higher thermal decomposition temperature than TPS and PLA.

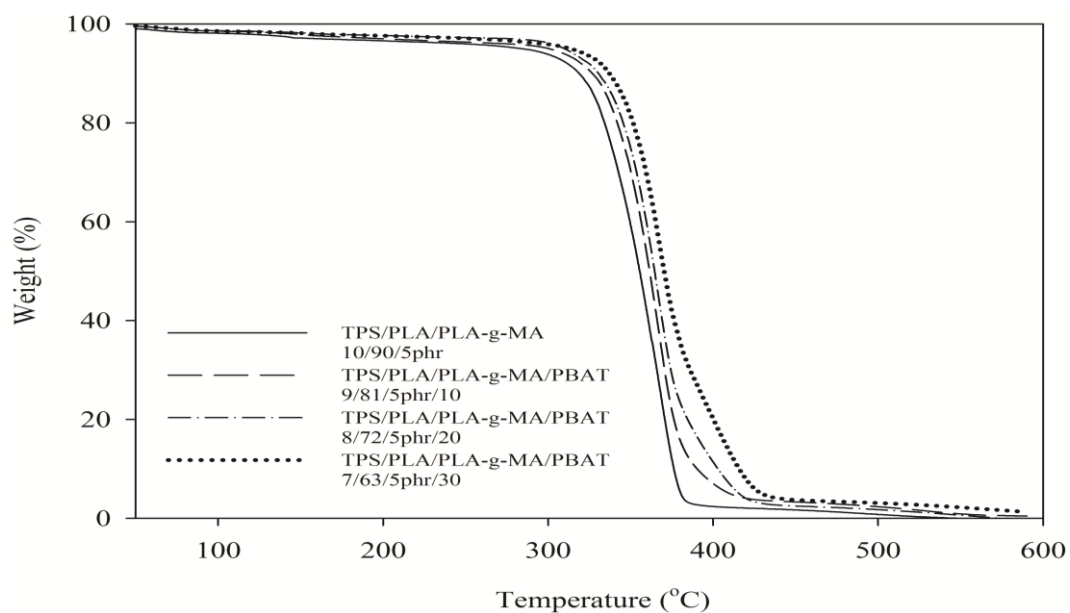


Figure 4.29 TGA thermograms of compatibilized TPS/PLA blend and compatibilized TPS/PLA/PBAT blends at various PBAT contents.

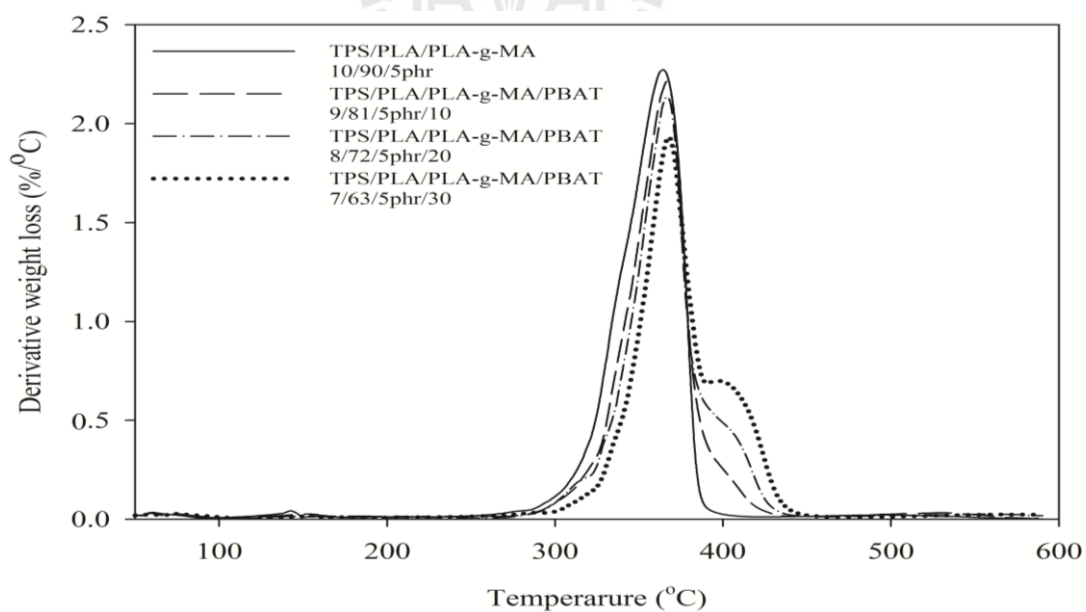


Figure 4.30 DTG thermograms of compatibilized TPS/PLA blend and compatibilized TPS/PLA/PBAT blends at various PBAT contents.

Table 4.9 The thermal decomposition temperature of compatibilized TPS/PLA blend and compatibilized TPS/PLA/PBAT blends at various PBAT contents.

Composition (%wt)	T₅ (°C)	T₅₀ (°C)	T_{d1} (°C)	T_{d2} (°C)
TPS/PLA/PLA-g-MA (10/90/5phr)	284.83	356.28	364.15	-
TPS/PLA/PLA-g-MA/PBAT (9/81/5phr/10)	290.83	359.33	367.54	403.83
TPS/PLA/PLA-g-MA/PBAT (8/72/5phr/20)	300.10	360.73	366.94	403.31
TPS/PLA/PLA-g-MA/PBAT (7/63/5phr/30)	302.84	361.42	366.93	402.96



4.4.2 Effect of ENR50 content on properties of compatibilized TPS/PLA blends

4.4.2.1 Mechanical properties

Mechanical properties of compatibilized TPS/PLA blend and compatibilized TPS/PLA/ENR50 blends at various ENR50 contents are shown in Table 4.10. The incorporation 10%wt ENR50 into the compatibilized TPS/PLA blend decreased tensile strength and tensile modulus but increased elongation at break as shown in Figure 4.31, Figure 4.32, and Figure 4.33, respectively. This was attributed to the flexibility of ENR (Yew, Mohd Yusof, Mohd Ishak, and Ishiaku, (2005); Zhang et al., (2013); Pongtanayut, Thongpin, and Santawitte, (2013)). Tensile strength and tensile modulus of the compatibilized TPS/PLA/ENR50 blends slightly decreased with increasing ENR50 content to 20% wt. Yew, Mohd Yusof, Mohd Ishak, and Ishiaku, (2005) also found a reduction in tensile strength and tensile modulus of PLA/starch/ENR50 blend with increasing ENR50 loading. Elongation at break of the compatibilized TPS/PLA/ENR50 blend was maximum at ENR50 content of 20%wt. ENR50 content of 30% wt, a little decrease in elongation at break of the blend was observed due to coalescence of ENR50. However, its value was still notably higher than that of the compatibilized TPS/PLA blend.

Impact strength of the compatibilized TPS/PLA/ENR50 blends was enhanced with increasing ENR50 content up to 20%wt as shown in Figure 4.34. The fracture crack ran along the interface between the PLA matrix and the rubber particle. The crack energy can be absorbed and dissipated by the dispersed rubber phase, thus the blend can avoid an abrupt breaking (Zhang et al., (2013)). Basically, the rubber particle in a rubber toughened polymer was a craze starter or a crack initiator

(Jaratrotkamjorn, Khaokong, and Tanrattanakul, (2012)). A further improvement of impact strength of the blend was occurred when 20%wt ENR50 was added. This indicated the fact that more acceptors of the dissipation energy were formed (Zhang et al., (2013)). However, impact strength of the blend was dramatically decreased when ENR50 content was 30%wt. The reduction in impact strength of the blend might be due to coalescence of the dispersed rubber phase (Zhang et al., (2013)). Large particle phases might induce severe stress concentration in wider regions than smaller phases resulting in hastening the initiation of fracture (Todo, Park, Takayama, and Arakawa, (2007)). Impact strength of compatibilized TPS/PLA/ENR50 blend showed similar trend as elongation at break results. The mechanical properties of the blends were dependent upon dispersion and size distribution of rubber particle. When rubber particle size was increased the discontinuity of PLA matrix was intensified (Pongtanayut, Thongpin, and Santawitte, (2013)). This led to a deterioration of mechanical properties of the blends.

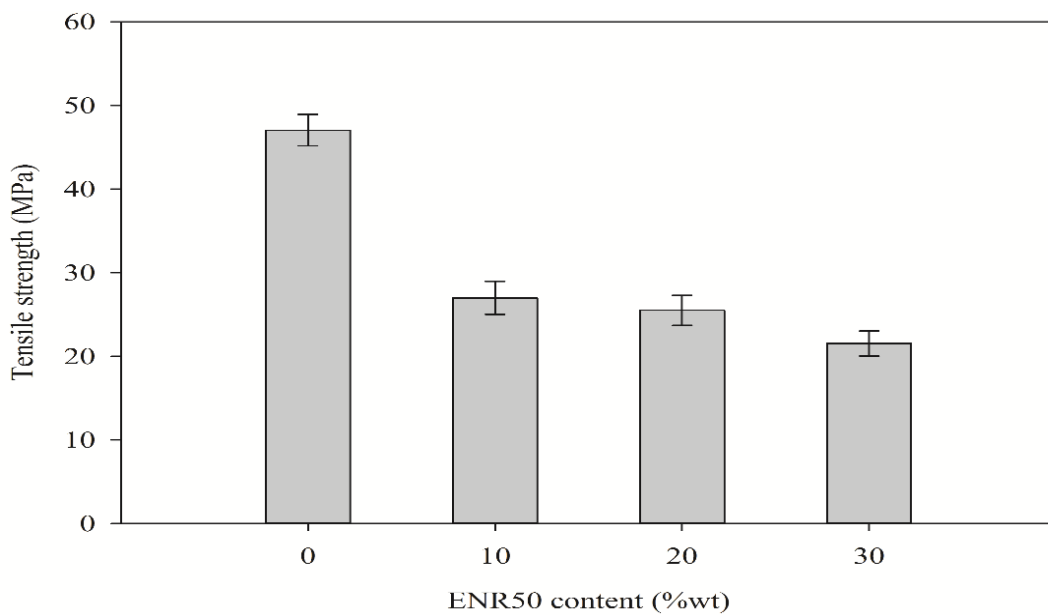


Figure 4.31 Tensile strength of compatibilized TPS/PLA blend and compatibilized TPS/PLA/ENR50 blends at various ENR50 contents.

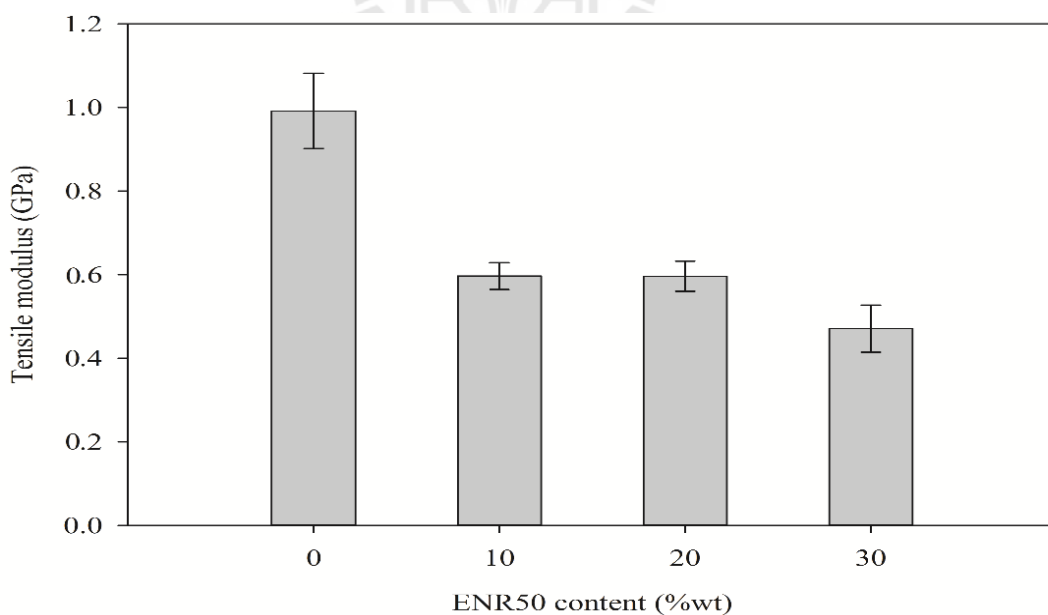


Figure 4.32 Tensile modulus of compatibilized TPS/PLA blend and compatibilized TPS/PLA/ENR50 blends at various ENR50 contents.

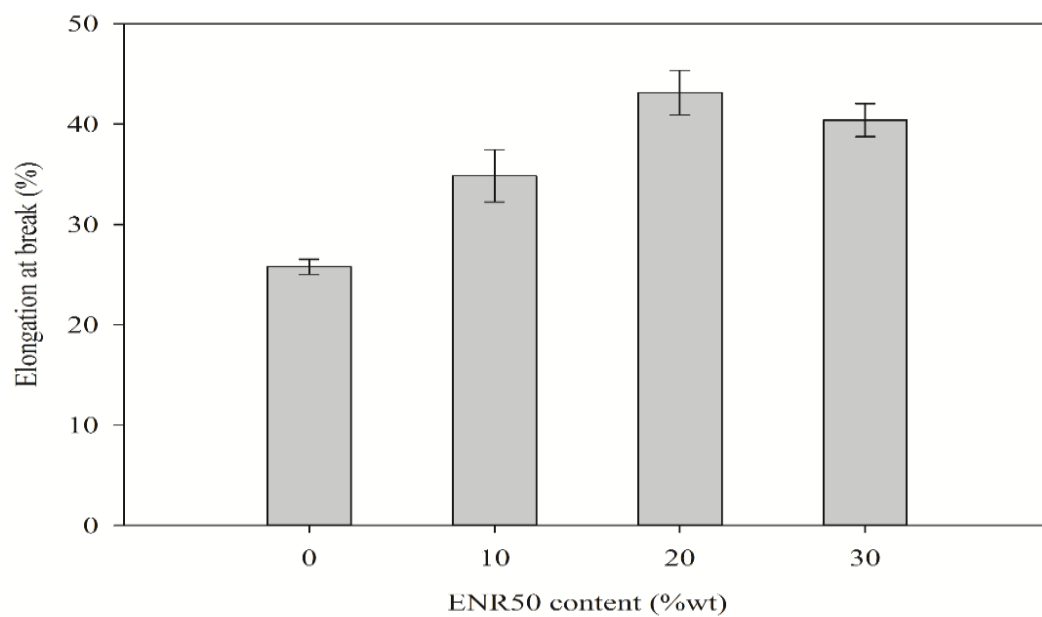


Figure 4.33 Elongation at break of compatibilized TPS/PLA blend and compatibilized TPS/PLA/ENR50 blends at various ENR50 contents.

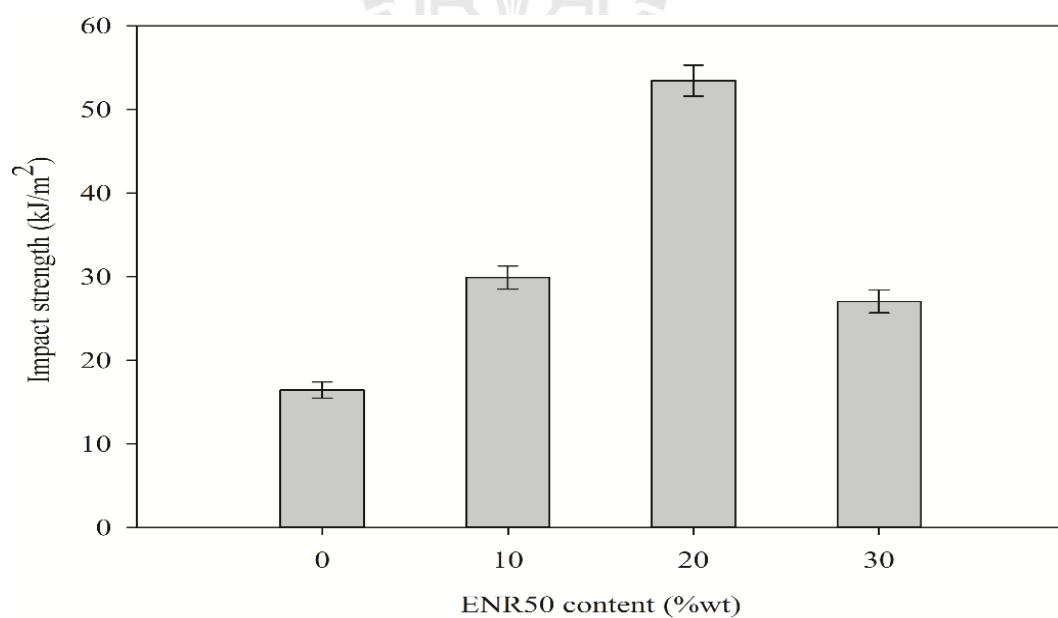


Figure 4.34 Impact strength of compatibilized TPS/PLA blend and compatibilized TPS/PLA/ENR50 blends at various ENR50 contents.

Table 4.10 Mechanical properties of compatibilized TPS/PLA blend and compatibilized TPS/PLA/ENR50 blends at various ENR50 contents.

Composition (%wt)	Tensile strength (MPa)	Tensile modulus (GPa)	Elongation at break (%)	Impact strength (kJ/m²)
TPS/PLA/PLA-g-MA (10/90/5phr)	47.06±1.88	0.99±0.09	25.79±0.75	16.43±0.96
TPS/PLA/PLA-g-MA/ENR50 (9/81/5phr/10)	26.99±1.98	0.59±0.03	34.84±2.61	29.90±1.38
TPS/PLA/PLA-g-MA/ENR50 (8/72/5phr/20)	25.49±1.81	0.59±0.03	43.14±2.23	53.45±1.85
TPS/PLA/PLA-g-MA/ENR50 (7/63/5phr/30)	21.53±1.49	0.47±0.05	40.39±1.65	28.76±2.87

4.4.2.2 Morphological properties

SEM micrographs of the freeze fractured surface of compatibilized TPS/PLA blend and compatibilized TPS/PLA/ENR50 blends at various ENR50 contents are shown in Figure 4.35. When 10%wt ENR50 was added into the compatibilized TPS/PLA blend, small size of ENR50 dispersed phase was observed. Pongtanayut, Thongpin, and Santawitte, (2013) found very fine particle of ENR50 dispersion in PLA matrix due to the partial compatibility between PLA and ENR50. Chemical interaction probably occurred between oxirane ring on ENR50 with hydroxyl group in PLA resulting in enhanced compatibility of the blend (Zhang et al., (2013)). This was reasonable to believe that ENR50 might have a good toughening effect on PLA due to enhanced compatibility with PLA. With increasing ENR50 content to 20%wt, ENR50 phase size was slightly increased due to coalescence phenomena as shown in Figure 4.35(c). ENR50 phase size at 30%wt in the blend was larger than 20%wt ENR50 indicated that a large particle size and weak adhesion would result in poor mechanical properties of the blends (Todo, Park, Takayama, and Arakawa, (2007)). Stress concentration usually took place in the vicinity of the dispersed phase due to the difference of elastic modulus between the rubber phase and the surrounding PLA matrix and initiated localized damages in this region resulting in the reduction of strength and toughness at high rubber content (Juntuek, Ruksakulpiwat, Chumsamrong, and Ruksakulpiwat, (2012)). Moreover, TPS phase size was large with adding 30%wt ENR50. This might be because ENR50 phase interrupted dispersion of TPS phase in the blend as shown in Figure 4.35(d). SEM micrographs of the tensile fractured surface of compatibilized TPS/PLA blend and compatibilized TPS/PLA/ENR50 blends at

various ENR50 contents are shown in Figure 4.36. Figure 4.36(b-d) showed ductile fracture in the blends toughened with ENR50.

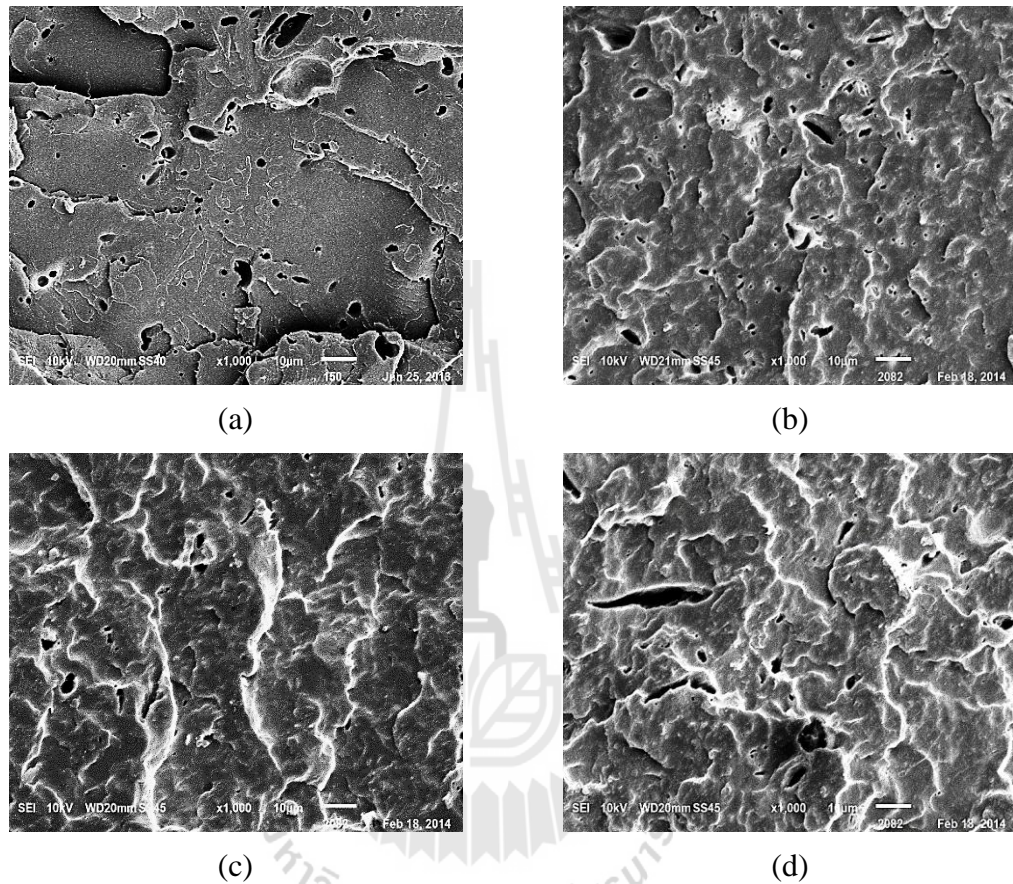


Figure 4.35 SEM micrographs of the freeze fractured surface at 1000x magnification (a) TPS/PLA/PLA-g-MA 10/90/5phr blend, (b) TPS/PLA/PLA-g-MA/ENR50 9/81/5phr/10 blend, (c) TPS/PLA/PLA-g-MA/ENR50 8/72/5phr/20 blend, and (d) TPS/PLA/PLA-g-MA/ENR50 7/63/5phr/30 blend.

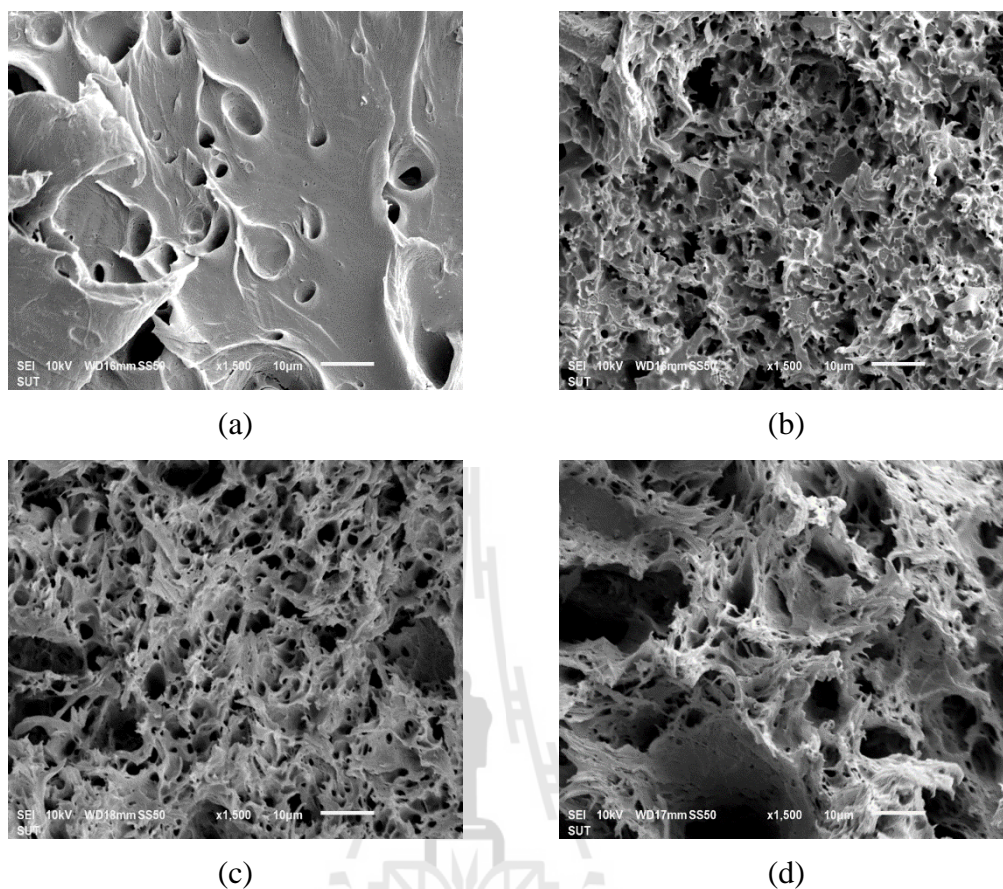


Figure 4.36 SEM micrographs of the tensile fractured surface at 1000x magnification (a) TPS/PLA/PLA-g-MA 10/90/5phr blend, (b) TPS/PLA/PLA-g-MA/ENR50 9/81/5phr/10 blend, (c) TPS/PLA/PLA-g-MA/ENR50 8/72/5phr/20 blend, and (d) TPS/PLA/PLA-g-MA/ENR50 7/63/5phr/30 blend.

4.4.2.3 Thermal properties

Thermal properties of compatibilized TPS/PLA blend and compatibilized TPS/PLA/ENR50 blends at various ENR50 contents were investigated by DSC. The determined data are listed in Table 4.11. DSC curves of compatibilized TPS/PLA blend and compatibilized TPS/PLA/ENR50 blends are shown

in Figure 4.37. T_g and T_m of PLA in the compatibilized TPS/PLA blend slightly decreased with increasing ENR50 content due to enhanced compatibility between PLA and ENR50 (Zhang et al., (2011)). T_{cc} of PLA in the compatibilized TPS/PLA blend increased with incorporating 10% wt ENR50. This implied that the rubber phase could hinder mobility of PLA in the blend (Pongtanayut, Thongpin, and Santawitte, (2013)). ΔH_m , ΔH_c , and χ_c of PLA in the compatibilized TPS/PLA/ENR50 blend were lower when compared with the compatibilized TPS/PLA blend. ENR50 probably hindered the formation of PLA crystal due to interaction between PLA and ENR molecular chains (Zhang et al., (2013)).

T_{cc} of PLA in the compatibilized TPS/PLA/ENR50 blend increased with increasing ENR50 content which indicated that large ENR phase size decreased chain mobility of PLA. Somdee, (2009) also found that T_{cc} of PLA was increased with increasing rubber content. On the other hand, increasing ENR50 content led to decrease in ΔH_m , ΔH_c , and χ_c . This was probably indicated that ENR phase restricted the crystallization of PLA (Maneechavakajone, 2011). Pongtanayut, Thongpin, and Santawitte, (2013) reported that increasing rubber content resulted in the formation of larger phase size and caused a lower interfacial contact area. The crystallinity was therefore decreased.

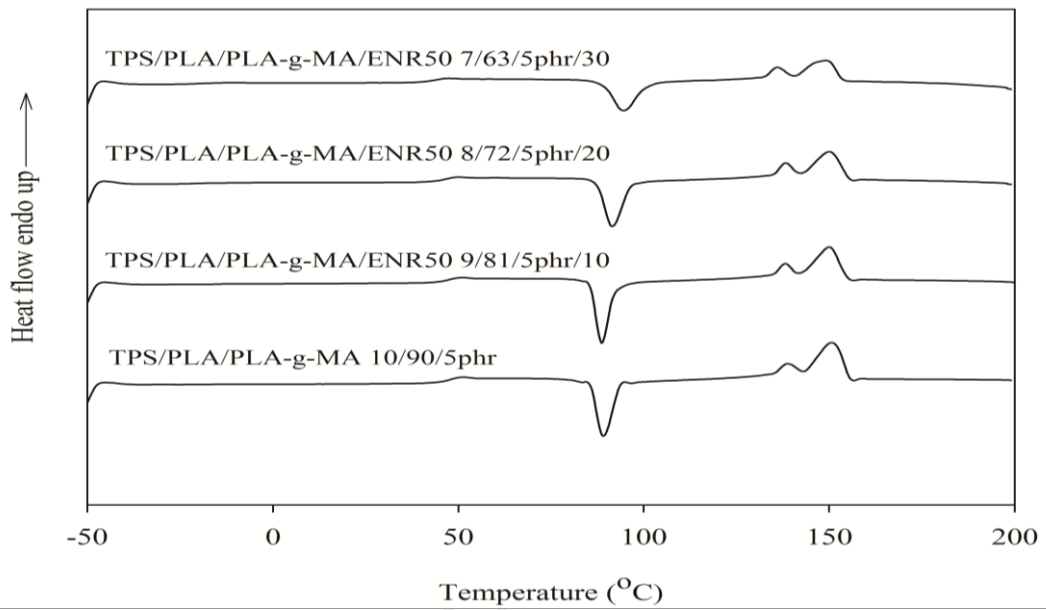


Figure 4.37 DSC thermograms of compatibilized TPS/PLA blend and compatibilized TPS/PLA/ENR50 blends at various ENR50 contents (the second heating, heating rate 5°C/min).

Table 4.11 Thermal characteristics of compatibilized TPS/PLA blend and compatibilized TPS/PLA/ENR50 blends at various ENR50 contents.

Composition (%wt)	T _g (°C)	T _{cc} (°C)	T _{m1} (°C)	T _{m2} (°C)	ΔH _c (J/g)	ΔH _m (J/g)	χ _c (%)
TPS/PLA/PLA-g-MA (10/90/5phr)	46.3	86.9	135.7	147.1	41.49	46.55	57.71
TPS/PLA/PLA-g-MA/ENR50 (9/81/5phr/10)	45.1	88.3	135.0	146.0	33.27	38.25	52.72
TPS/PLA/PLA-g-MA/ENR50 (8/72/5phr/20)	44.8	91.3	135.0	145.1	31.61	32.88	50.96
TPS/PLA/PLA-g-MA/ENR50 (7/63/5phr/30)	43.1	92.4	134.1	144.0	26.28	27.14	48.05



TGA and DTG curves of compatibilized TPS/PLA blend and compatibilized TPS/PLA/ENR50 blends at various ENR50 contents are demonstrated in Figure 4.38 and 4.39, respectively. All the compatibilized TPS/PLA/ENR50 blends illustrated two decomposition steps of TPS/PLA blend and ENR50. Thermal decomposition temperature at 5% weight loss (T_5), thermal decomposition temperature at 50% weight loss (T_{50}), and their thermal decomposition temperature of TPS/PLA (T_{d1}) and ENR50 (T_{d2}) in the compatibilized TPS/PLA blend and the compatibilized TPS/PLA/ENR50 blends are summarized in Table 4.12.

When 10% wt ENR50 was added, T_5 , T_{50} , T_{d1} , and T_{d2} of the compatibilized TPS/PLA/ENR50 blend were decreased. This suggested that thermal stability of the compatibilized TPS/PLA blend reduced with incorporating ENR50. Pongtanayut, Thongpin, and Santawitte, (2013) also found degradation temperature of PLA was decreased when ENR was added into PLA. With increasing ENR50 content, T_5 of the compatibilized TPS/PLA/ENR50 blends was increased. However, T_{50} , T_{d1} , and T_{d2} of the compatibilized TPS/PLA/ENR50 blend were decreased with increasing ENR50 content. Zhang et al, (2013) found that increasing ENR50 content greatly reduced thermal stability of PLA. However, T_{d2} of the compatibilized TPS/PLA/ENR50 blends insignificantly changed with increasing ENR50 content.

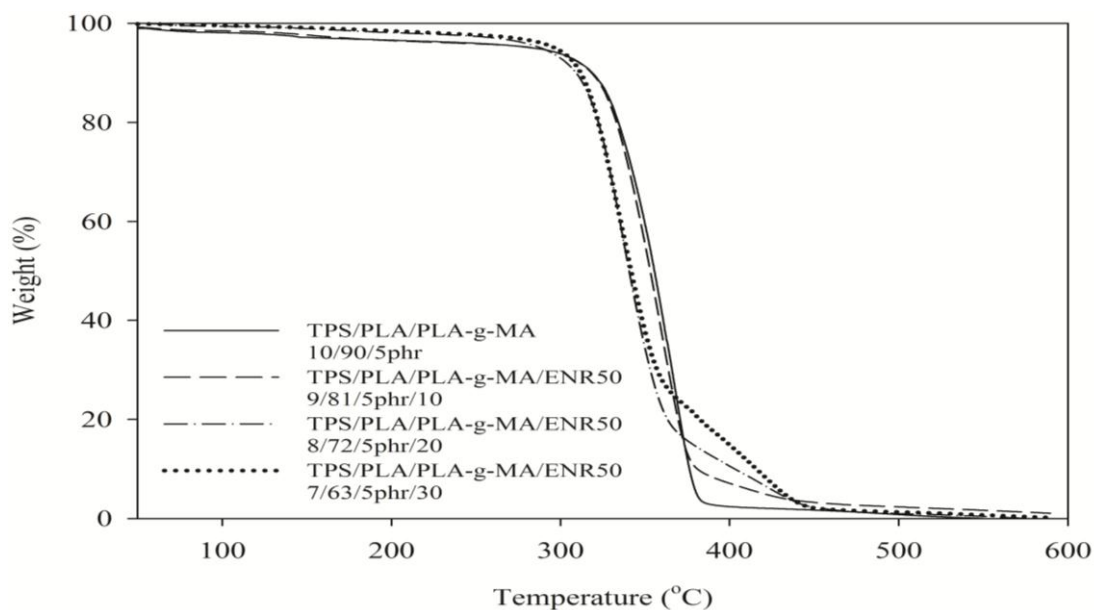


Figure 4.38 TGA thermograms of compatibilized TPS/PLA blend and compatibilized TPS/PLA/ENR50 blends at various ENR50 contents.

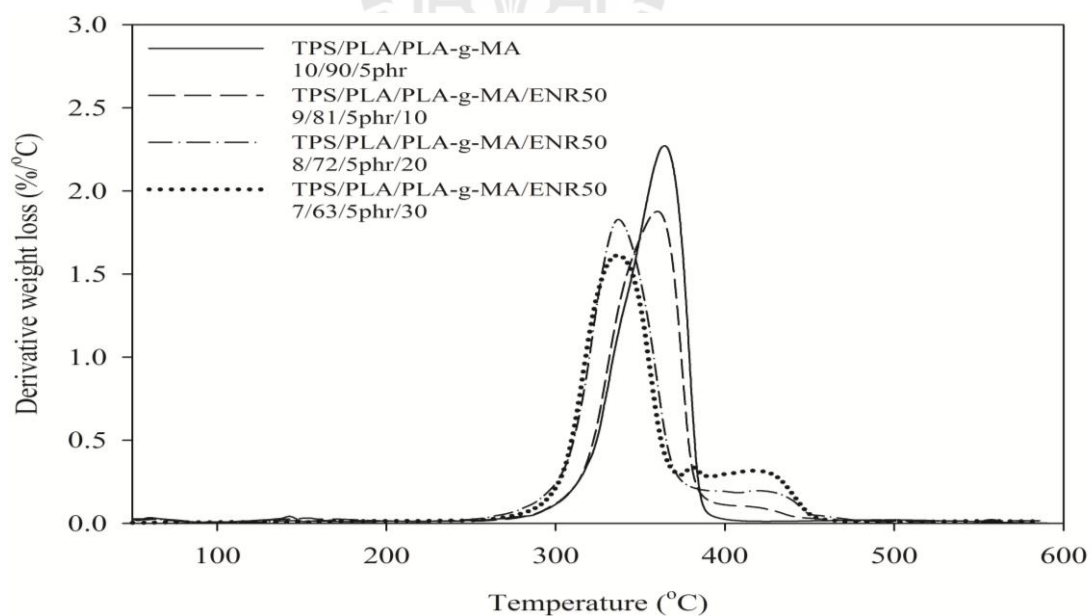
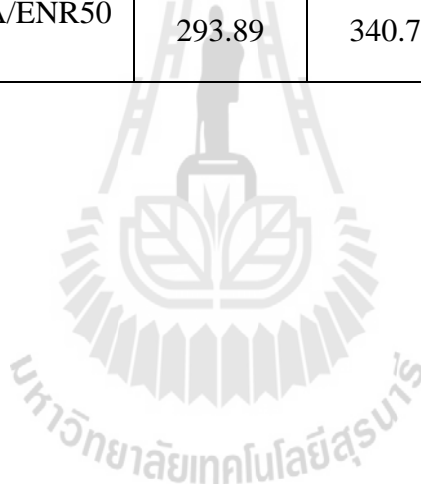


Figure 4.39 DTG thermograms of compatibilized TPS/PLA blend and compatibilized TPS/PLA/ENR50 blends at various ENR50 contents.

Table 4.12 The thermal decomposition temperature of compatibilized TPS/PLA blend and compatibilized TPS/PLA/ENR50 blends at various ENR50 contents.

Composition (%wt)	T₅ (°C)	T₅₀ (°C)	T_{d1} (°C)	T_{d2} (°C)
TPS/PLA/PLA-g-MA (10/90/5phr)	284.83	360.11	368.15	-
TPS/PLA/PLA-g-MA/ENR50 (9/81/5phr/10)	280.14	353.09	360.22	421.60
TPS/PLA/PLA-g-MA/ENR50 (8/72/5phr/20)	291.53	341.94	337.03	421.82
TPS/PLA/PLA-g-MA/ENR50 (7/63/5phr/30)	293.89	340.73	336.91	421.69



CHAPTER V

CONCLUSIONS

Effect of thermoplastic starch (TPS) content on mechanical, thermal, and morphological properties of TPS/poly(lactic acid) (PLA) blends were studied. TPS was obtained from cassava starch and glycerol at ratio of 70/30%wt. With the addition of 10%wt TPS, tensile strength, tensile modulus, and impact strength of PLA were decreased while elongation at break was increased due to ductile behavior of TPS. Tensile and impact properties of TPS/PLA blends were decreased with increasing TPS content due to poor interfacial adhesion between TPS and PLA. TPS/PLA (10/90) blend showed the highest tensile and impact properties. With incorporating 10%wt TPS into PLA, glass transition temperature (T_g) and melting temperature (T_m) of PLA in the blend were decreased. This indicated some degree of miscibility between the blend components. Cold crystallization temperature (T_{cc}) of PLA in the blend was decreased whereas degree of crystallinity (χ_c) was increased with adding 10%wt TPS due to nucleating effect of TPS. With increasing TPS content, T_g and T_m of PLA in the blends insignificantly changed while T_{cc} was decreased. Thermal stability of the blends was decreased with increasing TPS content because the products of pyrolytic decomposition of TPS involved thermal degradation of PLA. SEM micrographs revealed that the TPS/PLA blend was an immiscible blend.

Effect of PLA grafted with maleic anhydride (PLA-g-MA) content on mechanical, thermal, and morphological properties of the TPS/PLA blends was investigated. The addition of PLA-g-MA increased mechanical properties of the blends

due to enhanced compatibility between TPS and PLA. The highest mechanical properties of the blend was obtained when 5 phr of PLA-g-MA was incorporated. With increasing PLA-g-MA content to 7 phr, mechanical properties of the compatibilized blend were decreased. This was because more anhydride molecules were capable of activating chain scission of PLA molecules resulting in decreased mechanical properties of the blends. T_g and T_m of PLA in the blends were decreased with increasing PLA-g-MA content due to improved interfacial adhesion between TPS and PLA. T_{cc} was decreased with increasing PLA-g-MA content which indicated the enhancement of chain mobility of PLA. χ_c of PLA in the blends was increased when PLA-g-MA content was increased. Thermal stability of the compatibilized blends was higher than the uncompatibilized blend due to improved interfacial adhesion between TPS and PLA. PLA-g-MA content exhibited an insignificant effect on thermal stability of the blends. SEM micrographs of the compatibilized blends exhibited finer morphology when compared with the uncompatibilized blend.

Effect of poly(butylene adipate-co-terephthalate) (PBAT) content on mechanical, thermal, and morphological properties of the compatibilized blends was studied. Tensile strength and tensile modulus of the blends were decreased with increasing PBAT content while elongation at break and impact strength were increased due to the result of the rubber nature of PBAT. T_g of PLA in the blend was decreased with the addition of 10%wt PBAT due to partial miscibility between PLA and PBAT. On the other hand, the addition of PBAT reduced T_{cc} of PLA in the blend which was consistent with the fact that PBAT enhanced crystalline ability of PLA. However, the incorporation of 10%wt PBAT did not affect T_m of PLA in the blend. χ_c of PLA in the blends was increased with adding 10%wt of PBAT because PBAT acted as a nucleating

agent. As PBAT content was increased T_g , T_m , T_{cc} , and χ_c of PLA in the blends did not change. Thermal stability of the blends was increased with increasing PBAT content. SEM micrographs showed some features of ductile fracture in the blends toughened with PBAT.

Effect of epoxidized natural rubber with 50% epoxidation (ENR50) content on mechanical, thermal, and morphological properties of the compatibilized blends was investigated. Tensile strength and tensile modulus of the blend were decreased with the incorporation of 10%wt ENR50 whereas elongation at break and impact strength were increased due to the flexibility of ENR. With increasing ENR50 content to 20%wt, tensile strength and tensile modulus of the blend slightly decreased. However, elongation at break and impact strength of the blend was maximum at 20%wt ENR50. When 30%wt of ENR50 was added, mechanical properties of the compatibilized blend were dropped. This might be due to coalescence of ENR50. T_g and T_m of PLA in the blends were decreased with increasing ENR50 content due to partial miscibility between PLA and ENR50. T_{cc} of PLA in the blends increased with increasing ENR50 content. This implied that the rubber phase could hinder mobility of PLA in the blends. χ_c of PLA in the blends was decreased with increasing ENR50 content which indicated that ENR phase restricted the crystallization of PLA. Thermal stability of the blends was decreased with increasing ENR50 content due to chain scission of PLA. SEM micrographs showed ductile fracture in the blends toughened with ENR50. However, TPS phase size was increased with adding 30%wt of ENR. This might be because ENR50 phase interrupted the dispersion of TPS phase in the blend. This result led to poor mechanical properties of the compatibilized blend.

REFERENCES

- Ahmad, Z., Anuar, H., and Yusof, Y. (2011). The study of biodegradable thermoplastic sago starch. **Key Eng. Mater.** 471-472: 397-402.
- Bitinis, N., Verdejo, R., Cassagnau, P., Lopez-Manchado, M. A. (2011). Structure and properties of polylactide/natural rubber blends. **Mater. Chem. Phys.** 129: 823-831.
- Cai, J., Liu, M., Wang, L., Yao, K., Li, S., and Xiong, H. (2011). Isothermal crystallization kinetics of thermoplastic starch/poly(lactic acid) composites. **Carbohydr. Polym.** 86: 941-947.
- Da Roz, A. L., Carvalho, A. J. F., Gandini, A., and Curvelo, A. A. S. (2006). The effect of plasticizers on thermoplastic starch compositions obtained by melt processing. **Carbohydr. Polym.** 63: 417-424.
- Dong, W., Zou, B., Yan, Y., Ma, P., and Chen, M. (2013). Effect of chain-extenders on the properties and hydrolytic degradation behavior of the poly(lactide)/poly(butylene adipate-co-terephthalate) blends. **Int. J. Mol. Sci.** 14: 20189-20203.
- Ferrarezi, M. M. F., Taipina, M. D. O., Silva, L. C. E. D., Goncalves, M. D. C. (2013). Poly(ethylene glycol) as a compatibilizer for poly(lactic acid)/thermoplastic starch blends. **J. Polym. Environ.** 21: 151-159.
- Gao, H., Hu, S., Su, F., Zhang, J., Tang, G. (2011). Mechanical, thermal, and biodegradability properties of PLA/modified starch blends. **Polym. Compos.** 32: 2093-2100.

- Garlotta, D. (2001). A literature review of poly(lactic acid). **J. Polym. Environ.** 9: 63-84.
- Huang, M., Yu, J., and Ma, X. (2005). Ethanolamine as a novel plasticizer for thermoplastic starch. **Polym. Degrad. Stab.** 90: 501-507.
- Huneault, A., and Li, H. (2007). Morphology and properties of compatibilized polylactide/thermoplastic starch blends. **Polymer.** 48: 270-280.
- Jaratrotkamjorn, R., Khaokong, C. and Tanrattanakul, V. (2012). Toughness enhancement of poly(lactic acid) by melt blending with natural rubber. **J. Appl. Polym. Sci.** 124: 5027-5036.
- Jiang, L., Wolcott, M. P., and Zhang, J. (2006). Study of biodegradable polylactide/poly (butylene adipate-co-terephthalate) blends. **Biomacromolecules.** 7: 199-207.
- John, J., Tang, J., Yang, Z., Bhattacharya, M. (1997). Synthesis and characterization of anhydride-functional polycaprolactone. **J. Polym. Sci., Part A: Polym. Chem.** 35: 1139-1148.
- Juntuek, P., Ruksakulpiwat, C., Chumsamrong, P., and Ruksakulpiwat, Y. (2012). Effect of glycidyl methacrylate-grafted natural rubber on physical properties of polylactic acid and natural rubber blends. **J. Appl. Polym. Sci.** 125: 745-754.
- Karagoz, S. and Ozkoc, G. (2013). Effects of a diisocyanate compatibilizer on the properties of citric acid modified thermoplastic starch/poly(lactic acid) blends. **Polym. Eng. Sci.** 53: 2183-2193.
- Kaseem, M., Hamad, K., and Deri, F. (2012). Thermoplastic starch blends: A review of recent works. **Polym. Sci.** 54: 165-176.
- Ke, T., Sun, X. (2003). Thermal and mechanical properties of poly(lactic acid) and starch blends with various plasticizer. **Trans. Asae.** 44: 945-953.

- Kim, G.-M. and Michler, G. H. (1998). Micromechanical deformation processes in toughened and particle filled semicrystalline polymers. Part 2: Model representation for micromechanical deformation processes. **Polymer**. 39: 5699-5703.
- Kumar, M., Mohanty, S., Nayak, S. K., Rahail Parvaiz, M. (2010). Effect of glycidyl methacrylate (GMA) on the thermal, mechanical and morphological property of biodegradable PLA/PBAT blend and its nanocomposites. **Bioresour. Technol.** 101: 8406-8415.
- Leadprathom, J., Suttiruengwong, S., Threepopnatkul, P., and Seadan, M. (2010). Compatibilized polylactic acid/thermoplastic starch by reactive blend. **JOM**. 20: 87-90.
- Li, H., and Huneault, M.A. (2008). Crystallization of PLA/thermoplastic starch blends. **Int. Polym. Proc.** 5: 412-418.
- Li, H., and Huneault, M. A. (2011). Effect of chain extension on the properties of PLA/TPS blends. **J. Appl. Polym. Sci.** 122: 134-141.
- Li, S., Xiong, Z., Fei, P., Cai, J., Xiong, H., Tan, J., and Yu, Y. (2013). Parameter characterizing the kinetics of the nonisothermal crystallization of thermoplastic starch/poly(lactic acid) composites as determined by differential scanning calorimetry. **J. Appl. Polym. Sci.** 129: 3566-3573.
- Lin, S., Guo, W., Chen, C., Ma, J., and Wang, B. (2012). Mechanical properties and morphology of biodegradable poly(lactic acid)/poly(butylene adipate-co-terephthalate) blends compatibilized by transesterification. **Mater. Design.** 36: 604-608.

- Ma, X. F., Yu, J. G., and Ma, Y. B. (2005). Urea and formamide as a mixed plasticizer for thermoplastic wheat flour. **Carbohydr. Polym.** 60: 111-116.
- Maneechavakajorn, N. (2011). **Toughness improvement of polylactic acid blown film by adding carboxylated epoxidised natural rubber.** M. Eng. thesis, Chulalongkorn University. Thailand
- Mani, R., Bhattacharya, M., and Tang, J. (1999). Functionalization of polyesters with maleic anhydride by reactive extrusion. **J. Polym. Sci., Part A: Polym. Chem.** 37: 1693-1702.
- Mano, J. F., Koniarova, D., and Reis, R. L. (2003). Thermal properties of thermoplastic starch/synthetic polymer blends with potential biomedical applicability. **J. Mater. Sci. - Mater. Med.** 14: 127-135.
- McNeill, I. C. and Leiper, H. A. (1985). Degradation studies of some polyester and polycarbonates-1. Polylactide: General features of the degradation under programmed heating conditions. **Polym. Degrad. Stab.** 11: 267-285.
- Martin, O., and Averous, L. (2001). Poly(lactic acid): plasticization and properties of biodegradable multiphase systems. **Polymer.** 42: 6209-6219.
- Nashed, G., Rutgers, R. P. G. and Sopade, P. A. (2003). The plasticisation effect of glycerol and water on the gelatinisation of wheat starch. **Starch-Starke.** 55: 131-137.
- Park, J. W., Im, S. S., Kim, S. H., and Kim, Y. H., (2000). Biodegradable polymer blends of poly(l-lactic acid) and gelatinized starch. **Polym. Eng. Sci.** 40: 2539-2550.

- Petinakis, E., et al. (2010). Biodegradation and thermal decomposition of poly(lactic acid)-based material reinforced by hydrophilic fillers. **Polym. Degrad. Stab.** 95: 1704-1707.
- Phetwarotai, W., Potiyaraj, P. and Aht-Ong, D. (2010). Properties of compatibilized polylactide blend films with gelatinized corn and topical starches. **J. Appl. Polym. Sci.** 116: 2305-2311.
- Phetwarotai, W. and Aht-Ong, D. (2011). Reactive compatibilization of polylactide, thermoplastic starch and poly(butylene adipate-co-terephthalate) biodegradable ternary blend films. **Mater. Sci. Forum.** 695: 178-181.
- Ping, X., Kejian, W., Mingyin, J., Meijuan, Y. (2013). Biodegradation and mechanical property of polylactic acid/thermoplastic starch blends with poly(ethylene glycol). **J. Wuhan Univ. Technol.** 28: 157-162.
- Pongtanayut, K., Thongpin, C. and Santawitte, O. (2010). The effect of rubber on morphology, thermal properties and mechanical properties of PLA/NR and PLA/ENR blends. **Energy Procedia.** 34: 888-897.
- Qiao, X., Tang, Z., and Sun, K. (2011). Plasticization of corn starch by polyol mixtures. **Carbohydr. Polym.** 83:659-664.
- Oza, H., Thompson, M. R., Hrymak, A. N., Liu, Q. (2012). Influence of di-functional versus multi-functional chain extenders on the foamability of a potato starch-based biopolymer. **Starch-Starke.** 64: 944-954.
- Ren, J., Fu, H., Ren, T., and Yuan, W. (2009). Preparation, characterization and properties of binary and ternary blends with thermoplastic starch, poly (lactic acid), and poly(butylene adipate-co-terephthalate). **Carbohydr. Polym.** 77: 576-582.

- Rodriguez-Gonzalez, F. J., Ramsay, B.A, and Favis, B. D. (2004). Rheological and thermal properties of thermoplastic starch with high glycerol content. **Carbohyd. Polym.** 58: 139-147.
- Sailaja, R. R. N., Reddy, A. P., and Chanda, M. (2001). Effect of epoxy functionalized compatibilizer on the mechanical properties of low-density polyethylene/plasticized tapioca starch blends. **Polym. Int.** 50: 1352-1359.
- Sarazin, P., Li, G., Orts, W. J., and Favis, B. D. (2008). Binary and ternary blends of polylactide, polycaprolactone and thermoplastic starch. **Polymer.** 49: 599-609.
- Schwach, E., Six, J., and Averous, L. (2008). Biodegradable blends based on starch and poly(lactic acid): Comparison of different strategies and estimate of compatibilization. **J. Polym. Environ.** 16: 286-297.
- Sharma, N., et al. (2001). A study on the effect of pro-oxidant on the thermo-oxidative degradation behavior of sago starch filled polyethylene. **Polym. Degrad. Stab.** 71: 381-393.
- Shi, Q., Chen, C., Gao, L., Jiao, L., Xu, H., and Guo, W. (2011). Physical and degradation properties of binary or ternary blends composed of poly (lactic acid), thermoplastic starch and GMA grafted POE. **Polym. Degrad. Stab.** 96: 175-182.
- Shin, B. Y., Jang, S. H., and Kim, B. S. (2011). Thermal, morphological, and mechanical properties of biobased and biodegradable blends of poly(lactic acid) and chemically modified thermoplastic starch. **Polym. Eng. Sci.** 51: 826-834.
- Shin, B. Y., Jo, G. S., Kang, K. T., Lee, T. L., and Kim, B. S. (2007). Morphology and rheology on the blends of PLA/CMPS. **Macromol. Res.** 15: 291-301.

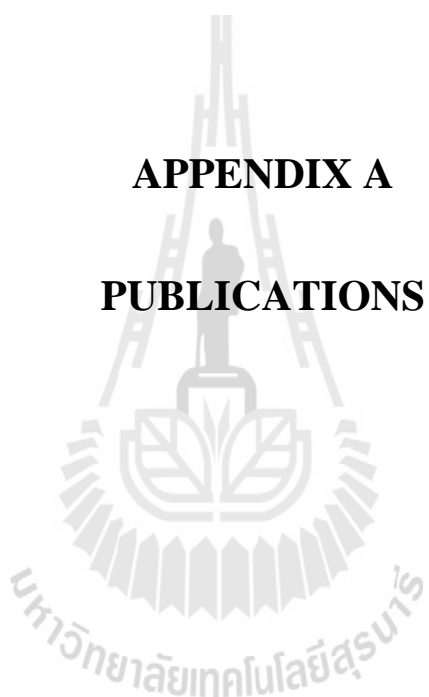
- Somdee, P. (2009). **Natural rubber toughened polylactic acid**. M. Eng. thesis, Suranaree University of Technology. Thailand.
- Sreekumar, P. A., Gopalakrishnan, P., Leblanc, N., and Saiter, J. M. (2010). Effect of glycerol and short sisal fibers on the viscoelastic behavior of wheat flour based thermoplastic. **Composites: Part A**. 41: 991-996.
- Sreekumar, P. A., Leblanc, N., and Saiter, J. M. (2013). Effect of glycerol on the properties of 100% biodegradable thermoplastic based on wheat flour. **J. Polym. Environ.** 21: 388-394.
- Teamsinsungvon, A. (2011). **Physical properties of poly(lactic acid)/poly(butylene adipate-co-terephthalate) blends and their composites**. M. Eng. thesis, Suranaree University of Technology. Thailand.
- Todo, M., Park, S.-D., Takayama, T., and Arakawa, K. (2007). Fracture micromechanisms of bioabsorbable PLLA/PCL polymer blends. **Eng. Fract. Mech.** 74: 1872-1883.
- Tserki, V., Matzinos, P., and Panayiotou, C. (2006). Novel biodegradable composites based on treated lignocellulosic waste flour as filler Part II. Development of biodegradable composites using treated and compatibilized waste flour. **Composites: Part A**. 37: 1231-1238.
- Tsuji, H. (2002). Autocatalytic hydrolysis of amorphous-made polylactides: effect of L-lactic content, tacticity, and enantiomeric polymer blending. **Polymer**. 43: 1789-1796.
- Teixeira, E. M., Da Roz, A. L., Carvalho, A. J. F., and Curvelo, A. A. S. (2007). The effect of glycerol/sugar/water and sugar/water mixtures on the plasticization of thermoplastic cassava starch. **Carbohydr. Polym.** 69: 619-624.

- Teixeira, E. M., et al. (2012). Properties of thermoplastic starch from cassava bagasse and cassava starch and their blends with poly(lactic acid). **Ind. Corp. Prod.** 37: 61-68.
- Vasques, C. T., et al. (2007). Effect of thermal treatment on the stability and structure of maize starch cast films. **Starch-Starke.** 59: 161-170.
- Victor, H. O., Brostow, W., Chonkaew, W., and Lopez, B. L. (2009). Preparation and characterization of poly(lactic acid)-g-maleic anhydride + starch blends. **Macromol. Symp.** 277: 69-80.
- Wang, H.-Y. and Huang M.-F. (2007). Preparation, characterization and performances of biodegradable thermoplastic starch. **Polym. Adv. Technol.** 18: 910-915.
- Wang, N., Yu, J., and Ma, X. (2008). Preparation and characterization of compatible thermoplastic dry starch/poly(lactic acid). **Polym. Compos.** 29: 551-559.
- Wang, N., Yu, J., Chang, P. R., and Ma, X. (2008). Influence of formamide and water on properties of thermoplastic starch/poly(lactic acid) blends. **Carbohydr. Polym.** 71: 109-118.
- Wootthikanokkhan, J., Wongta, N., Sombatsompop, N., Kositchaiyong, A., Wong-On, J., Isarankura na Ayuthaya, S., Kaabbuathong, N. (2012). Effect of blending conditions on mechanical, thermal, and rheological properties of plasticized poly(lactic acid)/maleated thermoplastic starch blends. **J. Appl. Polym. Sci.** 124: 1012-1019.

- Wootthikanokkhan, J., Kasemwananimit, P., Sombatsompop, N., Kositchaiyong, A., Isarankura na Ayutthaya, S., and Kaabuathong, N., (2012). Preparation of modified starch-grafted poly(lactic acid) and a study on compatibilizing efficacy of the copolymers in poly(lactic acid)/thermoplastic starch blends. **J. Appl. Polym. Sci.** 126: E389-E396.
- Xiao, H., Lu, W., and Yeh, J.-T. (2009). Crystallization behavior of fully biodegradable poly(lactic acid)/poly(butylene adipate-co- terephthalate) blends. **J. Appl. Polym. Sci.** 112: 3754-3763.
- Xiong, Z., Li, C., Ma, S., Feng, J., Yang, Y., Zhang, R., and Zhu, J. (2013). The properties of poly(lactic acid)/starch blends with a functionalized plant oil: Tung oil anhydride. **Carbohyd. Polym.** 95: 77-84.
- Yang, J. H., Yu, J. G., and Ma, X. F. (2006). Retrogradation of ethylenebisformamide and sorbitol plasticized corn starch (ESPTPS). **Starch-Starke.** 58: 580-586.
- Yasuniwa, M., Tsubakihara, S., Sugimoto, Y., Nakafuku, C. (2004). Thermal analysis of the double-melting behavior of poly(l-lactic acid). **J. Polym. Sci., Part B: Polym. Phys.** 42: 25-32.
- Yew, G. H., Mohd Yusof, A. M., MohdIshak, Z. A., and Ishiaku, U. S. (2005). Water absorption and enzymatic degradation of poly(lactic acid)/rice starch composites. **Polym. Degrad. Stab.** 90: 488-500.
- Yokesahachart, C. and Yoksan, R. (2011). Effect of amphiphilic molecules on characteristics and tensile properties of thermoplastic starch and its blends with poly(lactic acid). **Carbohyd. Polym.** 83: 22-31.
- Yu, L., and Christie, G., (2001). Measurement of starch thermal transitions using differential scanning calorimetry. **Carbohyd. Polym.** 52: 101-110.

- Yu, L., Petinakis, E., Dean, K., Liu, H., and Yuan, Q. (2011). Enhancing compatibilizer function by controlled distribution in hydrophobic polylactic acid/hydrophilic starch blends. **J. Appl. Polym. Sci.** 119: 2189-2195.
- Yunos, M. Z. B. and Rahman, W. A. W. A. (2011). Effect of glycerol on performance rice straw/starch based polymer. **J. Appl. Polym. Sci.** 11: 2456-2459.
- Zhang, C., Man., C., Pan, Y., Wang, W., Jiang, L., and Dan, Y. (2011). Toughening of polylactide with natural rubber grafted with poly(butyl acrylate). **Polym. Int.** 60: 1548-1555.
- Zhang, K., Ran, X., Zhuang, Y., Yao, B., and Dong, L. (2009). Blends of poly(lactic acid) with thermoplastic starch acetylated starch. **Chem. Res. Chinese U.** 25: 748-753.
- Zhang, J. S., Yu, J. G., Wu, Y., and Ma, X. F. (2008). Synthesis of aliphatic amidediol and used as a novel mixed plasticizer for thermoplastic starch. **Chin. Chem. Lett.** 19: 395-398.
- Zhang, C., Wang, W., Huang, Y., Pan, Y., Jiang, L., Dan, Y., Luo, Y., and Peng, Z. (2013). Thermal, mechanical and rheological properties of polylactide toughened by epoxidized natural rubber. **Mater. Design.** 45: 198-205.
- Zhao, P., Liu, W., Wu, Q., and Ren, J. (2010). Preparation, mechanical, and thermal properties of biodegradable polyester/poly(lactic acid) blends. **J. Nanomater.** 2010. doi: 10.1155/2010/287082.

APPENDIX A
PUBLICATIONS



List of Publications

- Tachaphiboonsap, S and Jarukumjorn, K. (2012). Mechanical and morphological properties of thermoplastic starch/poly(lactic acid) blends. **In Abstract of the 3rd Research Symposium on Petrochemical and Materials Technology and the 18th PPC Symposium on Petroleum, Petrochemicals, and Polymers** (pp 84-85). Bangkok, Thailand.
- Tachaphiboonsap, S and Jarukumjorn, K. (2013). Mechanical, thermal, and morphological properties of thermoplastic starch/poly(lactic acid) blends. **In Proceeding of Pure and Applied Chemistry International Conference 2013 (PACCON 2013)** (pp 677-680). Chonburi, Thailand.
- Tachaphiboonsap, S and Jarukumjorn, K. (2013). Toughness and compatibility improvement of thermoplastic starch/poly(lactic acid) blends. **Adv. Mater. Res.** 747: 67-71.
- Tachaphiboonsap, S and Jarukumjorn, K. (2013). Effect of poly(lactic acid) grafted with maleic anhydride on mechanical and morphological properties of thermoplastic starch/poly(lactic acid) blends. **In Proceeding of the 3rd International Conference on Biodegradable and Biobased Polymers (BIOPOL-2013)**. Rome, Italy.
- Tachaphiboonsap, S and Jarukumjorn, K. (2014). Mechanical, thermal, and morphological properties of thermoplastic starch/poly(lactic acid)/poly(butylene adipate-co-terephthalate) blends. **Adv. Mater. Res.** 970: 312-316.



The 3rd Research Symposium on Petrochemical and Materials Technology and The 18th PPC Symposium on Petroleum, Petrochemicals, and Polymers
 April 24, 2012, Ballroom, Queen Sirikit National Convention Center, Bangkok, Thailand

Poster Sessions

PA-P(10)-42 Mechanical and Morphological Properties of Thermoplastic Starch/ Poly(lactic acid) Blends

Sujaree Tachaphiboonsap^{a,b}, Kasama Jarukumjorn^{a,b}

^{a)}School of Polymer Engineering, Institute of Engineering, Suranaree University of Technology

^{b)}Center of Excellence on Petrochemical and Materials Technology

Biodegradable polymers have received considerable attention for replacement of petroleum-derived polymers due to environmental concern. Poly(lactic acid) (PLA), produced from renewable resources, is one of the most widely used biodegradable polymers. PLA has good mechanical properties (high strength and high modulus). However, its brittleness and high cost limit its application. Due to its low cost, biodegradable, and availability as a renewable source, starch has been used as filler for environmental friendly polymers. Thermoplastic starch (TPS) is a biodegradable material based on starch. Incorporation of TPS into PLA matrix can reduce material cost and increases its biodegradation rate. PLA and TPS form immiscible blend leading to poor mechanical properties of the blend. The compatibility of the blend can be improved by adding compatibilizers. PLA/TPS blends are prepared using an internal mixer. TPS is made by mixing cassava starch (70 wt%) and glycerol (30 wt%). Poly(lactic acid) grafted maleic anhydride (PLA-g-MA) is used as a compatibilizer. Mechanical and morphological properties of the blends are investigated.

MECHANICAL, THERMAL, AND MORPHOLOGICAL PROPERTIES OF THERMOPLASTIC STARCH/POLY(LACTIC ACID) BLENDS

Sujaree Tachaphiboonsap^{1,2}, Kasama Jarukumjorn^{1,2*}

¹ School of Polymer Engineering, Institute of Engineering, Suranaree University of Technology, Nakhon Ratchasima, 30000 Thailand

² Center of Excellence on Petrochemical and Materials Technology, Bangkok, 10330 Thailand

*Author for correspondence; E-mail: kasama@sut.ac.th, Tel. +66 44 224437, Fax. +66 44 224605

Abstract: Thermoplastic starch (TPS)/poly (lactic acid) (PLA) blends were prepared and their mechanical, thermal, and morphological properties were investigated. TPS was obtained from cassava starch and glycerol at ratio of 70:30 w/w. TPS contents were varied from 10 to 40 wt%. Poly(lactic acid) grafted maleic anhydride (PLA-g-MA) was used as a compatibilizer. Tensile and impact properties of the blends were decreased when the amount of TPS was increased. With increasing TPS content, the decomposition temperature of PLA was decreased while the decomposition temperature of TPS was increased. Incorporating PLA-g-MA resulted in an improvement of the mechanical properties of the blends. The compatibilized blends exhibited much finer dispersed phase size.

1. Introduction

Poly (lactic acid) (PLA), derived from renewable resources, is the most widely used biodegradable polymers. PLA possesses high strength and high modulus. However, its high cost and brittleness limit its applications.

Starch has been used as filler for polymers due to its low cost, biodegradable, and availability as a renewable resource. However, melting temperature of starch is close to degradation temperature [1, 2]. Therefore, starch has been modified to obtain thermoplastic starch (TPS). Glycerol is often used as a plasticizer due to its high boiling point and low cost [3]. TPS/PLA blends exhibit low mechanical properties due to poor compatibility between TPS and PLA [4, 5].

The compatibility of TPS/PLA blend can be achieved by adding compatibilizer [6, 7] or modified matrix [8, 9, 10, 11]. Schwach et al. [6] used PLA grafted with amylose (PLA-g-A) to enhance compatibility of TPS/PLA blends. With the addition of PLA-g-A, tensile modulus of the blend did not change but tensile strength and elongation at break increased. Woothikanokkhan et al. [7] reported that mechanical properties of TPS/PLA blends were increased when poly(lactic acid) grafted with maleated thermoplastic starch (PLA-g-MTPS) was used as a compatibilizer.

In this study, the effects of TPS content and adding compatibilizer on mechanical, thermal, and morphological properties of TPS/PLA blends were investigated.

2. Materials and Methods

2.1 Materials

Poly(lactic acid) (PLA, 4042D) was supplied from Natural Works LLC. Cassava starch was obtained from Bangkok Interfood Co., Ltd. Glycerol was supplied from Carlo Erba Reagenti Co., Ltd. 2, 5-bis (tert-butylperoxy)-2, 5 dimethylhexane (L101) and maleic anhydride (MA) were purchased from Sigma-Aldrich. Poly(lactic acid) grafted with maleic anhydride (PLA-g-MA) prepared in-house was used as a compatibilizer [12].

2.2 Preparation

TPS was obtained from cassava starch and glycerol at ratio of 70:30 w/w. Cassava starch was dried at 70°C for 4 h before mixing. Sample was prepared using an internal mixer (Hakke Rheomix, 3000P). The mixing temperature was kept at 120°C and the rotor speed of 60 rpm. The mixing time was 10 min.

TPS/PLA blends were prepared using an internal mixer (Hakke Rheomix, 3000P). TPS and PLA were dried at 70°C for 4 h before mixing. The mixing temperature was kept at 170°C and the rotor speed of 60 rpm. The specimens were processed by a compression molding machine (Labtech, LP20-B) at the temperature of 170°C and pressure of 100 MPa for 10 min. Designation and composition of TPS/PLA blends are shown in Table 1.

2.3 Characterization

Tensile properties of PLA and TPS/PLA blends were tested according to ASTM D638 using an universal testing machine (Instron, 5565) with a load cell 5 kN and crosshead speed of 1 mm/min.

Izod impact test was performed according to ASTM D256 using an impact testing machine (Atlas, BPI).

Thermal properties of PLA and TPS/PLA blends were analyzed using a thermogravimetric analyzer (Perkin Elmer, SDT 2960). The specimens were heat from room temperature to 600°C with heating rate of 10°C/min. under nitrogen atmosphere.

Morphological properties of PLA and TPS/PLA blends were performed by a scanning electron microscope (JEOL, JSM-6400). Acceleration voltage of 10 kV was used. The specimens were freeze-fractured in liquid nitrogen and treated with hydrochloric acid (HCl, 6N) for 3 h. After that the specimens were coated with gold before analysis.

Table 1: Designation and composition of TPS/PLA blends

Sample	TPS wt%	PLA wt%	PLA-g-MA phr
PLA	-	100	-
10TPS	10	90	-
20TPS	20	80	-
30TPS	30	70	-
40TPS	40	60	-
10TPS/PLA-g-MA	10	90	5
20TPS/PLA-g-MA	20	80	5
30TPS/PLA-g-MA	30	70	5
40TPS/PLA-g-MA	40	60	5

3. Results and Discussion

3.1 Mechanical Properties

Tensile properties of PLA and TPS/PLA blends are shown in Figure 1. Tensile strength and tensile modulus of PLA decreased with adding TPS but elongation at break increased. This suggested that the presence of TPS led to ductile behavior [8]. With increasing TPS content, tensile strength, tensile modulus, and elongation at break of the blends decreased due to poor interfacial adhesion between TPS and PLA [6]. Similar results were also found by Huneault and Li [11] and Woothikanokkhan et al. [7]. Tensile strength, tensile modulus, and elongation at break of the blends tended to increase with adding PLA-g-MA due to improved interfacial adhesion between TPS and PLA. Schwach et al. [6] and Woothikanokkhan et al [7] reported that tensile properties of TPS/PLA blends improved with the presence of compatibilizers.

Impact strength of PLA and TPS/PLA blends is shown in Figure 2. Impact strength of TPS/PLA blends reduced with adding TPS. When PLA-g-MA was incorporated into the blends impact strength increased due to enhanced interfacial adhesion between TPS and PLA. Huneault and Li [11] reported that the improvement of interfacial adhesion between TPS and PLA may enhance ductility of the materials.

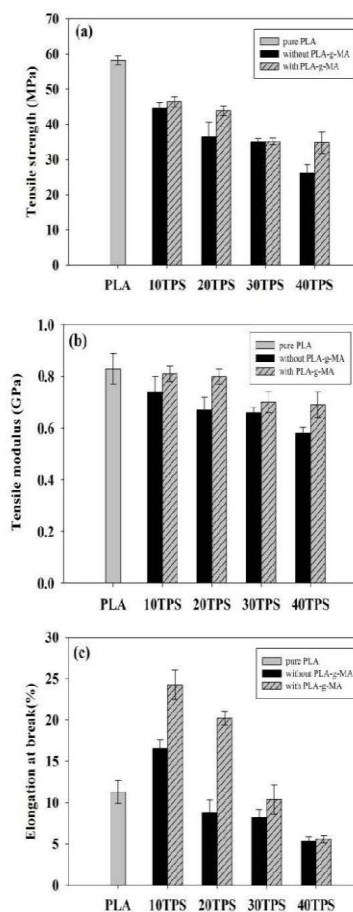


Figure 1. Tensile properties of PLA and TPS/PLA blends: (a) tensile strength, (b) tensile modulus, (c) elongation at break

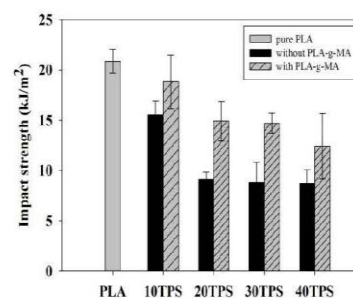


Figure 2. Impact strength of PLA and TPS/PLA blends

3.2 Thermal Properties

TGA curves of TPS, PLA, and TPS/PLA blends are shown in Figure 3. It can be seen that there were two steps in TGA curve of TPS. First step was obtained below 250°C which related to the volatilization of moisture and glycerol. The second step was observed from 280 to 350°C due to the decomposition of TPS [13]. While TGA curve of PLA showed one step relating to thermal decomposition of PLA polymer chain. DTG curves of TPS, PLA, and TPS/PLA blends are displayed in Figure 4. Thermal decomposition temperatures (T_d) of TPS and PLA in the TPS/PLA blends are listed in Table 2. T_d of PLA and TPS were observed at 349.46 and 317.79°C, respectively. It can be seen that PLA had better thermal stability than TPS. T_d of TPS and PLA in the blends decreased when compared with PLA and TPS. Similar results were also found by Wang et al. [4]. The reduction of T_d of PLA was probably because the degradation products of TPS involved thermal degradation of PLA [14]. Petinakis et al. [15] found that small polar molecules such as CO, CO₂, H₂O, CH₄, C₂H₄, and CH₂O were produced when starch decomposed. These molecules could break down PLA chain giving rise to a decrease in T_d of PLA. Shi et al. [16] reported that incorporating TPS into PLA resulted in reduced T_d of PLA. With increasing TPS content, T_d of TPS increased while T_d of PLA decreased. T_d of TPS increased with the addition of PLA-g-MA due to enhanced compatibility between TPS and PLA in the blends [4]. T_d of PLA in the blends did not change significantly when PLA-g-MA was added. Victor et al. [17] also reported that PLA-g-MA showed little effect on thermal stability of starch/PLA blends.

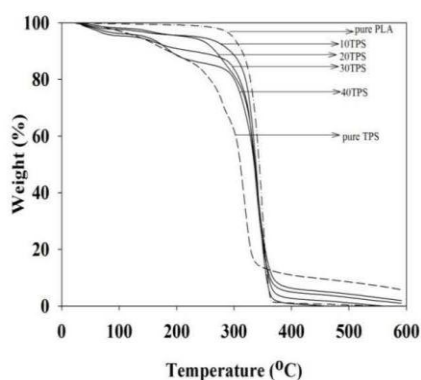


Figure 3. TGA curves of PLA, TPS, and TPS/PLA blends

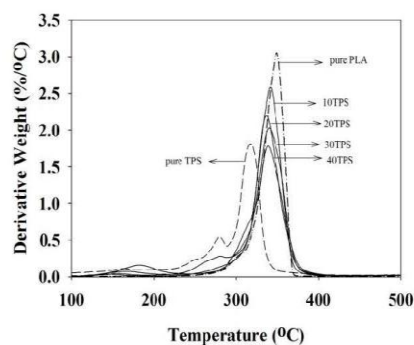


Figure 4. DTG curves of PLA, TPS, and TPS/PLA blends

Table 2: The decomposition temperature (T_d) of PLA, TPS, and TPS/PLA blends

Sample	T_d of TPS °C	T_d of PLA °C
PLA	-	349.46
TPS	317.79	-
10TPS	290.53	341.46
20TPS	301.49	340.19
30TPS	309.02	337.71
40TPS	310.52	337.08
10TPS/PLA-g-MA	309.27	339.30
20TPS/PLA-g-MA	312.78	341.74
30TPS/PLA-g-MA	313.80	337.12
40TPS/PLA-g-MA	314.92	337.77

3.3 Morphological Properties

SEM micrographs of the fracture surface of PLA and TPS/PLA blends are shown in Figure 5. From Figure 5(b) – (e), TPS droplets were observed in PLA matrix. This suggested that TPS/PLA blend was an immiscible blend. The number of the smaller TPS phase domains was observed when TPS content was increased. Similar result was observed by Wootthikanokkhan et al. [7]. With the addition of PLA-g-MA, the droplet size of TPS in the blends was finer than the blends without PLA-g-MA. Huneault and Li [11] found that the phase size of TPS in PLA was reduced with using PLA-g-MA. Wootthikanokkhan et al. [7] also reported that adding PLA-g-MTPS as a compatibilizer resulted in a decrease in particle size of TPS.

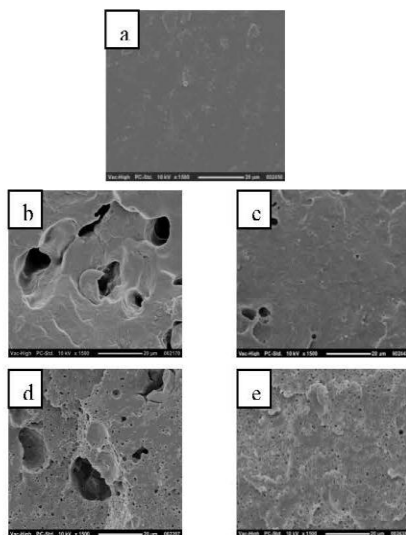


Figure 5. SEM micrographs at 1500x of (a) PLA, (b) 10TPS, (c) 10TPS/PLA-g-MA, (d) 30TPS, and (e) 30TPS/PLA-g-MA

4. Conclusions

Mechanical properties of TPS/PLA blends decreased with increasing TPS content. PLA-g-MA enhanced the compatibility of TPS/PLA blends. The compatibilized blends showed better mechanical properties than the uncompatibilized blends. The decomposition temperature of PLA in the blends was decreased with adding TPS. However, the decomposition temperature of PLA did not change significantly with the presence of PLA-g-MA. SEM micrographs of the compatibilized blends exhibited finer dispersed size.

Acknowledgements

The authors wish to acknowledge Suranaree University of Technology and Center of Excellence on Petrochemical and Materials Technology for financial supports.

References

- [1] G. Nashed, R. P. G. Rutgers and P. A. Sopade, *Starch/Stärke* **55** (2003) 131-137.
- [2] G. H. Yew, A. M. Mohd Yusof, Z. A. Mohd Ishak and U. S. Ishiaku, *Polym. Degrad. Stab.* **90** (2005) 488-500.
- [3] M. Kaseem, K. Haman and F. Deri, *Polym. Sci.* **54** (2012) 165-176.
- [4] N. Wang, J. Yu and X. Ma, *Polym. Compos.* **29** (2008) 551-559.
- [5] N. Wang, J. Yu, P. R. Chang and X. Ma, *Carbohydr. Polym.* **71** (2008) 109-118.
- [6] E. Schwach, J. Six and L. Averous, *J. Polym. Environ.* **16** (2008) 286-297.

- [7] J. Wootthikanokkhan, P. Kasemwananimit, N. Sombatsampop, A. Kositchaiyong, S. Isarankura na Ayutthaya and N. Kaabbuathong, *J. Appl. Polym. Sci.* **126** (2012) 388-395.
- [8] J. Leadprathom, S. Suttirungwong, P. Threepopnatkul and M. Seadan, *J. Met. Mater. Miner.* **20** (2012) 87-90.
- [9] G. Huliang, H. Shan, S. Fuhui, Z. Jun and T. Guanana, *Polym. Compos.* **8** (2011) 2093-2100.
- [10] J. Wootthikanokkhan, N. Wongta, N. Sombatsampop, A. Kositchaiyong, J. Wong-On, S. Isarankura an Ayutthaya and N. Kaabbuathong, *J. Appl. Polym. Sci.* **124** (2012) 1012-1219.
- [11] M. A. Huneault and H. Li, *Polymer* **48** (2007) 270-280.
- [12] A. Teamsinsungvon, *Physical properties of poly(lactic acid)/poly(butylene adipate-co-terephthalate) blends and their composites*, Master's Thesis, Suranaree University of Technology (2011).
- [13] K. Zhang, X. Ran, Y. Zhuang, B. Yao and L. Doung, *Chem. Res. Chin. Univ.* **25** (2009) 748-753.
- [14] C. T. Vasques, S. C. Domenech, V. L. S. Severgnini, L. A. O. Belmonte, M. S. Soldi, P. L. M. Barreto, and V. Soldi, *Starch/Stärke* **59** (2007) 161-170.
- [15] E. Petinakis, X. Liu, L. Yu, C. Way, P. Sangwan, K. Dean, S. Bateman and G. Edward, *Polym. Degrad. Stab.* **95** (2010) 1704-1707.
- [16] Q. Shi, C. Chen, L. Gao, L. Jiao, H. Xu and W. Guo, *Polym. Degrad. Stab.* **96** (2011) 175-182.
- [17] O. H. Victor, B. Witold, C. Wunpen and L. L. Betty, *Macromol. Symp.* **277** (2009) 69-80.

Advanced Materials Research Vol. 747 (2013) pp 67-71
 Online available since 2013/Aug/30 at www.scientific.net
 © (2013) Trans Tech Publications, Switzerland
 doi:10.4028/www.scientific.net/AMR.747.67

Toughness and Compatibility Improvement of Thermoplastic Starch/Poly(lactic acid) Blends

Sujaree Tachaphiboonsap^{1, 2, a} and Kasama Jarukumjorn^{1, 2, b}

¹School of Polymer Engineering, Suranaree University of Technology,
 Nakhon Ratchasima, Thailand

²Center of Excellence on Petrochemical and Materials Technology,
 Bangkok, Thailand

^asuj.sut@gmail.com, ^bkasama@sut.ac.th

Keywords: PLA, TPS, PBAT, PLA-g-MA, TPS/PLA Blend

Abstract. Poly(lactic acid) (PLA), produced from renewable resources, is one of the most widely used biodegradable polymers. PLA has high strength and high modulus. However, its brittleness and high cost limit its application. Starch has been used as filler for environmental friendly polymers due to its low cost, biodegradable, and availability as a renewable source. Thermoplastic starch (TPS) is a biodegradable material based on starch. Incorporation of TPS into PLA matrix can reduce material cost and increases its biodegradation rate. However, PLA and TPS form immiscible blend leading to poor mechanical properties of the blend. The compatibility of the blend can be improved by adding compatibilizers. Moreover, in order to improve toughness of the TPS/PLA blend, poly(butylenes adipate-co-terephthalate) (PBAT), is introduced into the blend. In this study, PLA/TPS blends are prepared using an internal mixer and test specimens are molded using a compression molding. TPS is obtained from cassava starch and glycerol at ratio of 70/30 wt%. The ratio of TPS/PLA blend is 10/90 wt%. Poly(lactic acid) grafted maleic anhydride (PLA-g-MA) is used as a compatibilizer at contents of 3, 5, and 7 phr. PBAT content is 10 wt%. Mechanical, morphological, and thermal properties of the blends are investigated.

Introduction

Poly(lactic acid) (PLA) is one of the most widely used biodegradable polymers. PLA provides high strength, high modulus, and excellent degradability. However, its high brittleness and high cost limit its application. Starch has been used as filler for environmental friendly polymer due to its low cost and biodegradability. Since melting temperature of starch is close to its degradation temperature. Starch has been modified to obtain thermoplastic starch (TPS) [1,2]. Glycerol is the most used plasticizer in TPS preparation due to its high boiling point and low cost [3]. The addition of TPS into PLA can decrease material cost and increase its biodegradation rate. However, TPS/PLA blends have poor mechanical properties due to poor compatibility between TPS and PLA [4]. The compatibility of TPS/PLA blends can be enhanced by adding compatibilizers [5,6]. In order to improve toughness of TPS/PLA blends, flexible polymers e.g. polycaprolactone (PCL) [7], Poly(butylenes adipate-co-terephthalate) (PBAT) [8] have been incorporated into the blends.

The objective of this work was to investigate the effects of PBAT and PLA-g-MA content on mechanical, morphological, and thermal properties of TPS/PLA blends.

Experimental

Materials. Poly(lactic acid) (PLA, 4043D) was supplied from Natural Works LLC. Poly(butylenes adipate-co-terephthalate) (PBAT, BASF Ecoflex FBX 7011) was purchased from BASF. Cassava starch was obtained from Bangkok Interfood Co., Ltd. Glycerol was supplied from Carlo Erba Reagent Co., Ltd. 2, 5-bis (tert-butylperoxy)-2, 5 dimethylhexane (L101) and maleic anhydride (MA) were purchased from Sigma-Aldrich. Poly(lactic acid) grafted with maleic anhydride (PLA-g-MA) prepared in-house was used as a compatibilizer [9].

Preparation. TPS was obtained from cassava starch and glycerol at ratio of 70:30 w/w. Cassava starch was dried at 70°C for 4 h before mixing. Sample was prepared using an internal mixer (Hakke Rheomix, 3000P). The mixing temperature was kept at 120°C and the rotor speed was 60 rpm. The mixing time was 10 min.

TPS/PLA/PBAT blends were prepared using an internal mixer (Hakke Rheomix, 3000P). TPS, PLA, and PBAT were dried at 70°C for 4 h before mixing. The mixing temperature was kept at 170°C and the rotor speed was 60 rpm. The specimens were processed by a compression molding machine (Labtech, LP20-B) at temperature of 170°C and pressure of 100 MPa for 10 min. Designation and composition of TPS/PLA blend and TPS/PLA/PBAT blends are shown in Table 1.

Table 1. Designation and composition of the blends

Designation	TPS [wt%]	PLA [wt%]	PBAT [wt%]	PLA-g-MA [phr]
TPS/PLA	10	90	-	-
nc-10PBAT	9	81	10	-
3c-10PBAT	9	81	10	3
5c-10PBAT	9	81	10	5
7c-10PBAT	9	81	10	7

Characterization. Tensile properties of TPS/PLA blend and TPS/PLA/PBAT blends with various PLA-g-MA contents were tested according to ASTM D638 using a universal testing machine (Instron, 5565) with a load cell of 5 kN and a crosshead speed of 1 mm/min.

Izod impact test was performed according to ASTM D256 using an impact testing machine (Atlas, BPI).

Thermal properties of TPS/PLA blend and TPS/PLA/PBAT blends with various PLA-g-MA contents were analyzed using a thermogravimetric analyzer (Perkin Elmer, SDT 2960). The specimens were heated from room temperature to 600°C with heating rate of 10°C/min under nitrogen atmosphere.

Morphological properties of TPS/PLA blend and TPS/PLA/PBAT blends with various PLA-g-MA contents were performed by a scanning electron microscope (NeoScope, JCM-5000). Acceleration voltage of 10 kV was used. The specimens were freeze-fractured in liquid nitrogen and treated with hydrochloric acid (HCl, 6N) for 3 h. Then the samples were coated with gold before analysis.

Results and Discussion

Mechanical Properties. Mechanical properties of TPS/PLA blend and TPS/PLA/PBAT blends with various PLA-g-MA contents are shown in Fig. 1. Elongation at break of TPS/PLA blend increased with adding PBAT whereas tensile strength and tensile modulus decreased. This was due to the result of the rubbery nature of PBAT. Similar results were also found by Ren et al. [8]. Tensile strength, tensile modulus, and elongation at break of TPS/PLA/PBAT blend increased with adding 3 phr PLA-g-MA due to improved interfacial adhesion [8,10]. However, tensile properties of the blends decreased with further increasing PLA-g-MA content. This may be because increasing PLA-g-MA content provided more anhydride molecules which were capable of activating chain scissions of PLA molecules. The reduction in molecular weight of PLA in the blends contributed to a decrease in the tensile properties of the blends [11].

Impact strength of TPS/PLA blend increased with adding PBAT. When PLA-g-MA at content of 3 phr was incorporated into the blends impact strength was increased. However, with adding 5 or 7 phr PLA-g-MA, impact strength of the blends was reduced.

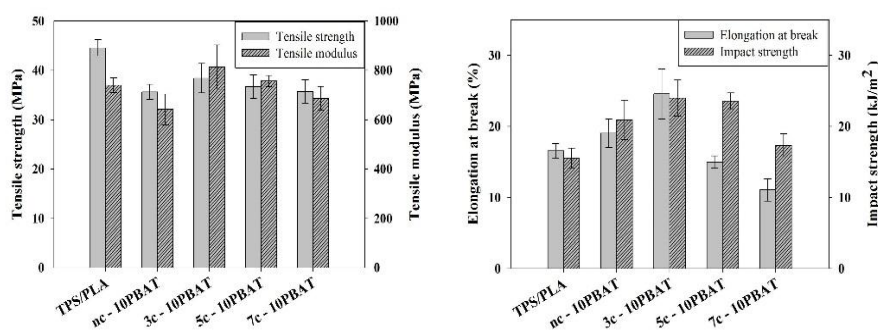


Figure 1. Mechanical properties of TPS/PLA blend and TPS/PLA/PBAT blends with various PLA-g-MA contents

Thermal Properties. TGA curves of TPS/PLA blend and TPS/PLA/PBAT blends with various PLA-g-MA contents are shown in Fig. 2. Their thermal decomposition temperatures (T_d) are summarized in Table 2. TGA curve of TPS/PLA blend showed two steps. The first step was observed below 300°C relating to thermal decomposition of TPS. The second step was obtained from 300 to 360°C due to thermal decomposition of PLA [12]. T_d of TPS and PLA in TPS/PLA blend were observed at 290.53 and 341.46°C, respectively. It can be seen T_d of TPS was lower than that of PLA. While TGA curve of TPS/PLA/PBAT blend showed three steps. The first step was attributed to the loss of TPS. The second step was thermal decomposition of PLA. The third step presented thermal decomposition of PBAT. T_d of TPS, PLA, and PBAT in TPS/PLA/PBAT blend were appeared at 314.68, 360.87, and 405.91°C, respectively. T_d of TPS and PLA in TPS/PLA/PBAT blend were increased with adding PBAT indicating the improvement of thermal stability of TPS and PLA in the blend [10,13]. T_d of TPS, PLA, and PBAT in the compatibilized blends did not change significantly when PLA-g-MA content was increased. Phetwarotai et al. [10] also reported that content of compatibilizer slightly affected thermal behaviors of the TPS/PLA/PBAT blends.

Table 2. The decomposition temperature (T_d) of TPS/PLA blend and TPS/PLA/PBAT blends with various PLA-g-MA contents

Sample	T_d of TPS [°C]	T_d of PLA [°C]	T_d of PBAT [°C]
TPS/PLA	290.53	341.46	-
nc-10PBAT	314.68	360.87	405.91
3c-10PBAT	311.95	360.87	402.24
5c-10PBAT	309.63	361.79	402.24
7c-10PBAT	309.44	363.02	402.60

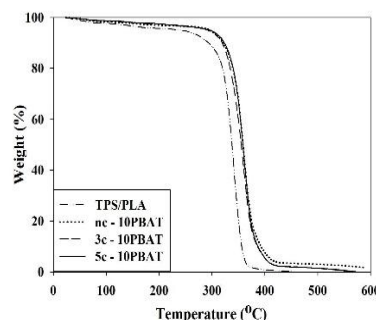


Figure 2. TGA curves of TPS/PLA blend and TPS/PLA/PBAT blends with various PLA-g-MA contents

Morphological Properties. SEM micrographs of the fractured surface of TPS/PLA blend and TPS/PLA/PBAT blends with various PLA-g-MA contents are shown in Fig. 3. TPS phase in the blend was removed by 6 N HCl solution. From Fig. 3(a), the holes of TPS were observed in PLA matrix. This indicated that TPS/PLA blend was an immiscible blend [8]. When PBAT was added into the TPS/PLA blend, PBAT droplets were observed as shown in Fig. 3(b). With the addition of 3 phr PLA-g-MA, not only the size of TPS was decreased but also PBAT droplets were finer as

shown in Fig. 3(c). The compatibilizer improved the interfacial adhesion of the blend components and provided a finer morphology [8,10]. This led to the blend with better mechanical properties. From Fig. 3(d), the size of TPS was increased with increasing PLA-g-MA content. This may result in reduced mechanical properties of the blend.

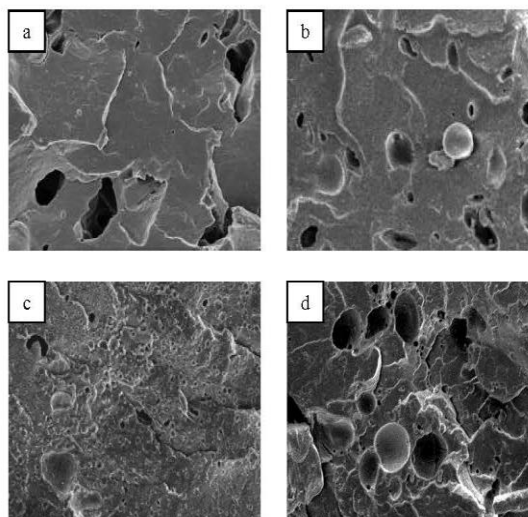


Figure 3. SEM micrographs at 1000x of (a) TPS/PLA blend, (b) nc-10PBAT blend, (c) 3c-10PBAT blend, and (d) 7c-10PBAT blend

Summary

Elongation at break and impact strength of TPS/PLA blend increased with adding PBAT while tensile strength and tensile modulus decreased. The presence of 3 phr PLA-g-MA promoted good interfacial adhesion of the blend and led to an increase in the mechanical properties of the blend. PBAT led to an increase in thermal stability of the TPS/PLA blend. However, PLA-g-MA content insignificantly affected thermal behaviors of the blends.

Acknowledgements

The authors wish to acknowledge Suranaree University of Technology and Center of Excellence on Petrochemical and Materials Technology for financial supports.

References

- [1] G. Nashed, R. P. G. Rutgers, P. A. Sopade, *Starch/Stärke*. 55 (2003) 131-137.
- [2] J. H. Yang, J. G. Yu, X. F. Ma, *Starch/Stärke*. 58 (2006) 580-586.
- [3] M. Kaseem, K. Hamad, F. Deri, *Polym. Sci.* 54 (2012) 165-176.
- [4] W. Ning, Y. Jiugao, M. Xiaofei, *Polym. Compos.* 29 (2008) 551-559.
- [5] E. Schwach, J. L. Six, L. Averous, *J. Polym. Environ.* 16 (2008) 286-297.
- [6] J. Wootthikanokkhan, P. Kasemwananimit, N. Sombatsampop, A. Kositchaiyong, S. Isarankura na Ayutthaya and N. Kaabbuathong, *J. Appl. Polym. Sci.* 126 (2012) 388-395.
- [7] P. Sarazin, G. Li, W. J. Orts, B. D. Favis, *Polymer* 49 (2008) 599-609.
- [8] J. Ren, H. Fu, T. Ren, W. Yuan, *Carbohydr. Polym.* 77 (2009) 576-582.
- [9] A. Teamsinsungvon, Physical properties of poly(lactic acid)/poly(butylene adipate-co-terephthalate) blends and their composites, Master's Thesis, Suranaree University of Technology (2011).

-
- [10] W. Phetwarotai, D. Aht-Ong, Mater. Sci. Forum 695 (2011) 178-181.
- [11] H. Tsuji, Polymer 43 (2002) 1789-1796.
- [12] K. Y. Zhang, X. H. Ran, Y. G. Zhuang, B. Yao, L. S. Dong, Chem. Res. Chin. Univ. 25 (2009) 748-753.
- [13] M. Kumar, S. Mohanty, S. K. Nayak, M. R. Parvaiz, Bioresour. Technol. 101 (2010) 8406-8415.



EFFECT OF POLY(LACTIC ACID) GRAFTED WITH MALEIC ANHYDRIDE ON MECHANICAL AND MORPHOLOGICAL PROPERTIES OF THERMOPLASTIC STARCH/POLY(LACTIC ACID) BLENDS

Kasama Jarukumjorn and Sujaree Tachaphiboonsap

School of Polymer Engineering, Institute of Engineering, Suranaree University of Technology,
Nakhon Ratchasima, 30000 Thailand
E-mail: kasama@sut.ac.th

Introduction

Poly(lactic acid) (PLA) is the most widely used biodegradable polymers. PLA possesses high strength, high modulus, and excellent degradability. However, its high cost and brittleness limit its applications. Starch has been used as filler for environmental friendly polymers due to its low cost, biodegradability, and availability as a renewable resource. However, melting temperature of starch is close to degradation temperature (1). Therefore, starch has been modified to obtain thermoplastic starch (TPS). Glycerol is often used as a plasticizer due to its high boiling point and low cost (2). TPS/PLA blends exhibit low mechanical properties due to poor compatibility between TPS and PLA (3, 4). The compatibility of TPS/PLA blends can be achieved by adding compatibilizers (5, 6) or matrix modification (7, 8).

In this study, poly(lactic acid) grafted with maleic anhydride (PLA-g-MA) was used as a compatibilizer. The effect of PLA-g-MA content on mechanical and morphological properties of TPS/PLA blends was investigated.

Experimental

Poly(lactic acid) (PLA, 4043D) was supplied from Natural Works LLC. Cassava starch was obtained from Bangkok Interfood Co., Ltd. Glycerol was supplied from Carlo Erba Reagenti Co., Ltd. Poly(lactic acid) grafted with maleic anhydride (PLA-g-MA) was prepared in-house (9).

TPS was obtained from cassava starch and glycerol at a ratio of 70:30 w/w. TPS was prepared using an internal mixer (Hakke Rheomix, 3000P). The mixing temperature was kept at 120°C and the rotor speed of 60 rpm. The mixing time was 10 min. TPS/PLA blend and TPS/PLA/PLA-g-MA blends were prepared using an internal mixer. The mixing temperature was kept at 170°C and the rotor speed of 60 rpm. The mixing time was 10 min. TPS content was fixed at 10 wt%. PLA-g-MA content was varied as 3, 5, and 7 phr. The specimens were processed by a compression molding machine (Labtech, LP20-B) at the temperature of 170°C and pressure of 100 MPa.

Tensile properties of PLA and TPS/PLA blends were tested according to ASTM D638 using a universal testing machine (Instron, 5565) with a load cell 5 kN and crosshead speed of 5 mm/min.

Izod impact test was performed according to ASTM D256 using an impact testing machine (Atlas, BPI).

Morphological properties of PLA and TPS/PLA blends were performed by a scanning electron microscope (JEOL, JSM-6400). Acceleration voltage of 10 kV was used. The specimens were freeze-fractured in liquid nitrogen and treated with hydrochloric acid (HCl, 6N) for 3 h. The specimens were coated with gold before analysis.

Results and Discussion

Tensile strength and modulus of PLA decreased with adding TPS but elongation at break increased as shown in Figure 1 and 2. This suggested that the presence of TPS led to ductile behavior (7). Tensile properties of the blends tended to increase with the addition of PLA-g-MA due to improved interfacial adhesion between TPS and PLA. Tensile properties of the blends were slightly increased when PLA-g-MA content was increased up to 5 phr. With incorporating 7 phr of PLA-g-MA, tensile properties of the blend did not change significantly. Impact strength of TPS/PLA blends reduced with adding TPS as shown in Figure 2. When PLA-g-MA was incorporated into the blends impact strength

increased due to enhanced interfacial adhesion between TPS and PLA. Huneault and Li. (10) reported that the improvement of interfacial adhesion between TPS and PLA may enhance ductility of the materials. With increasing PLA-g-MA content, the impact strength of the blends exhibited the similar trend as the tensile properties.

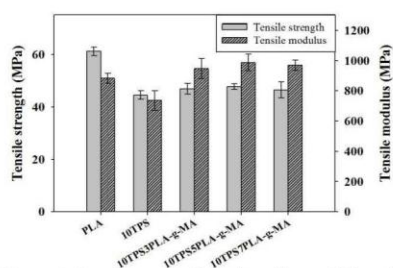


Figure 1 Tensile strength and tensile modulus of PLA, TPS/PLA blends, and TPS/PLA/PLA-g-MA blends

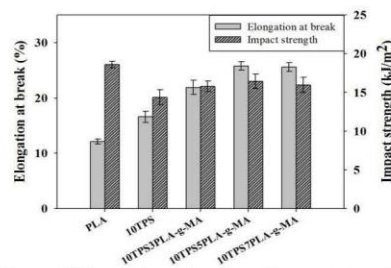


Figure 2 Elongation at break and impact strength of PLA, TPS/PLA blends, and TPS/PLA/PLA-g-MA blends

SEM micrographs of the fractured surface of TPS/PLA blend and TPS/PLA/PLA-g-MA blends are shown in Figure 3. TPS phase was removed by 6 N HCl solution. The holes of TPS were observed in PLA matrix as shown in Figure 3(a). This suggested that TPS and PLA were immiscible. From Figure 3(b-d), the size of TPS phase in the PLA-g-MA compatibilized blends was smaller than the uncompatibilized blends. Similar result also found by Huneault et al. (10). Wootthikanokkhan et al. (6) suggested that reduction of coalescence and surface tension of minor phase were acted by compatibilizer. The size of TPS was insignificantly changed when PLA-g-MA content was increased.

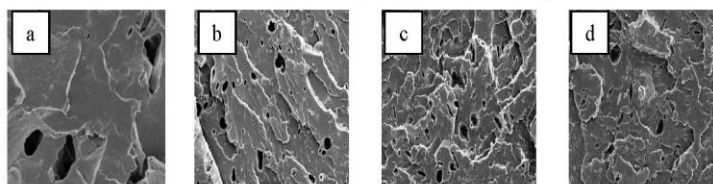


Figure 3 SEM micrographs at 1000x of (a) 10TPS, (b) 10TPS3PLA-g-MA, (c) 10TPS5PLA-g-MA, and (d) 10TPS7PLA-g-MA blends

Conclusion

Tensile strength, tensile modulus, and impact strength of PLA decreased with adding TPS whereas elongation at break increased. The addition of PLA-g-MA improved the mechanical properties of TPS/PLA blend due to enhanced compatibility between TPS and PLA. The mechanical properties of TPS/PLA blend increased with increasing PLA-g-MA content up to 5 phr. When PLA-g-MA content was 7 phr the mechanical properties of the blend did not change significantly. SEM results revealed that TPS phase was finer when PLA-g-MA was incorporated in the blends, resulting in the improvement of mechanical properties of the blends.

References

1. G. Nashed; R. P. G. Rutgers; P. A. Sopade *Starch/Stärke* **2003**, *55*, 131-137.
2. M. Kaseem; K. Haman; F. Deri *Polym. Sci.* **2012**, *54*, 165-176.
3. N. Wang; J. Yu; X. Ma *Polym. Compos.* **2008**, *29*,551-559.
4. N. Wang; J. Yu; P. R. Chang; X. Ma *Carbohydr. Polym.* **2008**, *71*,109-118.
5. E. Schwach; J. Six; L. Averous *J. Polym. Environ.* **2008**, *16*, 286-297.
6. J. Wootthikanokkhan; P. Kasemwananimit; N. Sombatsampop; A. Kositchaiyong; S. Isarankurana Ayuthaya; N. Kaabbuathong *J. Appl. Polym. Sci.* **2012**, *126*, 388-395.
7. J. Leadprathom; S. Suttiruengwong; P. Threepopnatkul; M. Seadan *J. Met. Mater. Miner.* **2012**, *20*, 87-90.
8. G. Huliang; H. Shan; S. Fuhui; Z. Jun; T. Guanana *Polym. Compos.* **2011**, *8*, 2093-2100.
9. A. Teamsinsungvon, Physical properties of poly(lactic acid)/poly(butylene adipate-co-terephthalate) blends and their composites, **2011**, Master's Thesis, Suranaree University of Technology.

10. M. A. Huneault; H. Li *Polymer* **2007**, *48*, 270-280.

Advanced Materials Research Vol. 970 (2014) pp 312-316
Online available since 2014/Jun/18 at www.scientific.net
 © (2014) Trans Tech Publications, Switzerland
 doi:10.4028/www.scientific.net/AMR.970.312

Mechanical, Thermal, and Morphological Properties of Thermoplastic Starch/Poly(lactic acid)/Poly(butylene adipate-co-terephthalate) Blends

Sujaree Tachaphiboonsap^{1,a}, Kasama Jarukumjorn^{1,b*}

¹School of Polymer Engineering, Institute of Engineering, Suranaree University of Technology, Nakhon Ratchasima, 30000 Thailand

^asuj.sut@gmail.com, ^bkasama@sut.ac.th

Keywords: Poly(lactic acid), Thermoplastic starch, Poly(butylene adipate-co-terephthalate), Poly(lactic acid) grafted with maleic anhydride, Mechanical properties, Thermal properties, Morphological properties

Abstract. Thermoplastic starch (TPS)/poly(lactic acid) (PLA) blend and thermoplastic starch (TPS)/poly(lactic acid) (PLA)/poly(butylene adipate-co-terephthalate) (PBAT) blend were prepared by melt blending method. PLA grafted with maleic anhydride (PLA-g-MA) was used as a compatibilizer to improve the compatibility of the blends. As TPS was incorporated into PLA, elongation at break was increased while tensile strength, tensile modulus, and impact strength were decreased. Tensile properties and impact properties of TPS/PLA blend were improved with adding PLA-g-MA indicating the enhancement of interfacial adhesion between PLA and TPS. With increasing PBAT content, elongation at break and impact strength of TPS/PLA blends were improved. The addition of TPS decreased glass transition temperature (T_g), crystallization temperature (T_c), and melting temperature (T_m) of PLA. T_g and T_c of TPS/PLA blend were decreased by incorporating PLA-g-MA. However, the presence of PBAT reduced T_c of TPS/PLA blend. Thermal properties of TPS/PLA/PBAT blends did not change with increasing PBAT content. SEM micrographs revealed that the compatibilized TPS/PLA blends exhibited finer morphology when compared to the uncompatibilized TPS/PLA blend.

Introduction

Poly(lactic acid) (PLA) is thermoplastic aliphatic polyester derived from renewable resources. PLA is one of the most widely used biodegradable polymers. PLA exhibits high strength, high modulus, and excellent degradability. However, its high brittleness and high cost limit its application. Blending PLA with low cost fillers and flexible polymers presents a practical and economical way to obtain economical products. Starch has been used as filler for environmental friendly polymers because its low cost and biodegradability. However, melting temperature of starch is close to degradation temperature [1,2]. Therefore, starch has been modified to obtain thermoplastic starch (TPS). The most commonly used plasticizer for TPS is glycerol due to its high boiling point and low cost [3]. The addition of TPS into PLA can decrease material cost and increase degradation rate. However, TPS/PLA blends exhibit poor mechanical properties due to poor compatibility between TPS and PLA [4]. The compatibility of TPS/PLA blends can be enhanced by adding compatibilizers [5,6]. In order to improve toughness of TPS/PLA blends, flexible polymers e.g. polycaprolactone (PCL) [7] and poly(butylene adipate-co-terephthalate) (PBAT) [8] have been incorporated into TPS/PLA blends. PBAT is considered as a good candidate for toughening PLA due to its high toughness and biodegradability. The objective of this work was to investigate the effect of PLA-g-MA on mechanical, thermal, and morphological properties of TPS/PLA blends and TPS/PLA/PBAT blends.

Experimental

Materials. Poly(lactic acid) (PLA, 4043D) was supplied from Natural Works LLC. Poly(butylene adipate-co-terephthalate) (PBAT, BASF Ecoflex FBX7011) was purchased from BASF. Cassava starch was obtained from Bangkok Interfood Co., Ltd. Glycerol was supplied from Carlo Erba

Reageti Co., Ltd. 2, 5-bis (tert-butylperoxy)-2, 5 dimethylhexane (L101) and maleic anhydride (MA) were purchased from Sigma-Aldrich. Poly(lactic acid) grafted with maleic anhydride (PLA-g-MA) prepared in-house was used as a compatibilizer [9].

Preparation. TPS was obtained from cassava starch and glycerol at ratio of 70:30 w/w. Cassava starch was dried at 70°C for 4 h before mixing. TPS was prepared using an internal mixer (Hakke Rheomix, 3000P). The mixing temperature was kept at 120°C and the rotor speed was 60 rpm. The mixing time was 10 min.

TPS/PLA blends and TPS/PLA/PBAT blends were prepared using an internal mixer (Hakke Rheomix, 3000P). PLA, TPS, and PBAT were dried at 70°C for 4 h before mixing. The mixing temperature was kept at 170°C and the rotor speed was 60 rpm. The mixing time was 10 min. The specimens were processed by a compression molding machine (Labtech, LP20-B) at temperature of 170°C and pressure of 100 MPa for 10 min. Designation and composition of TPS/PLA blends and TPS/PLA/PBAT blends are shown in Table 1.

Table 1. Designation and composition of the blends

Designation	TPS [%wt]	PLA [%wt]	PBAT [%wt]	PLA-g-MA [phr]
PLA	-	100	-	-
TPS/PLA	10	90	-	-
5c-TPS/PLA	10	90	-	5
5c-10PBAT	9	81	10	5
5c-20PBAT	8	72	20	5

Characterization.

Mechanical Properties. Tensile properties of PLA, TPS/PLA blends, and TPS/PLA/PBAT blends at various PBAT contents were tested according to ASTM D638 using a universal testing machine (Instron, 5565) with a load cell of 5 kN and a crosshead speed of 5 mm/min.

Izod impact test was performed according to ASTM D256 using an impact testing machine (Atlas, BPI).

Thermal Properties. Thermal properties of PLA, TPS/PLA blends, and TPS/PLA/PBAT blends at various PBAT contents were analyzed using a differential scanning calorimeter (NETZSCH, DSC204F1 Phoenix). All samples were heated from 25°C to 200°C with heating rate of 10°C/min (heat scan) and kept isothermal for 5 min under a nitrogen atmosphere to erase previous thermal history. Then, the sample was cooled to -50°C with cooling rate of 10°C/min and heated again to 200°C with heating rate of 10°C/min (2nd heating scan).

Morphological Properties. Morphological properties of PLA, TPS/PLA blends, and TPS/PLA/PBAT blends at various PBAT contents were performed by a scanning electron microscope (JEOL, JSM-6010LV). Acceleration voltage of 10 kV was used. The fractured specimens were treated with hydrochloric acid (HCl, 6N) for 3 h. The specimens were coated with gold before analysis.

Results and Discussion

Mechanical Properties. Tensile strength and tensile modulus of PLA decreased with adding TPS while elongation at break increased as shown in Fig. 1 and Fig. 2, respectively. This result indicated that TPS led to ductile behavior [10]. With incorporating PLA-g-MA, tensile properties of TPS/PLA blend were increased due to enhanced compatibility between TPS and PLA. Tensile

strength and tensile modulus decreased whereas elongation at break increased when PBAT was added into TPS/PLA blend. This was because PBAT had lower tensile strength and tensile modulus than PLA resulting in improvement of PLA ductility. Phetwarotai et al. [11] also found that adding PBAT increased elongation at break of TPS/PLA blend but decreased tensile strength because PBAT had lower tensile strength than PLA. With increasing PBAT content, elongation at break of TPS/PLA/PBAT blend significantly increased. Impact strength of PLA reduced when TPS was added due to poor interfacial adhesion between TPS and PLA as shown in Fig. 2. When PLA-g-MA was incorporated into the blends, impact strength was increased due to enhanced interfacial adhesion between TPS and PLA. Huneault et al. [12] reported that the improvement of interfacial adhesion between TPS and PLA may enhance ductility of the materials. Impact strength of TPS/PLA blend increased with adding PBAT and further increased with increasing PBAT content.

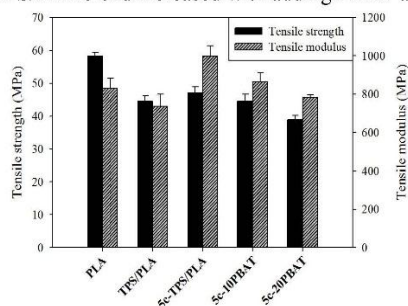


Figure 1. Tensile strength and tensile modulus of PLA, TPS/PLA blends, and TPS/PLA/PBAT blends at various PBAT contents

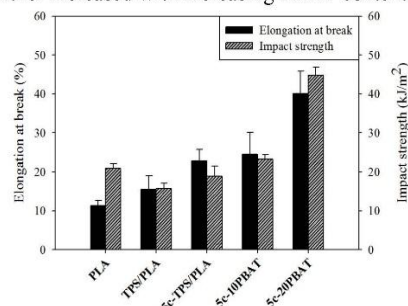


Figure 2. Elongation at break and impact strength of PLA, TPS/PLA blends, and TPS/PLA/PBAT blends at various PBAT contents

Thermal Properties. DSC thermograms of PLA, TPS/PLA blends, and TPS/PLA/PBAT blends are shown in Fig. 3 and their DSC data are listed in Table 2. There was no detectable change of the thermogram of TPS which was explained that thermal signal of TPS was weaker than conventional polymers [13]. Glass transition temperature (T_g) and crystallization temperature (T_c) of pure PLA were observed at 57.2°C and 110.3°C, respectively. PLA displayed melting temperature (T_m) at 148.6°C accompanied with shoulder-melting peak at 153.2°C. The addition of TPS decreased T_g and T_m of PLA due to the plasticizing effect of glycerol. Moreover, T_c of PLA in TPS/PLA blends was lower than pure PLA. Li et al. [14] explained that plasticizer such as water and glycerol could potentially migrate into PLA matrix leading to enhanced PLA polymer chain mobility thus increased crystallization of PLA. T_g and T_c of compatibilized TPS/PLA blend were lower than the uncompatibilized TPS/PLA blend due to improved interfacial adhesion between TPS and PLA. Karagoz et al. [15] reported that T_g and T_c of PLA in TPS/PLA blend were decreased with the addition of phenylene diisocyanate (PDI) as a compatibilizer due to the improvement of interfacial adhesion of the blend. T_g and T_m of TPS/PLA blend did not change when PBAT was incorporated. Shi et al. [16] also reported that T_g and T_m of TPS/PLA blends insignificant changed with adding glycidyl methacrylate grafted poly(ethylene octane) (GPOE) as a toughening agent. However, the presence of PBAT reduced T_c of PLA which was consistent with the fact that PBAT enhanced crystalline ability of PLA [17]. Thermal properties of TPS/PLA/PBAT blends insignificantly changed with increasing PBAT content. Shi et al. [16] found that the increasing toughening agent content exhibited no effect on the thermal properties of TPS/PLA blend.

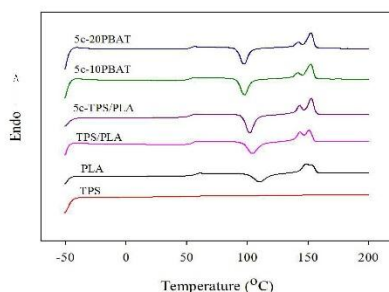


Figure 3. DSC thermograms of PLA, TPS/PLA blends, and TPS/PLA/PBAT blends (the second heating, heating rate of 10°C/min)

Table 2. Thermal properties of PLA, TPS/PLA blends, and TPS/PLA/PBAT blends

Designation	T _g [°C]	T _c [°C]	T _{m1} [°C]	T _{m2} [°C]
PLA	57.2	110.3	148.6	153.2
TPS/PLA	54.9	104.2	143.4	151.2
5c-TPS/PLA	52.1	100.5	141.3	151.0
5c-10PBAT	52.1	96.1	139.8	150.3
5c-20PBAT	52.2	95.8	140.0	150.6

Morphological Properties. SEM micrographs of the fractured surface of PLA, TPS/PLA blends, and TPS/PLA/PBAT blends are shown in Fig. 4. TPS phase in the blends was removed by 6 N HCl solution. Dispersed phase of TPS was observed in PLA matrix indicating that TPS/PLA blend was immiscible. With the addition of PLA-g-MA, the dispersed phase size of TPS in the blend was smaller than the blend without PLA-g-MA due to enhanced interfacial adhesion between TPS and PLA. Li et al. [18] also reported that PLA-g-MA compatibilized TPS/PLA blend exhibited finer morphology when compared with uncompatibilized TPS/PLA blend.

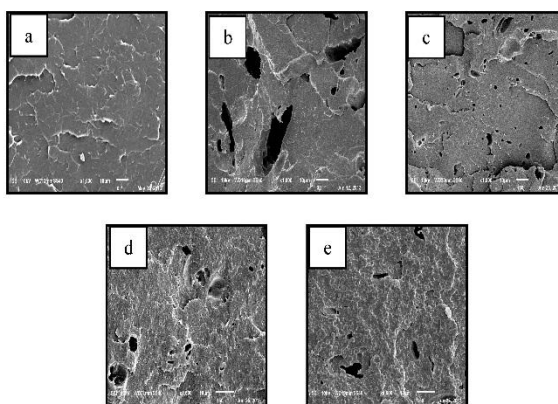


Figure 4. SEM micrographs of (a) PLA, (b) TPS/PLA, (c) 5c-TPS/PLA, (d) 5c-10PBAT, and (e) 5c-20PBAT

Summary

Tensile strength, tensile modulus, and impact strength of PLA decreased with adding TPS while elongation at break increased. The compatibilized TPS/PLA blend showed better mechanical properties than that of the uncompatibilized TPS/PLA blend. The incorporation of PBAT into the compatibilized TPS/PLA blend increased elongation at break and impact strength. The addition of TPS decreased T_g, T_c, and T_m of PLA. T_g and T_c of TPS/PLA blend were decreased by incorporating PLA-g-MA. However, the presence of PBAT reduced T_c of TPS/PLA blend. Thermal properties of TPS/PLA/PBAT blends did not change with increasing PBAT content. The compatibilized TPS/PLA blends exhibited finer morphology when compared to the uncompatibilized TPS/PLA blend.

References

- [1] G. Nashed, R. P. G. Rutgers, P. A. Sopade, *Starch/Stärke* 55 (2003) 131-137.
- [2] G. H. Yew, A. M. Mohd Yusof, Z. A. Mohd Ishak, U. S. Ishiaku, *Polym. Degrad. Stab.* 90 (2005) 488-500.
- [3] M. Kaseem, K. Haman, F. Deri, *Polym. Sci.* 54 (2012) 165-176.
- [4] W. Ning, Y. Jiugao, M. Xiaofei, *Polym. Compos.* 29 (2008) 551-559.
- [5] E. Schwach, J. L. Six, L. Averous, *J. Polym. Environ.* 16 (2008) 286-297.
- [6] J. Wootthikanokkhan, P. Kasemwananimit, N. Sombatsampop, A. Kositchaiyong, S. Isarankurana Ayutthaya, N. Kaabbuathong, *J. Appl. Polym. Sci.* 126 (2012) E388-E395.
- [7] P. Sarazin, G. Li, W. J. Orts, B. D. Favis, *Polymer* 49 (2008) 599-609.
- [8] J. Ren, H. Fu, T. Ren, W. Yuan, *Carbohydr. Polym.* 77 (2009) 576-582.
- [9] A. Teamsinsungvon, Physical properties of poly(lactic acid)/poly(butylene adipate-co-terephthalate) blends and their composites, Master's Thesis, Suranaree University of Technology (2011).
- [10] J. Leadprathom, S. Suttiruengwong, P. Threepopnatkul, M. Seadan, *J. Met. Mater. Miner.* 20 (2010) 87-90.
- [11] W. Phetwarotai, D. Aht-Ong, *Mater. Sci. Forum* 695 (2011) 178-181.
- [12] M. A. Huneault, H. Li, *Polymer* 48 (2007) 270-280.
- [13] L. Yu, E. Petinakis, K. Dean, H. Liu, Q. Yuan, *J. Appl. Polym. Sci.* 119 (2011) 2189-2195.
- [14] H. Li, M. A. Huneault, *Int. Polym. Proc.* 5 (2008) 412-418.
- [15] S. Karagoz, G. Ozkoc, *Polym. Eng. Sci.* DOI 10.1002 (2013) 1-11.
- [16] Q. Shi, C. Chen, L. Geo, L. Jiao, H. Xu, W. Guo, *Polym. Degrad. Stab.* 96 (2011) 175-182.
- [17] L. Jiang, M. P. Wolcott, J. Zhang, *Biomacromolecules* 7 (2006) 199-207.
- [18] H. Li, M. A. Huneault, *J. Appl. Polym. Sci.* 122 (2011) 134-141.

BIOGRAPHY

Miss Sujaree Tachaphiboonsap was born on December 1, 1987 in Nakhon Ratchasima Province, Thailand. She finished high school from Mahitsarathibodee School in 2005. She attended Suranaree University of Technology (SUT) and graduated in 2010 with a Bachelor's degree of Polymer Engineering. After graduation, she pursued her Master's degree in Polymer Engineering, Institute of Engineering, Suranaree University of Technology (SUT) in Nakhon Ratchasima Province. Her research was about thermoplastic starch/poly(lactic acid) blends. During her graduate study, she got a research assistantship from Suranaree University of Technology and Center of Excellence on Petrochemical and Materials Technology. In the period of her Master's degree study, she presented two posters and one oral presentation entitled: **“Mechanical, thermal, and morphological properties of thermoplastic starch/poly(lactic acid) blends”** in Pure and Applied Chemistry International Conference 2013 (PACCON 2013), Chonburi, Thailand, **“Toughness and compatibility improvement of thermoplastic starch/poly(lactic acid) blends”** in the 4th International Conference on Multi-Functional Materials and Structures (MFMS 2013), Bangkok, Thailand, and **“Mechanical, thermal, and morphological properties of thermoplastic starch/poly(lactic acid)/poly(butylene adipate-co-terephthalate) blends”** in the 1st International Conference on the Science and Engineering of Materials (ICoSEM 2013), Kuala Lumpur, Malaysia.